snowpex

SnowPEx – The Satellite Snow Product Intercomparison and Evaluation Exercise

Review of Algorithms and Products

Deliverable D3

Prepared by

Thomas Nagler / ENVEO , Austria
Chris Derksen / EC, Canada,
Richard Fernandes / CCRS, Canada,
Masahiro Hori / JAXA, JP
Kari Luojus / FMI, Finland
Thomas Mote / University of Georgia, USA
George Riggs / NASA, USA
David Robinson / Rutgers University, USA
Rune Solberg / NR, Norway
Bartolomeo Ventura/EURAC, Bolzano, ITALY
Gabriele Bippus / ENVEO , Austria
Nicolo DiGirolamo / NASA, USA
Dorothy Hall / NASA GSFC, USA
Richard Kelly / University of Waterloo, CA
Sari Metsämäki / SYKE, Finland,
Claudia Notarnicola / EURAC, Italy
Elisabeth Ripper / ENVEO, Austria
Peter Romanov / NOAA, USA
Marco Tedesco / City College, New York USA
Fuqun Zhou / CCRS, Government of Canada

Issue / Revision: 1.0 / 0

Date: 18.12.2015

Document controlled by: [Thomas Nagler]

SnowPEx Report

Subject: Review of Algorithms and Products	**Project Coordinator**: ENVEO
Issue / Revision: 1 / 0	**Contractor's Ref:** Deliverable D3

This document provides an overview on the 13 snow extent products and 3 snow water equivalent products participating in SnowPEx. For each of the products the main characteristics are summarized and an example for the snow product is given. The overall processing line and required input and auxiliary data are described. Algorithms for detecting snow, cloud screening and optionally post-processing steps are explained. We also summarize the published methods and results for quality assessment and validation of the product and provide information on the strengths and weaknesses of the products and algorithms. Information on the product availability, contact person and relevant publications are also given for each product.

This project was funded by the European Space Agency. Responsibility for the contents resides in the author or organisation that prepared it.

Authors: Nagler T. et al.,

This page is intentionally left blank.

DOCUMENT CHANGE LOG

Issue/ Revision	*Date*	*Modification*	*Modified pages*	*Comment*
1/0		Document created	ALL	Authors

This page is intentionally left blank.

TABLE OF CONTENTS

1. INTRODUCTION 1

1.1 Purpose 1
1.2 Outline 1
1.1 Acronyms 1

2. OVERVIEW OF SNOW EXTENT PRODUCTS 5

3. MOD10 - DAILY GRIDDED MODIS SNOW COVER FRACTION PRODUCT 8

3.1 Product overview and specification 8
3.1.1 Snow mapping algorithm 10
3.1.1.1 Algorithm Description 11
3.1.1.2 Fractional snow cover 11
3.1.2 Cloud screening 13
3.1.3 Auxiliary data sets (Static) 14
3.2 Quality and validation of product 14
3.3 Strength and weaknesses of product 14
3.4 Contact 16
3.5 References 16

4. SCAG 18

4.1 Product overview and specification 18
4.2 Processing line and algorithm 18
4.3 Contact 18

5. GLOBSNOW V2.1 19

5.1 Product overview and specification 19

5.2 Processing lines and Algorithm 21
5.2.1 Snow mapping algorithm 22
5.2.2 Cloud screening 23
5.2.3 Input data 25
5.2.4 Auxiliary data sets (Static) 25
5.3 Quality and validation of product 27
5.4 Strength and weaknesses of product 28
5.5 Contact 29
5.6 References 29

6. GLOBAL MULTISENSOR AUTIMATED SNOW AND ICE MAPS- GMASI (ASNOW) 31

6.1 Product overview and specification 31
6.2 Processing line and algorithm 33
6.2.1 Snow mapping algorithms (visible/infrared and microwave) 34
6.2.1.1 Snow mapping with satellite observations in optical and infrared spectral bands 34
6.2.1.2 Snow mapping with satellite observations in the microwave 37
6.2.2 Blending Approach and Algorithm 38
6.2.3 Input Data 39
6.2.4 Auxiliary Data Sets 39
6.3 Quality and Validation of Product 40
6.3.1 Validation with NOAA Interactive Snow Maps (IMS) 40
6.3.2 Validation with in situ snow observations 41
6.4 Strengths and weaknesses of product 42
6.5 Contact 43
6.6 References 43

7. NOAA IMS 45

7.1 Product overview and specification 45
7.2 Processing line and algorithm 45
7.3 Contact 45

8. CRYOCLIM 46

8.1 Product Overview and Specification 46
8.2 Processing chain and algorithm 48
8.2.1 Single-sensor algorithms for snow probabilities 48
8.2.2 Hidden Markov model algorithm for sensor fusion 48
8.2.3 Processing chain 50
8.3 Quality and Validation of Product 52
8.4 Strength and weaknesses of product 53
8.5 Contact 53
8.6 References 53

9. JASMES MDS10C (JXM10) 55

9.1 Product overview and specification 55
9.2 Processing line and algorithm 56
9.2.1 Snow Mapping Algorithm 57
9.2.2 Cloud Screening 58
9.2.3 Input Data 58
9.2.4 Auxiliary Data Sets (Static) 58
9.2.5 Quality and Validation of Product 58
9.3 Strength and weaknesses of product 59
9.4 Contact 60
9.5 References 60

10. GHRM5C (JXAM5) 61

10.1 Product overview and specification 61
10.2 Processing line and Algorithm 62
10.2.1 Snow mapping algorithm 64
10.2.2 Cloud screening 65
10.2.3 Input data 65
10.2.4 Auxiliary data sets 65

10.2.5 Quality and validation of product 65
10.3 Strength and weaknesses of product 66
10.4 Contact 67
10.5 References 67

11. AVHRR PATHFINDER 68

11.1 Product Overview and Specification – 2 pages 68
11.2 Processing line and Algorithm (max 5 pages) 69
11.2.1 Input Data 70
11.2.2 Data Processing 70
11.2.3 Output Data Formatting 71
11.3 Quality and Validation 72
11.4 Strength and weaknesses of product 72
11.5 Contact 73
11.6 References 73

12. MEASURES SNOW PRODUCT 75

12.1 Product overview and specification 75
12.2 Processing line and algorithm 76
12.2.1 Conversion of source products 77
12.2.1.1 IMS 77
12.2.1.2 CGF 77
12.2.1.3 MW 78
12.2.2 Merged snow extent product 80
12.2.3 MEaSUREs maximum SE for SnowPEx 80
12.2.4 Snow mapping algorithm 81
12.2.5 Cloud screening 81
12.2.6 Input data 81
12.2.7 Auxiliary data sets 81
12.3 Quality and validation of product 81

12.4 Strength and weaknesses of product 82
12.5 Contact 82
12.6 References 82

13. CRYOLAND FSC (CRYOL) 85

13.1 Product Overview and Specification 85
13.2 Processing line and Algorithm 86
13.2.1 Snow Mapping Algorithm 87
13.2.2 Cloud Screening 88
13.2.3 Input Data 89
13.2.4 Auxiliary Data Sets (Static) 89
13.3 Quality and Validation of Product 90
13.4 Strengths and weaknesses of product 92
13.5 Contact 92
13.6 References 92

14. H-SAF10 / H-SAF31 SNOW EXTENT PRODUCT 94

14.1 Product Overview and Specification 94
14.2 Processing line and Algorithm 95
14.3 Cloud Screening 98
14.4 Contact 99
14.5 References 99

15. EURACSNOW – BINARY SNOW EXTENT PRODUCT 100

15.1 Product overview and specification 100
15.2 Processing line and algorithm 101
15.2.1 Snow mapping algorithm 101
15.2.1.1 Pre-processing of MODIS data 102
15.2.1.2 Snow module 103
15.2.1.3 Module for snow detection in forest 103

15.2.2 Cloud screening 105
15.2.3 Input data 105
15.2.4 Auxiliary data sets 105
15.3 Quality and validation of product 105
15.4 Strength and weaknesses of the product 106
15.5 Contact 106
15.6 References 107

16. SNOW WATER EQUIVALENT ALGORITHMS AND PRODUCTS 108

16.1 Overview 108
16.2 Common Approaches 112
16.3 References 113

17. GLOBSNOW SWE PRODUCT 118

17.1 Algorithm 118
17.2 Input and Auxiliary Data 120
17.3 Product Specs 121
17.4 Validation 123
17.4.1 INTAS-SCCONE snow course data 123
17.4.2 Finnish snow course data 124
17.4.3 Canadian Reference Data 124
17.5 References 127

18. NASA STANDARD AMSR-E SWE PRODUCT 129

18.1 Algorithm 129
18.2 Input and Auxiliary Data 131
18.3 Product Specs 132
18.4 Validation 132
18.5 References 133

19. NASA PROTOTYPE AMSR-E PRODUCT 135

19.1 Algorithm 135
19.2 Input and Auxiliary Data 137
19.3 Product Specs 137
19.4 Validation 137
19.5 References 138

1. INTRODUCTION

1.1 Purpose

This document provides information on the snow extent products participating in the SnowPEx intercomparison and validation exercise. The algorithm, processing lines, required input data and auxiliary data needed for generating the product are given. The document provides information on product generation and support the understanding and interpretation of differences in the snow extent by different products revealed in the intercomparison and validation exercise.

1.2 Outline

Section 2 gives an overview on the snow extent products participating in the snow product intercomparison and validation exercise. It includes snow extent product from optical satellite data and snow water equivalent from passive microwave satellite data.

Section 3 to Section 15 provides information on the product specifications and their applied algorithms and processing lines are given for each of the participating products.

Section 16 to Section 19 give the specifications of SWE products and describes the algorithms.

1.1 Acronyms

AATSR	Advanced Along-Track Scanning Radiometer
AMSR-E	Advanced Microwave Scanning Radiometer - Earth Observing System
ASCII	American Standard Code for Information Interchange
ATBD	Algorithm Theoretical Basis Document
ATSR-2	Along-Track Scanning Radiometer -2, onboard of ERS-2
AVHRR	Advanced Very High Resolution Radiometer (AVHRR)
BERMS	Boreal Exosystem Research and Monitoring Sites
BU	Boston University
BU-MODIS	Boston University MOD12Q1 V004 Land Cover Product
CDR	Climate Data Record
CGF	Cloud Gap Filled
CGF	Cloud-Gap-Filled

CLC	Corinne Land Cover
CM SAF	Climate Monitoring SAF
CONUS	Continental United States
CPC	Cloud-Persistence Count
D4FSC	Daily 4 Classes Snow Cover
DFSC	Daily Fractional Snow Cover
DMSP	Defense Meteorological Satellite Program
EASE	Equal-Area Scalable Earth grid
ECMWF	European Center for Medium Range Weather Forecast
EEA	European Environmental Agency
ESA	European Space Agency
ETM+	Enhanced Thematic Mapper
FIR	Finite Impulse Response
GAC	Global Area Coverage (data set of AVHRR)
GDEM	Global Digital Elevation Model
GETASSE	Global Earth Topography And Sea Surface Elevation
GHCN-D	Global Historical Climatology Network Daily
GHRM5C	Japanese Global Snow Cover Extent for Climate Dataset
GHz	Giga Hertz
GLSSE	GlobSnow Snow Extent Product
GMASI	Global Multisensor Automated Snow and Ice
GMT	Generic Mapping Tool
GOES	Geostationary Operational Environmental Satellite)
GSFC	NASA Goddard Space Flight Center
GSGRDA	GMES (Copernicus) Service for Geospatial Reference Data Access
GTS	Global Telecommunication System
HMM	Hidden Markov Model
IMS	Interactive Multisensor Snow and Ice Mapping System
IMS	Interactive Multisensor Snow and Ice Mapping System
INTAS	International Association for the promotion of cooperation with scientists from the New Independent States of the former Soviet Union
-SCCONE	Snow Cover Changes Over Northern Eurasia
ISCCP	International Cloud Climatology Project

JASMES	JAXA Satellite Monitoring for Environmental Studies
JAXA	Japan Aerospace Exploration Agency
JXM10	JAXA Daily Snow Extent product
LOCI	Land-Ocean-Coast-Ice mask
MCST	MODIS Calibration Support Team
MEaSUREs	Making Earth System Data Records for Use in Research Environments
METOP	Meteorological Operational Satellite
MFSC	Monthly aggregated Fractional Snow Cover
MODAPS	MODIS Adaptive Processing System
MODIS	Moderate Resolution Imaging Spectroradiometer
MSG	Meteosat Second Generation
MW	Microwave
NASA	National Aeronautics and Space Administration
NCL	NCAR Command Language
NDSI	Normalized Difference Snow Index
NDVI	Normalizes Difference Vegetation Index
NetCDF	Network Common Data Format
NHTSD25E2	Northern Hemisphere Terrestrial Snow Cover Extent Daily 25km EASE-Grid 2.0
NIC	National Ice Centre
NOAA	National Oceanic and Atmospheric Administration
NR	Norwegian Computing Center
NSIDC	National Snow and Ice Data Center
NWP	Numerical Weather Prediction Model
PDF	Probability Density Function
PMR	Passive Microwave Radiometer
PRCSF	Preliminary Cloud and Snow Cover Flag
QA	Quality Assessment
RIHMI-WDC	All Russion Research Institute of Hydrometeorological Information - World Data Center
RMSE	Root Mean Square Error
SAF	Satellite Application Facility
SCAG	Snow Cover and Grain size (SCAG) spectral unmixing algorithm
SCDA	Simple Cloud Detection Algorithm
SCE	Snow Cover Extent

SCF	Snow Cover Fraction
SD	Snow Depth
SDS	Scientific Data Sets, from MODIS
SE	snow extent
SLSTR	Sea and Land Surface Temperature Radiometer
SMMR	Scanning Multichannel Microwave Radiometer
SNWFG	Snow Cover Flag
SRTM	Shuttle Radar Topography Mission
SSM/I	Special Sensor Microwave/Imager
SSMI/S	Special Sensor Microwave Imager/Sounder
SWE	Snow Water Equivalent
SYKE	Finnish Environment Institute
TM	Thematic Mapper
USGS	United States Geological Survey
UTC	Universal Time Count
UTM	Universal Transverse Mercator
VIIRS	Visible Infrared Imaging Radiometer Suite
WFSC	Weekly aggregated Fractional Snow Cover
WMO	World Meteorological Organisation

2. OVERVIEW OF SNOW EXTENT PRODUCTS

Table 2.1 summarizes the products participating in the SnowPEx intercomparison and validation exercise. Overall, 14 snow extent products are intercompared and validated. In the following sections information on products, their specifications and algorithms and processing lines are given. Table 2.2 summarizes the participating snow water equivalent products.

Table 2.1:
Overview of snow extent products participating in SnowPEx.

Section	SnowPEx PRODID	SnowPEx PRODID_VXX	Product Name	Thematic Parameter	Pixel Sp.	Frequency	Period	Contact Organisation
3	M10C05	V01	MOD10_C5	Fractional / Viewable Snow, Global	0.5 km	daily	2000 – present (Terra)	dorothy.k.hall@nasa.gov NASA
4	SCAG	V01	SCAG	Fractional / Viewable Snow & **Snow on Ground**, NH	0.5 km	daily	2000 - 2013	thomas.painter@jpl.nasa.gov karl.rittger@nsidc.org JPL, NSIDC
5	GLSSE	V01	GlobSnow v2.1	Fractional / **Snow on Ground**, NH	1 km	daily - monthly	1996 - 2012	sari.metsamaki@ymparisto.fi SYKE
6	ASNOW	V01	Autosnow	Fractional / Viewable Snow, NH	4 km	daily	2006 - present	peter.romanov@noaa.gov NESDIS
7	IMS01	V01	IMS	Binary / **Snow on Ground**, NH	1 km	daily	2014 ->	sean.helfrich@noaa.gov NOAA
7	IMS04	V01	NOAA IMS	Binary / **Snow on Ground**, NH	4 km	daily	2004 - present	sean.helfrich@noaa.gov NOAA
7	IMS24	V01	NOAA IMS	Binary / **Snow on Ground**, NH	24 km	daily	1997 - 2004	sean.helfrich@noaa.gov NOAA

Section	SnowPEx PRODID	SnowPEx PRODID_VXX	Product Name	Thematic Parameter	Pixel Sp.	Frequency	Period	Contact Organisation
8	CRCLIM	V01	CryoClim	Binary / **Snow on Ground**, Global	5km	daily	1982 - present	rune.solberg@nr.no NR,METNO
9	JXM10	V01	JASMES MDS10C	Binary / Viewable Snow, NH	5 km	Daily weekly half-monthly	2000 – 2013	hori.masahiro@jaxa.jp JAXA
10	JXAM5	V01	JASMES GHRM5C	Binary / Viewable Snow, NH	5 km	Daily weekly half-monthly	1979 – 2013	hori.masahiro@jaxa.jp JAXA
11	PATHF	V01	AVHRR Pathfinder	Binary / **Snow on Ground**, NH	5 km	daily	1985 - 2004	Richard.fernandes@nrcan.gc.ca CCRS
12	MEASU	V01	MEaSUREs	Binary / **Snow on Ground**, Global	25 km	daily	1999 - 2012	dorothy.k.hall@nasa.gov NASA
13	CRYOL	V01	CryoLand	Fractional / **Snow on Ground** (PanEur)	0.5 km	daily	2000 - present	thomas.nagler@enveo.at ENVEO
14	HSAF10 / HSAF31	V01	HSAF H10 / HSAF H31	Binary / Viewable Snow (PanEur)	5 km	daily	2009 / 2008 - present	matias.takala@fmi.fi, niilo.siljamo@fmi.fi FMI
15	EURAC	V01	EURAC Snow	Binary / **Snow on Ground** (Alps)	0.25 km	daily	2002 - present	claudia.notarnicola@eurac.edu EURAC

Table 2.2:
Overview of snow water equivalent products participating in SnowPEx.

Section	SnowPEx PRODID	SnowPEx Vxx	Product Name	Coverage	Algorithm	Pixel Sp.	Frequency	Period	Contact Organisation
17	GLSWE	V01	ESA GlobSnow	Northern Hemis. (non Alpine)	PMW + Ground stations	25 km	Daily N	1979-present	kari.luojus@fmi.fi FMII
18	NASSTD	V01	NASA AMSR-E (standard)	Northern Hemis.	PMW	25 km	daily	2002-2011	rejkelly@uwaterloo.ca cryocity@gmail.com (Tedesco)
19	NASPR	V01	NASA AMSR-E (prototype)	Northern Hemis.	PMW + Ground stations climatology	25 km	daily	2002-2011	cryocity@gmail.com City College, New York

3. MOD10 - DAILY GRIDDED MODIS SNOW COVER FRACTION PRODUCT

Authors: Dorothy Hall, George Riggs and Nicolo DiGirolamo (NASA, USA)

3.1 Product overview and specification

The daily gridded MODIS snow cover fraction (SCF) snow product, MOD10A1 is derived from a series of MODIS snow cover data products that originate at the swath processing level. The fractional snow cover algorithm is applied at the swath level then the swath products are composited to make a daily gridded product then the 'best' observation of the day from the many that may have been acquired is selected to make the MOD10A1 fractional snow product used in SnowPEx. The MOD10A1 daily tiled products are mosaicked to make the M10C05 SnowPEx single day, 500 m, hemisphere product. Only the Terra MOD10_L2 standard MODIS snow-cover product (Riggs and Hall, 2014 has been contributed. There is also an Aqua MODIS MYD10_L2 generated but Aqua was not contributed to this intercomparison. The MODIS snow cover products in Collection 5 have both a binary snow cover area and a fractional snow cover map. Only the fractional snow cover map is contributed to SnowPEx because it is considered the better snow map and only the factional snow product will be in MODIS collection 6 (C6) processing.

Table 3.1:
Summary on MODIS fractional snow cover product.

Parameter	***Specification***
Thematic variable	Fractional Snow Cover (SCF)
Thematic resolution	1% FSC
Thematic range	[1, 100] FSC
Thematic accuracy	~20%
Thematic uncertainty estimate	RMSE per pixel; not estimated.
Product Quality Map	General quality setting attached to daily products
Spatial resolution	0.005° × 0.005° (ca 500m)
Spatial coverage	global
Product available since	Daily products, since March2000
Delivery time period	MOD10A1 typically 1-3 days after acquisition
Temporal frequency	Daily
Projection/Datum	Geographical (lat/lon) / WGS84
Cloud Screening	Standard MODIS Cloud Product
Invalid / Masked Areas	Oceans, polar darkness
Sensor	Terra MODIS

Parameter	*Specification*
Satellite data level	Level 1B Swath data
File format	GeoTIFF
Developed by	MODIS Snow/Ice Project
Provider / Generated by	MODIS Snow/Ice Project
Product available at	
Contact	Dorothy Hall / NASA / GSFC Dorothy.k.hall@nas.gov

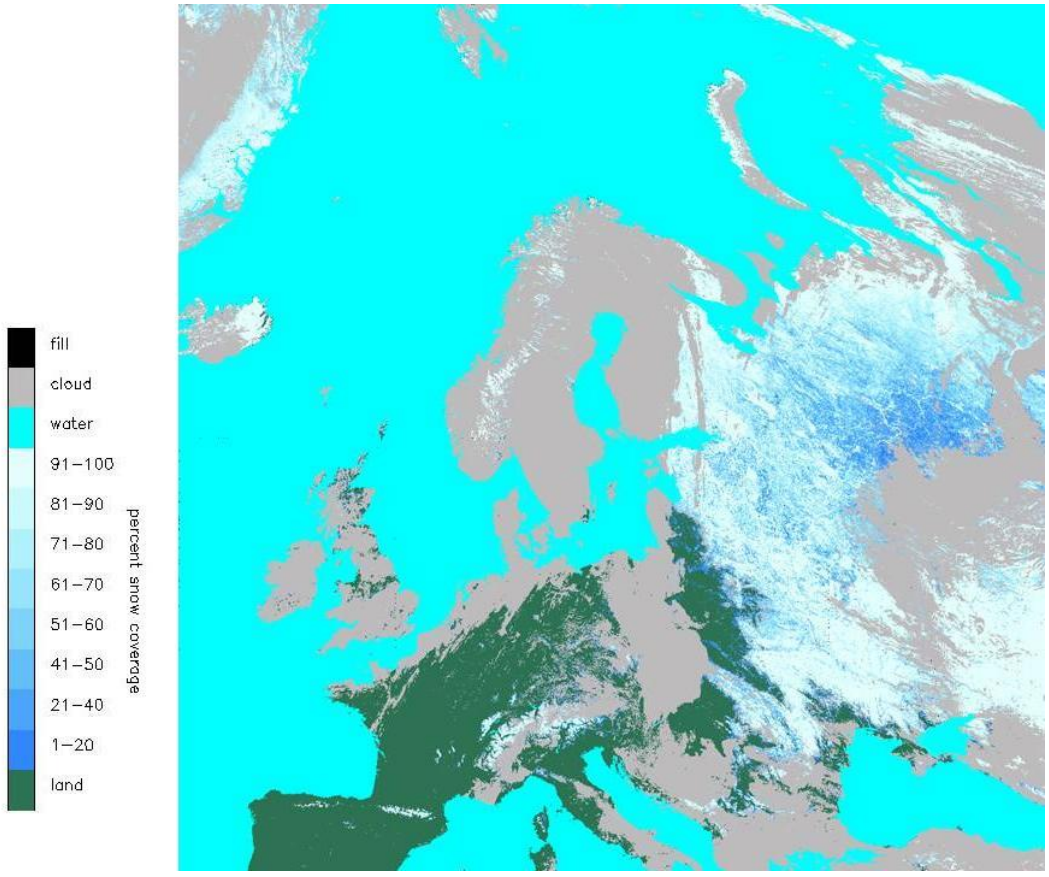

Figure 3.1: Example of MOD10A1 Fractional Snow Extent product, 9 March 2012.

Figure 3.2 shows a processing flowchart of the standard MODIS fractional snow cover products. Input data are satellite data from MODIS / Terra.

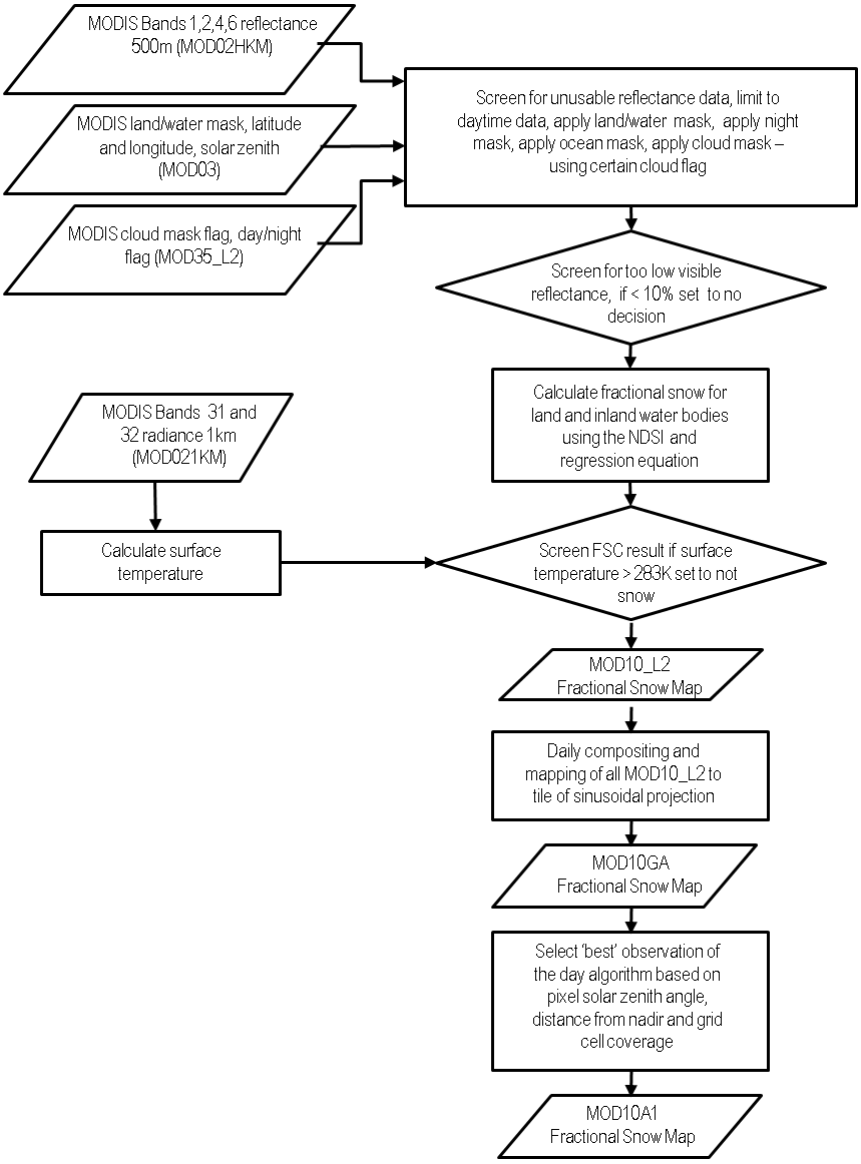

Figure 3.2: Flowchart of the MODIS fractional snow-cover algorithm and products from the swath level to the daily gridded MOD10A1 products (Riggs and Hall, 2014).

3.1.1 Snow mapping algorithm

The swath product is generated using the MODIS calibrated radiance data products (MOD02HKM and MOD021KM), the geolocation product (MOD03) and the cloud mask product (MOD35_L2) as inputs. The MODIS snow cover algorithm output product, MOD10_L2, contains two SDS of snow cover, a quality assessment (QA) SDS, latitude and longitude SDSs, local attributes and global attributes. The snow cover algorithm identifies snow-covered land, snow-covered ice on inland water and computes

fractional snow cover. There are approximately 288 swaths of Terra orbits acquired in daylight so there are approximately 288 MOD10_L2 snow products per day.

3.1.1.1 Algorithm Description

The snow algorithm is described in detail in the Algorithm Theoretical Basis Document (ATBD) (Riggs et al., 2006) and the Snow Product User Guide (Riggs and Hall, 2006 (for C5) and Riggs and Hall, 2014 (for C6). Analysis for snow in a MODIS swath is done on pixels of land or of inland water that have usable L1B radiance data, are in daylight, have greater than 10% visible reflectance, and to which the cloud mask was applied. Snow detection is also screened for surface temperature to reduce the occurrence of erroneous snow in some situations. Land and inland waters are masked with the 1 km resolution land/water mask, contained in the MODIS geolocation product (MOD03). In Collection 5 (C5) the land/water mask made by the Boston University (BU) team based on EOS data is used. (More information is given on the land/water mask in QA sections below.) The 1 km data of the land/water mask is applied to the four corresponding 500 m pixels in the snow algorithm. Ocean waters are not analysed for snow. Inland waters, lakes and rivers, are analysed for snow-covered ice conditions.

The MODIS L1B is screened for missing data and for unusable data. Unusable data results from the processing at L1B when the sensor radiance data fails to meet acceptable criteria. MODIS data may be unusable for several reasons. Specifics of L1B processing and criteria can be found at the MODIS Calibration Support Team (MCST) webpage {http://mcst.gsfc.nasa.gov/} and in supporting documentation. If missing data is encountered those pixels are identified as missing data in MOD10_L2. If unusable data is encountered, then a no decision result is written for those pixels. Usable L1B calibrated radiance data is converted to at-satellite reflectance for use in the snow algorithm.

Fractional snow cover is computed for all land and inland water body pixels in a swath that passed the above screenings. Fractional snow cover is calculated using the NDIS and regression equation of Salomonson and Appel (2004 and 2006). The fractional snow cover calculation is applied to the full range of NDSI values, 0.0 -1.0. Fractional snow is constrained to an upper limit of 100%. All pixels with fractional snow cover are screened for surface temperature, calculated in the algorithm, snow pixels with surface temperature > 283 K are reset to 0% FSC.

3.1.1.2 Fractional snow cover

Results of the fractional snow cover algorithm are stored as coded integers in the Fractional_Snow_Cover SDS. The fractional snow algorithm calculates fractional snow in the 0 – 100%

range, including for inland water bodies. Pixels that are not identified as snow are labelled as water, cloud or other condition. A fractional snow map is shown in Figure 3.1.

Local attributes, listed below are also stored with the SDS:

- Local attributes with Fractional_Snow_Cover SDS:
- Attribute name: Fractional Snow Cover
- long_name MOD10A1, 500m
- units none
- Key: Key to meaning of data in the SDS
    - 0-100=fractional snow,
    - 200=missing data,
    - 201=no decision,
    - 211=night,
    - 225=land,
    - 237=inland water,
    - 239=ocean,
    - 250=cloud,
    - 254=detector
    - saturated, 255=fill
- Nadir_data_resolution: Nominal pixel resolution at nadir 500 m

The next processing level is L2G where the MOD10_L2 swath products for a day are composited and gridded to the sinusoidal projection to make the MOD10GA product. The MODAPS built a generic gridding algorithm for many of the MODIS data products to create the L2G daily gridded data products (Wolfe et al., 1998). The Earth is divided into an array of 36 x 18, longitude by latitude, tiles, about 10°x10° in size in the sinusoidal projection. The gridding algorithm maps MODIS Level-2 swath products into a tile of the grid and creates the relevant gridding projection data structures in the product.

The MOD10A1 algorithm selects the ‘best’ observation of the single to many MOD10_L2 pixels stored in the MOD10GA product. The observation selection criteria used are solar elevation, distance from

nadir, observation cover (pixel coverage in a grid cell of the projection), to map an observation into the first data layer. Thus the 'best' observation for each product is based only on those criteria so that the observation selected is nearest local solar noon time, nearest the orbit nadir track and with most coverage in a grid cell, which is considered the best sensor view of the surface on a day relevant to snow cover detection. Those 'best' observations are mapped into the MOD10A1 product. This strategy results in a contiguous mapping of swaths with a weave or checkerboard pattern along stitched together swath edges. That weave pattern is sometimes apparent where cloud cover changed between acquisition times of overlapping swaths.

The MOD10A1 products are converted to SnowPEx format by mapping of FSC values to SnowPEx value set and converting to Geotiff format and making the metadata file. SnowPEx takes all the MOD10A1 tiled products, approximately 175 per day for the Northern Hemisphere and mosaics them to a single day, hemispheric 500 m resolution, M10C05 product.

3.1.2 Cloud screening

Clouds are masked using data from the MODIS Cloud Mask data product (MOD35_L2). The MOD35_L2 data is checked to determine if the cloud mask algorithm was applied to a pixel. If it was applied, then results of the cloud mask algorithm are used. If it was not applied then the cloud mask is not used and the snow algorithm will process for snow assuming that the pixel is unobstructed by

cloud. Only the summary cloud result, the unobstructed field-of-view flag, from

MOD35_L2 is used to mask clouds in the snow algorithm. If the summary cloud flag is certain cloud, then cloud is mapped in the snow product. Documentation of the cloud mask is available at *MODIS cloud mask* (http://modis-atmos.gsfc.gov/index.html).

Input Data

- MOD02HKM MODIS Level 1B Calibrated and Geolocated Radiances Reflectance for MODIS bands:
    - 1 (0.645 µm)
    - 2 (0.865 µm)
    - 4 (0.555 µm)
    - 6 (1.640 µm)
- MOD021KM MODIS Level 1B Calibrated and Geolocated Radiances

- band 31 (11.28 µm)
- band 32 (12.27 µm)

- MOD03 MODIS Geolocation
- Land/Water Mask, Solar Zenith Angles, Sensor Zenith Angles, Latitude, Longitude
- MOD35_L2 MODIS Cloud Mask
  - Cloud Mask Flag, Unobstructed Field of View Flag, Day/Night Flag

3.1.3 Auxiliary data sets (Static)

Auxiliary data are static data sets, which means they are the same for the complete time series of products. The product MODIS C5 uses the MODIS land/water mask described in Salomon et al. 2004.

3.2 Quality and validation of product

The accuracy of the MODIS snow extent product varies with land-cover type, but overall, the accuracy under clear sky conditions has been assessed at 92% in various peer-reviewed publications. Validation at stage 2 has been achieved for the snow-cover product (MOD10). Stage 2 Validation is defined as follows: "*Product accuracy is estimated over a significant set of locations and time periods by comparison with reference in situ or other suitable reference data. Spatial and temporal consistency of the product and with similar products has been evaluated over globally representative locations and time periods. Results are published in the peer-reviewed literature.*"

Validation of the MODIS product is well documented in various publications, e.g. Lee et al., 2005; Ault et al., 2006; Parajka and Bloschl, 2006; Hall and Riggs, 2007. Numerous other peer-reviewed journal articles have discussed the validation of the MOD10A1 products and a list of those publications may be found here: http://modis-snow-ice.gsfc.nasa.gov/?c=publications. Validation activities have largely been conducted by conducting comparisons with other snow maps, in-situ data and optical satellite imagery. A summary of the validation of the standard MODIS snow products is available at http://landval.gsfc.nasa.gov/MODIS/ProductStatus.php?ProductID=MOD10/29.

3.3 Strength and weaknesses of product

The biggest uncertainty in the standard MODIS snow and ice products rests with the cloud mask, MOD35. The standard MODIS cloud mask is overly conservative over snow and ice targets. There is an

additional major uncertainty in Collection 5. Because of the surface temperature screen, some spring snow cover in mountainous areas is screened out, causing it to look like the snow melted earlier than it really did. This has been corrected in Collection 6 (see Riggs and Hall, 2014).

A surface temperature screen was applied in the algorithm in C5 to reverse all snow detections that were too warm to be snow. Any pixel detected as snow cover and having an estimated surface temperature >283 K was reversed to a snow free pixel. That temperature screening was successful at greatly reducing the occurrence of erroneous snow cover in warm regions of the world and along warm coastal regions especially those with wide, sandy beaches. However, it was discovered that the temperature screen also caused snow omission errors. Snow omission errors in spring and summer on snow covered mountain ranges could be very large as the seasonal surface temperature increased above 283 K. The effect of the temperature screen on mapping of snow cover on the Sierra Nevada from 1 May to 1 August 2010 is exhibited at http://modis-snow-ice.gsfc.gov/?c=collection6. Snow omission errors were around 10% at start of that time period then rose to near 90% at the end. It is probable that snow omission errors associated with seasonally increasing temperatures occurred on some mountain ranges depending on the climate they are located.

The effectiveness of the surface temperature screen varied as the surface changed over seasons. Bright surface features that were cold, below the surface temperature threshold, and snow free could be detected as snow cover, a commission error and the temperature screen would not reverse that result. As the surface warmed through the season the temperature screen would take effect and the snow free surface would at some point be mapped as snow free. If that surface was cold and snow covered then a correct detection would occur.

Low solar illumination conditions occurring when the solar zenith angle is > 70.0 degrees and near to the day/night terminator are a challenge to snow detection. Low reflectance, less than about 0.30 across the visible bands from a landscape is also a challenge for snow detection. In either case and depending on presence or absence of snow cover, snow commission or omission errors are possible. Low reflectance across the spectrum combined with the nature of a ratio can result in relatively small differences between the visible and NIR bands used to calculate the NDSI to have a high NDSI value. However, the very low visible reflectance is cause for large uncertainly in detection of snow cover. Investigation and discussion with some users who encountered errors associated with low reflectance surface conditions resulted in setting a low reflectance limit in the algorithm. If reflectance is too low a pixel is not processed, it is set to “no decision.” This is considered a low limit to accurately detect snow cover on the landscape. Low reflectance associated with shadowed landscape, clouds or terrain, and unmapped water bodies or inundated landscape can possibly exhibit reflectance characteristics

similar to snow and could be erroneously detected as snow in the algorithm. Reflectance values in the range above the low limit and below about 0.30 may cause uncertainty in a snow detection.

3.4 Contact

Institution	NASA Goddard Space Flight Center
Contact Person	Dorothy K. Hall , George A. Riggs
Email	Dorothy.k.hall@nasa.gov George.a.riggs@nasa.gov
Website for downloading the product:	http://reverb.echo.nasa.gov/

3.5 References

Ackerman, S. A., K. Strabala, W.P. Menzel, R.A. Frey, C.C. Moeller, and L.E. Gumley, 1998: Discriminating clear sky from clouds with MODIS. *Journal of Geophysical Research: Atmospheres* (1984–2012), 103(D24):32141-32157.

Ault, T.W., K.P. Czajkowski , T. Benko, J. Coss, J. Struble, A. Spongberg, M. Templin and C. Gross, 2006: Validation of the MODIS snow product and cloud mask using student and NWS cooperative station observations in the Lower Great Lakes Region, *Remote Sensing of Environment,* 105:341-353.

Hall, D. K., G.A. Riggs, and V.V. Salomonson, 1995: Development of methods for mapping global snow cover using moderate resolution imaging spectroradiometer data, *Remote sensing of Environment*, 54(2):127-140.

Hall, D.K., G.A. Riggs, V.V. Salomonson, N.E. DiGiromamo and K.J. Bayr, 2002: MODIS snow-cover products, *Remote Sensing of Environment*, 83:181–194.

Hall, D.K. and G.A. Riggs, 2007: Accuracy assessment of the MODIS snow products, *Hydrological Processes*, 21, 1534-1547.

Hall, D.K., Riggs, G.A., Foster, J.L. and Kumar, S.V., 2010: Development and evaluation of a cloud-gap-filled MODIS daily snow-cover product, *Remote Sensing of Environment,* 114:496-503.

Jarvis A, H. Reuter, A. Nelson, E. Guevara, 2008: Hole-filled SRTM for the globe Version 4, available from the CGIAR-CSI SRTM 90m Database. Available at: http://srtm.csi.cgiar.org

Parajka, J. and G. Blöschl, 2006: Validation of MODIS Snow Cover Images Over Austria, *Hydrology and Earth System Sciences*, 10(5): 679-689.

Lee, S., A.G. Klein and T.M. Over, 2005: A comparison of MODIS and NOHRSC snow-cover products for simulating streamflow using the Snowmelt Runoff Model, *Hydrological Processes,* 19:2951-2972.

Riggs, G. A., Hall, D. K., and Salomonson, V. V., 2006. MODIS snow products user guide. http://modis-snow-ice.gsfc.nasa.gov/sug_c5.pdf.

Riggs, G.A. and D.K. Hall, 2014: MODIS Snow Products User Guide to Collection 6, 1 October 2014, URL TBD, 58 pp.

Rossow, W. B. and L.C. Garder, 1993: Cloud detection using satellite measurements of infrared and visible radiances for ISCCP, *Journal of Climate*, *6*(12):2341-2369.

Salomonson, V.V. and Appel, I., 2004. Estimating the fractional snow cover using the normalized difference snow index, *Remote Sensing of Environment*. 89(3):351-360.

Salomon, J.; Hodges, J.C.F.; Friedl, M.; Schaaf, C.; Strahler, A.; Gao, F.; Schneider, A.; Zhang, X.; El Saleous, N.; Wolfe, R.E .20045. Global Land–Water Mask Derived from MODIS Nadir BRDF–Adjusted Reflectances (NBAR) and the MODIS Land Cover Algorithm. Proc. IGARSS 2004.

Salomonson, V., and I. Appel, 2006: Development of the Aqua MODIS NDSI fractional snow cover algorithm and validation results, *Geoscience and Remote Sensing, IEEE Transactions on*, *44*(7):1747-1756.

Wolfe, R.E., D.P. Roy, E. Vermote, 1998: MODIS land data storage, 1998: gridding and compositing methodology: Level 2 Grid, *IEEE Transactions on Geoscience and Remote Sensing*, 36:1324–1338

4. SCAG

4.1 Product overview and specification

An online help section about the MODSCAG (MODIS Snow Covered-Area and Grain size retrieval algorithm) products is available at http://snow.jpl.nasa.gov/portal/data/help_modscag.

4.2 Processing line and algorithm

The SCAG algorithm is based on a multiple endmember linear spectral mixture analysis applied on MODIS, VIIRS or Landsat data. Descriptions of the basic MODSCAG algorithm are available in the following publications:

Painter, T. H., Rittger, K., McKenzie, C., Slaughter, P., Davis, R. E. & Dozier, J. (2009) Retrieval of subpixel snow covered area, grain size, and albedo from MODIS. Remote Sensing of Environment 113(4), 868–879. doi:10.1016/j.rse.2009.01.001: currently online available from

http://digitalcommons.unl.edu/cgi/viewcontent.cgi?article=1082&context=usarmyresearch.

Rittger, K., Painter, T. H. & Dozier, J. (2013) Assessment of methods for mapping snow cover from MODIS. Advances in Water Resources 51(35th Year Anniversary Issue), 367–380. doi:10.1016/j.advwatres.2012.03.002: currently available from

ftp://ftp.eri.ucsb.edu/pub/org/snow/users/krittger/20131203_MeritReview/RittgerPainterDozierADWR2012.pdf.

4.3 Contact

Institution	NASA / JPL, NSIDC
Contact Person	Thomas Painter, Karl Rittger, Kat Bormann
Email	thomas.painter@jpl.nasa.gov, karl.rittger@nsidc.org
Website for downloading the product:	Only on request, email to snowds-dev@jpl.nasa.gov

5. GLOBSNOW V2.1

Authors: Sari Metsämäki (SYKE), Kari Luojus (FMI), Gabriele Bippus, Elisabeth Ripper, Thomas Nagler (ENVEO)

5.1 Product overview and specification

GlobSnow Snow Extent (SE) product portfolio comprises a set of product which all are generated from daily product providing sub-pixel Snow Cover Fraction (SCF) in 0.01 deg grid over the Northern Hemisphere, for time period 1995-2012. Grid cells classified as „Cloud" as well as water bodies are excluded in the SCF provision. The SCF retrieval is based on SCAmod algorithm (Metsämäki et al. (2005, 2012). SCAmod is particularly designed to map SCF in boreal forests, essentially based on the pre-determined information on forest transmissivity employed by the radiative transfer model-originated reflectance modelling.

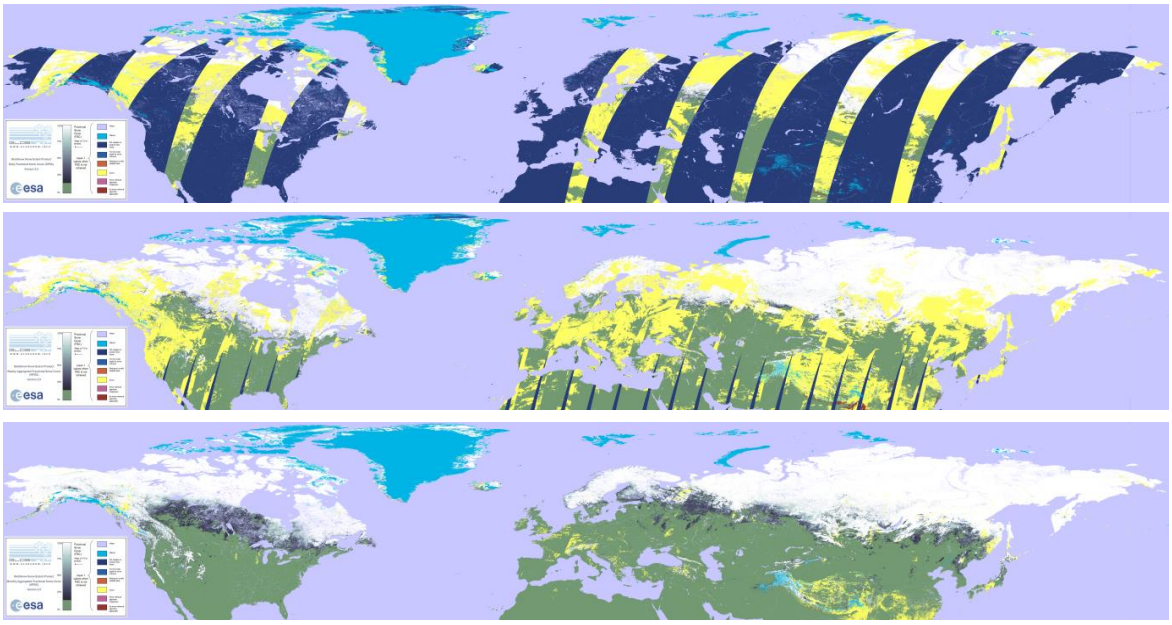

Figure 5.1: A sample set of GlobSnow v2.0 SE products for April 2006. *Top*: daily product 13 April, *Middle*: weekly product 15 April, *Bottom*: monthly product.

GlobSnow v2.1 and v2.0 SE product portfolio includes maps on Snow Cover Fraction (range 0-100 % or 0-1) in 0.01º×0.01º geographical grid and they cover the Northern Hemisphere in latitudes 25ºN - 84ºN

and longitudes 168W-192E. v2.1 cover years 2003-2012, while the years 1995-2002 are available as v2.0). The *Daily Fractional Snow Cover* (DFSC) product provides fractional snow cover in percentage (%) per grid cell for all satellite overpasses of a given day. If there are multiple snow observations (only far north within a day), the satellite observations applied are those giving the highest solar elevation. SCF is provided only for observations at sun zenith angle < 74º. The *Weekly Aggregated Fractional Snow Cover* (WFSC) product is based on the latest satellite overpasses within a seven-day period. The *Monthly Aggregated Fractional Snow Cover* (MFSC) product is provided as an average of all satellite overpasses within a calendar month period. The *Daily 4-classes Snow Cover* (D4FSC) product provides snow cover classified into four categories per grid cell for all satellite overpasses of a given day. In terms of SCF, the four classes represent: 0 % ≤ SCF ≤ 10 %; 10 % < SCF ≤ 50 %; 50 % < SCF ≤ 90 %; 90 % < SCF ≤ 100 %.

Table5.5.1:
Summary on GlobSnow (GLSSE) snow product.

Parameter	***Specification***
Thematic variable	Fractional Snow Cover (SCF)
Thematic resolution	1% SCF
Thematic range	[1, 100] SCF
Thematic accuracy	~20%
Thematic uncertainty estimate	RMSE per pixel;
Product Quality Map	Uncertainty map calculated and attached to daily products
Spatial resolution	0.01° × 0.01° (ca 1000m)
Spatial coverage	~Northern Hemisphere : 25N-84N; 168W-192E
Product available since	Daily products, since 1995
Delivery time period	Full Year, daily
Temporal frequency	Daily
Projection/Datum	Geographical (lat/lon) / WGS84
Cloud Screening	GlobSnow
Invalid / Masked Areas	Open Water (sea, lakes, rivers)
Sensor	ERS-2/ATSR-2, Envisat/AATSR
Satellite data level	Level 1B Swath data
File format	Netcdf
Developed by	GlobSnow team
Provider / Generated by	FMI
Product available at	www.globsnow.info/SE
Contact	Sari Metsämäki (email: sari.metsamaki@environment.fi) Kari Luojus (email: kari.luojus@fmi.fi)

The weekly and monthly products based on D4FSC are also provided, with same specifications as for daily products. The dataset is available at http://www.globsnow.info/se/archive_v2.0/ for years 1995-2003 and http://www.globsnow.info/se/archive_v2.1/ for years 2003-2011. Figure 5.1 presents an example of daily, weekly and monthly SE products for April 2006.

5.2 Processing lines and Algorithm

A high-level conceptual diagram of the SE processing system is given in Figure 5.2.

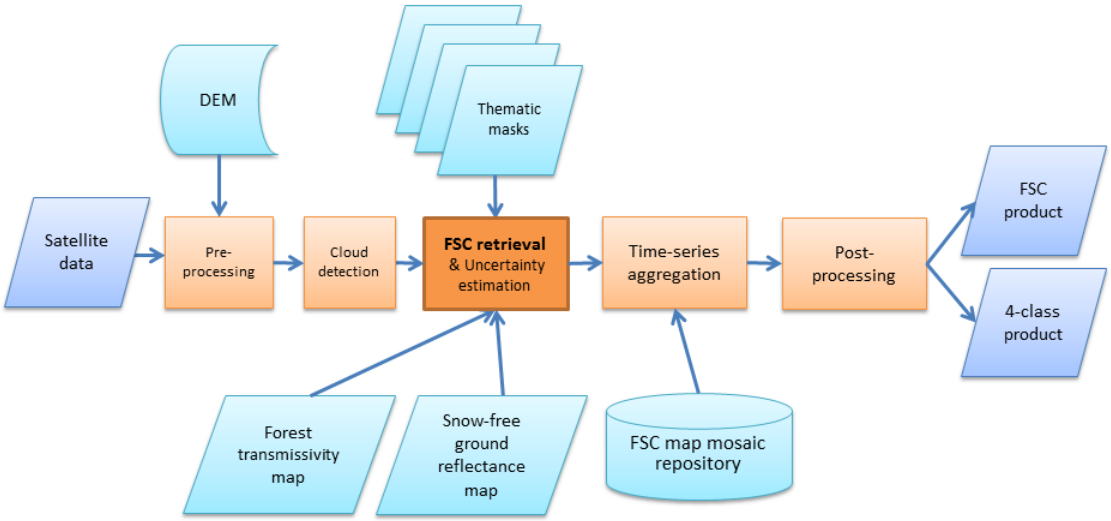

Figure 5.2: Conceptual model for the SE processing system.

The main data elements and buildings blocks of the system are:

- Satellite data: ATSR-2 and AATSR data as processed and delivered from the ESA
- DEM: Digital Elevation Model data applied for topographic geometrical and radiometric correction
- Pre-processing:
    - geometrical correction (geo-referencing),
    - radiometric calibration and topographic correction
    - cloud detection
- SFC retrieval algorithm and uncertainty estimation

- Thematic masks: Providing thematic map information, like forest, mountain, water etc.
- Forest transmissivity map: applied in the SCF retrieval algorithm
- Snow-free ground reflectance map
- Time-series aggregation: Algorithm aggregating satellite data over a period (a few days) in order to obtain better spatial coverage
- Post-processing: Product generation from the SCF map and uncertainty data coming from the retrieval algorithms
- SCF and 4-classes products: Final SE products, including data on accuracy and other metadata.

5.2.1 Snow mapping algorithm

The SCF retrieval is based on SCAmod algorithm (Metsämäki et al. (2005, 2015). SCAmod is particularly designed to map SCF in boreal forests, essentially based on the pre-determined information on forest transmissivity employed by the radiative transfer model-originated reflectance modelling. The model describes the scene reflectance as a mixture of three major constituents – opaque forest canopy, snow and snow-free ground, which are interconnected through the *apparent forest transmissivity* and the snow fraction. Transmissivity can be derived from reflectance observations under conditions that highlight the presence of forest canopy – namely in the presence of full snow cover on the ground. Given that the transmissivity can be determined with an appropriate accuracy, SCAmod enables the consideration for the masking effect of forest canopy in fractional snow cover estimation (Metsämäki et al., 2005, 2012). SCAmod expresses the observed reflectance as follows:

$$\rho_{\lambda,obs}(SCF) = (1-t_\lambda^2) * \rho_{\lambda,\,forest} \quad + \quad t_\lambda^2 * \left[SCF * \rho_{\lambda,snow} + (1-SCF) * \rho_{\lambda,ground}\right] \qquad \text{(Equ. 5.1)}$$

where $\rho_{\lambda,snow}$, $\rho_{\lambda,ground}$ and $\rho_{\lambda,forest}$ are generally applicable pre-determined reflectances of (wet) snow, snow-free ground and forest canopy at wavelength λ, respectively. $\rho_{\lambda,obs}$ stands for the observed reflectance from calculation unit area. t_λ^2 stands for the apparent two-way transmissivity for the unit area. The generally applicable value for snow reflectance $\rho_{\lambda,snow}$ in eq. (5.1) is empirically derived from i) MODIS band 4 reflectance observations from snow-covered non-forested areas (Metsämäki et al., 2012) and ii) at-ground spectral measurements conducted in Finland (Salminen et al., 2009; Niemi et al., 2012). Value of 0.65 is used for GlobSnow SCF provision. The applied value of $\rho_{\lambda,forest}$ was mainly derived from MODIS reflectance observations from carefully selected very dense boreal forests over Finland and Russia (Metsämäki et al., 2012), but also from reflectance measurement of thick layers of

Scots pine branches at laboratory condition (Niemi et al., 2012). A value of 0.08 for $\rho_{\lambda,forest}$ is considered reasonable for SCF estimation. SCF (range 0-1 here) is solved from Equ. 5.1 as follows:

$$SCF = \frac{\frac{1}{t_\lambda^2} * \rho_{\lambda,obs} + (1 - \frac{1}{t_\lambda^2}) * \rho_{\lambda,forest} - \rho_{\lambda,ground}}{\rho_{\lambda,snow} - \rho_{\lambda,ground}}. \quad \text{(Equ. 5.2)}$$

SCAmod may result in SCF>1 (100 %) if the observed reflectance is higher than the maximum allowed by the model with the applied parameters. This may be e.g. due to the non-representative transmissivity. Likewise, SCAmod may result in SCF<0 if the observed reflectance is lower than the minimum allowed by the model. Consequently, fractional snow cover is constrained to upper and lower limits of 100 % and 0 % respectively.

An additional test for identification of snow-free conditions is applied to avoid false snow detection if the observed reflectance from snow-free terrain is higher than assumed by the model. Normalized Difference Snow Index (NDSI) is used to identify confident snow-free cases. Since NDSI decreases with the decreasing snow fraction it is possible to determine a threshold to identify the snow-free situation. The value 0.4 (or 0.1 for forested areas) as proposed by Klein et al., (1998) is however not feasible for SCAmod purposes, as the intention is to identify also small snow fractions accurately without too conservative thresholding. A empirical threshold of -0.02 is used in GlobSnow:

IF (NDSI < -0.02) THEN SCF = 0

Temperature screening is applied to avoid false snow identifications caused by highly reflective non-snow targets like certain non-identified cloud types or warm bright mineral surfaces. A pixel is designated 'snow-free' if its temperature > threshold. In GlobSnow the thresholding is based on a single band (centred at 12µm) approximation of the surface brightness temperature:

IF (temperature > 288 K) THEN SCF=0

A more detailed description of the algorithm is given in Metsämäki et al. (2014) and Metsämäki et al. (2015).

5.2.2 Cloud screening

A simple and computationally low-cost binary (cloud/clear) classifier method SCDA (Simple Cloud Detection Algorithm) was developed during the GlobSnow project.

The current version SCDA2.0 was designed to be used for optical and infrared data from sensors such as Terra/MODIS, ERS-2/ATSR-2, ENVISAT/AATSR, NPP Suomi/VIIRS and the future Sentinel-3 SLSTR. The method uses wavelength bands 550 nm, 1.6 µm, 3.7 µm, 11 µm and 12 µm, common for these sensors. Figure 5.2 presents the cloud screening scheme, with these bands referred to as R550, R1.6, BT3.7, BT11 and BT12, correspondingly.

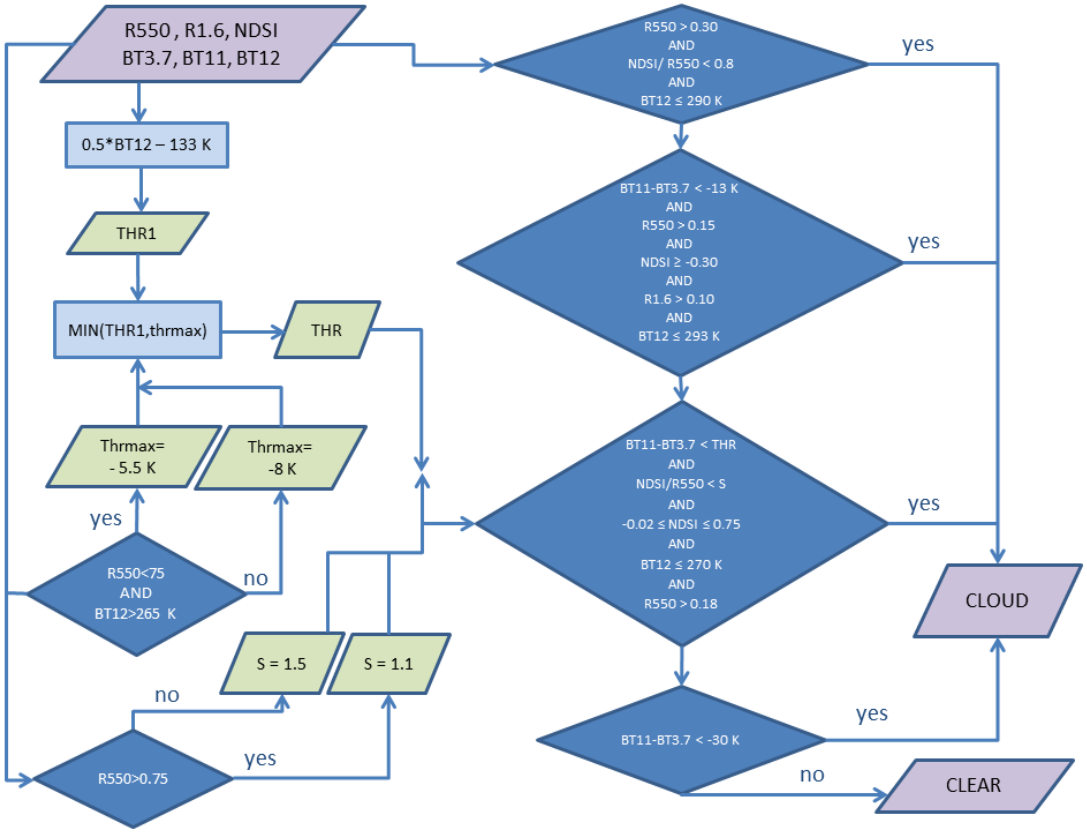

Figure 5.3: Cloud detection scheme for GlobSnow SE production.

The methodology is based on the several empirically determined decision rules, determined from selected training areas representing (by visual judgment) clouds, snow-covered terrain, partially snow-covered terrain and snow-free terrain. NPP Suomi/VIIRS and Terra/MODIS acquisitions from several dates and from different regions over Northern Hemisphere provided the training data. The development work for SCDA2.0 was intended particularly for identification of clouds throughout potential snow seasons for such regions where snow events are typical. Identification of clouds over regions without even ephemeral snow is therefore not given any specific attention, which means that

thin semi-transparent clouds over areas confidently assumed to be snow-free may not be classified as cloud. This kind of 'liberal' mask would retain more area for snow/non-snow mapping purposes. As a drawback, some non-detected clouds still may confuse the snow mapping method, leading to false snow commissions during summer months. In most cases however, non-detected clouds in summertime images are assigned 'snow-free' by the SCF retrieval method. Finally, the original cloud mask is enhanced by expanding it by a width of 1–3 pixels. This would diminish the presence of partly cloud-contaminated pixels at the cloud edges and removes most of the shadows cast by clouds.

5.2.3 Input data

GlobSnow SE products are based on data provided by ERS-2/ATSR-2 (1995-2003) and Envisat/AATSR (2002-2012), so that a contiguous dataset spanning for 17 years is obtained. Swath width for both these sensors is only ~500 km so that the complete spatial coverage at mid-latitudes cannot be reached daily. The relevant bands for GlobSnow SE are Band 1 (0.545-0.565 µm) and Band 4 (1.58-1.64 µm) used for SCF-retrievals; thermal bands 5, 6 and 7 centred at 3.7 µm, 10.85 µm and 12 µm, respectively, are used for cloud screening. SCAmod employs top-of-atmosphere reflectance acquisitions of ATSR-2/AATSR Band 1 (545-565nm) as $\rho_{\lambda,obs}$ i.e. as daily input. The feasible values for the SCAmod parameters (including the three reflectance constituents and transmissivity) are based on MODIS band 4 (550nm) reflectance observations and field spectroscopy. MODIS reflectance data are used in model parametrization due the narrow swath width of ATSR-2/AATSR which would drastically reduce the amount of suitable observations while MODIS provides daily global coverage. The ATSR-2/AATSR spectral bands used in GlobSnow SE product generation well correspond to the ones provided by MODIS, so this is considered a feasible approach.

5.2.4 Auxiliary data sets (Static)

A set of auxiliary data is used in SE processing:

- *The transmissivity map* is essential to SCAmod fractional snow computation. Transmissivity was first determined from MODIS reflectance acquisitions for several extensive 'training areas' in the Northern Hemisphere. For each area, transmissivity statistics (mean and standard deviation) were determined for the present GlobCover classes; these were then combined to obtain class-stratified values. Then the transmissivity for each 0.01º pixel was determined as a linear combination of class-wise average transmissivity and the occurrence of the corresponding classes in that pixel (4×4 GlobCover 0.0025º pixels in one GlobSnow grid cell).

- *The snow-free ground reflectance map* used by SCAmod is based on the GlobCover class-stratified average values for the MODIS-observed snow-free ground reflectance. For seasonally snow-covered areas in the Northern Hemisphere, the snow-free ground reflectance statistics were determined using MODIS reflectance observations and GlobSnow data for training areas in Europe and in North America. The observations representing post-melt (assumed mostly wet) snow-free ground were extracted from the MODIS reflectance time-series using methodology by Salminen et al., (2013). The extracted pixel-wise values were then related to the GlobCover data to generate class-stratified snow-free ground reflectance statistics.
- The provision of these data sets is part of the conducted research work in GlobSnow-2; the data are not publicly available.
- A more detailed description of the auxiliary data is given in Metsämäki et al., (2014).

Thematic masks are used in the GlobSnow SE processing system to 1) label areas where SE processing is not applied, such as oceans, and other open water areas and 2) to identify different kind of regions in the uncertainty calculations and 3) to derive the snow-free ground reflectance maps. The following masks are used:

- Open water mask
- Mask of mountainous areas (> 2 deg. local slope)
- Forest mask

The primary data sources for generating the masks are:

- Land cover maps from the GlobCover project with about 300 m pixel size (Bicheron et al., 2008).
- Digital elevation model (GETASSE30 DEM)

GETASSE30 stands for Global Earth Topography And Sea Surface Elevation at 30 arc second resolution. GETASSE30 is a composite of four DEM datasets. It is using the SRTM30 dataset, ACE dataset, Mean Sea Surface (MSS) data and the EGM96 ellipsoid as sources. The resulting GETASSE30 dataset represents the Earth Topography And Sea Surface Elevation with respect to the WGS84 ellipsoid at 30 arc second resolution. The GETASSE30 DEM is provided available at: http://www.brockmann-consult.de/beam/doc/help/visat/GETASSE30ElevationModel.html.

5.3 Quality and validation of product

The GLSSE product was extensively validated during the GlobSnow-2 project. The results are not published yet. The methodology used for validation was to directly compare at-pixel SCF estimates against i) in-situ SCF observations made at Finnish Snow courses ii) Snow Depth (SD) observations made at Finnish and Austrian weather stations (different threshold for both SCF and SD observations to classify pixel as 'snow' were tested) and iii) Landsat TM/ETM+ derived Fractional snow cover maps on pixel-by-pixel basis. Only reference data acquired or observed coincidently with the GLSSE product were used for assessing the product performance.

In-situ snow depth measurements were compared with binary snow maps generated from the GLSSE product using 50% and 15% to identify a pixel as snow covered, respectively. Additionally, the thresholds 1 cm and 15 cm were applied on the in-situ snow depth measurements to assimilate full snow cover for the associated GLSSE pixel. For describing the GLSSE performance based on the binary intercomparison with in-situ data, the statistical measures Hit Rate, Kuiper's Skill Score, Probability of Detection and False Alarm Ratio were used.

For generating snow maps from Landsat scenes, 4 different algorithms are applied: (1) the binary snow classification after Dozier and Painter (2004), (2) binary snow classification after Klein et al. (1998), (3) fractional snow cover classification after Salomonson and Appel (2004, 2006), (4) fractional snow cover classification by multi-spectral unmixing method with end-member selection for high-alpine, non-forested areas, and a binary snow classification for forested areas.

Intercomparisons of the GlobSnow DFSC product with snow maps from Landsat imagery were performed considering beside the total area the surface classes forest, non-forested areas, mountains, plains, and all combinations of mountains/plains with forested/non-forested areas, as well as different seasons, in particular for the main winter season from January to March, and for the melting season from April to June.

The statistical measures Root Mean Square Error, unbiased RMSE, Bias, and Correlation Coefficient were used to assess the performance of the GLSSE compared to the snow maps derived from the selected Landsat scenes. Overall, the quality of the GLSSE product compared with punctual or gridded reference data sets is within 15 % considering the total area covered by both data sets. For particular surface classes the accuracy of the GLSSE product compared to the reference data ranges between about 7 % and 22 %.

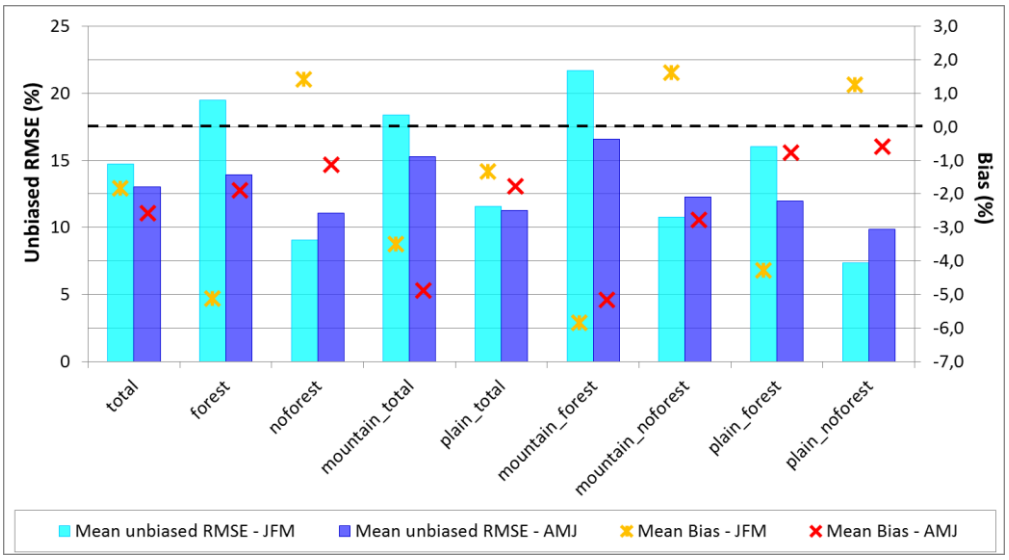

Figure 5.4: Mean unbiased Root Mean Square Error and Bias resulting from the intercomparison of 70 Landsat snow maps generated with different algorithms with the GlobSnow DFSC V2.1 product, considering different surface classes and distinguishing the results for the main winter season (January – March) and for the melting season (April – June).

In Figure 5.4 the mean statistical measures of unbiased RMSE and Bias, retrieved for the intercomparison of the GLSSE product with snow maps generated by applying the four different snow detection approaches on the selected Landsat scenes, are shown for different surface classes, and divided for the main winter season from January to March, and the main melting season, from April to June. As one might expect, smallest differences were found for plain non-forested areas, and largest differences were found for forested mountainous areas in both seasons.

5.4 Strength and weaknesses of product

Strengths of the GLSSE product:

- SCAmod reflectance model compensates the forest canopy effect on the observed reflectance and thus allows more accurate SCF retrieval in forested areas
- In many cases (but not persistently) the cloud detection over fractional snow areas performs relatively well i.e. fractional snow is not misclassified as cloud.

Weaknesses of the GLSSE product are:

- SCAmod reflectance model, when applying several pre-fixed parameters either as spatially varying or static values, is sensitive to the representativeness of these parameters.
- SCF retrieval is sensitive to the representativeness of the applied forest transmissivity; it is based on static land cover classification and thus dos not follow the possible changes in forest density/coverage.
- Data loss due to the gaps in the input data (ATSR-2 and AATSR have narrow swath width). This has strong implications to statistical calculations (e.g. to monthly statistics).
- A source of inaccuracy is the misclassification/outdated information in GlobCover, as the transmissivity map and snow-free ground reflectance map are generated using GlobCover to obtain the NH coverage.
- SCAmod is optimized for springtime (ablation) conditions, which is evident from the way the parameters are determined. The applied limitation for the sun zenith angle (max. 73º is accepted) in GlobSnow SE production, which limits the mapped area quite drastically during the late accumulation period and the high snow season in northern latitudes. However, this limitation is not crucial for snow mapping during the melting period in boreal forest and tundra zones, and of course has no impact on mid-latitude snow retrieval.

5.5 Contact

Institution	Finnish Environment Institute
Contact Person	Sari Metsämäki
Email	sari.metsamaki@environment.fi
Website for downloading the product:	http://www.globsnow.info/se/

5.6 References

Klein, A. G., Hall, D. K. & Riggs, G. A. (1998). Improving snow-cover mapping in forests through the use of a canopy reflectance model. Hydrological Processes, 12, 1723–1744.

Metsämäki, S., Anttila, S., Huttunen, M. and Vepsäläinen, J. (2005). A feasible method for fractional snow cover mapping in boreal zone based on a reflectance model. Remote Sensing of Environment, 95, 77-95.

Metsämäki, S., Mattila, O.-P., Pulliainen, J., Niemi, K., Luojus, K. and Böttcher, K. (2012). An optical reflectance model-based method for fractional snow cover mapping applicable to continental scale. Remote Sensing of Environment, 123, 508-521.

Metsämäki, S., Salminen, M., Pulliainen, J., Luojus, K., Nagler, T., Bippus, G., Solberg, R., Salberg, A.-B., Trier, O. D. & Wiesmann, A. (2014). Algorithm Theoretical Basis Document - SE-algorithm, GlobSnow-2 Deliverable-9 . Available at: http://www.globsnow.info/docs/GS2_SE_ATBD.pdf.

Metsämäki, S., Pulliainen, J., Salminen, M., Luojus, K., Wiesmann, A., Solberg, R., Böttcher, K., Hiltunen, M., Ripper, E. (2015). Introduction to GlobSnow SE-products with considerations for accuracy assessment. Remote Sensing of Environment, 156 (2015) 96–108.

Niemi, K., Metsämäki, S., Pulliainen, J., Suokanerva, H., Böttcher, K., Leppäranta, M. and Pellikka, P. (2012). The behaviour of mast-borne spectra in a snow-covered boreal forest. Remote Sensing of Environment, 124, 551-563.

Salminen, M., Pulliainen, J., Metsämäki, S., Kontu, A. and Suokanerva, H. (2009). The behaviour of snow and snow-free surface reflectance in boreal forests: Implications to the performance of snow covered area monitoring. Remote Sensing of Environment, 113, 907-918.

Salminen, M., Pulliainen, J., Metsämäki, S., Böttcher, K. and Heinilä, K. (2013). MODIS-derived snow-free ground reflectance statistics of selected Eurasian non-forested land cover types for the application of estimating fractional snow cover. Remote Sensing of Environment, 138, 51-64.

6. GLOBAL MULTISENSOR AUTIMATED SNOW AND ICE MAPS- GMASI (ASNOW)

Author: Peter Romanov (NOAA USA)

6.1 Product overview and specification

Global Multisensor Automated Snow and Ice (GMASI) Maps provide spatially continuous (gap-free) characterization of the global snow and ice cover distribution at 4 km spatial resolution. Snow and ice maps are generated daily using a fully-automated unsupervised data processing algorithm. The retrieval technique is based on a synergy of snow and ice retrievals from satellite observations in the visible/infrared and microwave spectral bands. The primary input to the system is provided by the Advanced Very High Resolution Radiometer (AVHRR) on-board NOAA and METOP satellites and by Special Sensor Microwave Imager/Sounder instruments on-board DMSP satellites. The system is also capable of processing and assimilating in the product of snow and ice retrievals from geostationary satellites GOES and Meteosat Second Generation (MSG). The output product is a binary snow/ice maps where every “land” pixel is labelled as either “snow” or “snow-free land surface” and every “water” pixel is labelled as either “ice-free water” or “ice”. No estimates of the subpixel snow fraction and subpixel ice fraction/concentration are performed.

The primary intent behind the development of the GMASI system was to routinely provide up-to-date information on snow and ice for NOAA operational applications, particularly for Numerical Weather Prediction (NWP) models and interactive snow/ice analysis. Therefore, the system is built to use data only from operational meteorological satellites and is designed to ensure near-real time data processing and product generation. The system was first implemented into operations at NESDIS in the end of 2005. Changes to the system were mostly related to changes in available operational satellite instruments. The archived product presents the output of the operational algorithm. No reprocessing of the data has been performed.

Since the focus of this project is on the snow cover, the following review covers mostly the snow portion of the GMASI algorithms and output product.

Table 6.1:
Summary of GMASI global snow cover product.

Parameter	*Specification*
Thematic variable	Binary Snow Cover (BSC)
Thematic resolution	0/1
Thematic range	[0,1] Binary Snow Cover
Thematic accuracy	~80-90% agreement with in situ observations
Thematic uncertainty	10-15% per pixel
Product Quality Map	Not available
Spatial resolution	0.04° × 0.04° (ca 4km)
Spatial coverage	Global
Product available since	Daily products, since January 2006
Delivery time period	Full Year, daily
Temporal frequency	Daily
Projection/Datum	Geographical (lat/lon) / WGS84
Cloud Screening	Built in the AVHRR data processing algorithm
Invalid / Masked Areas	Open Water (sea, lakes, rivers)
Sensor	AVHRR (NOAA, METOP), SSMI/SSMIS (DMSP F-15, ….-19), Imager (GOES), SEVIR (MSG)I
Satellite data level	Level 1B Swath data
Output File format	GeoTIFF, flat binary
Developed by	NOAA/NESDIS
Provider / Generated by	NOAA/NESDIS
Product available at	ftp://ftp.star.nesdis.noaa.gov/pub/smcd/emb/snow/binary/multisensor/global
Contact	Peter Romanov / NOAA / peter.romanov@noaa.gov

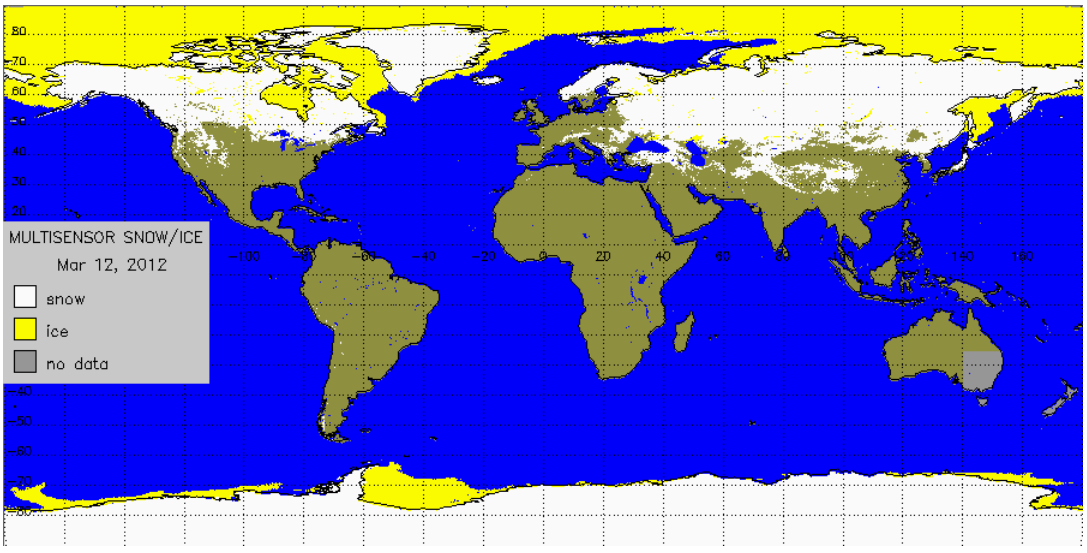

Figure 6.1: Example of GMASI binary snow/ice product, 9 March 2012.

6.2 Processing line and algorithm

The principal approach to the snow and ice cover mapping within the GMASI system consists in the use of synergy of satellite observations in the visible/infrared and in the microwave spectral bands from operational meteorological polar orbiting and geostationary satellites. In the algorithm we tried to make maximum use of strengths of both types of remote sensing observations (visible/infrared and microwave) and to most efficiently compensate for their weaknesses. A brief description of the algorithm and its main processing stages with the focus on snow cover retrievals is presented in this section. A detailed description is provided in the system Algorithm Theoretical Basis Document at www.star.nesdis.noaa.gov/smcd/emb/snow/documents/Global_Auto_Snow-Ice_4km_ATBD.pdf

Figure 6.2 presents the system level and the detailed processing flow of GMASI. Within the current configuration the primary input to the system includes calibrated and navigated (level 1B) data from METOP AVHRR, GOES-E and –W Imager, MSG SEVIRI and from all operational SSMIS sensors on-board DMSP satellites (currently operational are F-16, -17, -18 and -19). Several auxiliary datasets are used to improve the classification accuracy and to make snow/ice identification and mapping more reliable. The system output consists of a global blended snow and ice cover map (which is the primary product of the system) and a processing log file containing run-time service messages.

Within the system, daily observations from each satellite sensor are processed separately and corresponding individual daily maps of snow and ice cover are derived (see the system level processing chart in Figure 6.2, right). Daily retrievals made with two groups of sensors (optical/infrared and microwave) are then merged to generate corresponding two snow/ice maps. At the next step daily visible/infrared and microwave snow/ice maps are combined into a blended product which provides near-continuous spatial coverage of the area. Lastly, a recurrent gap-filling technique is applied to provide a full spatial continuity of the daily blended product. Execution of these steps yields a global, continuous (gap-free) daily map of snow and ice cover extent. Maps are generated daily on a latitude-longitude equal angle (Plate Carree) grid with about 4 km (0.04^0 x 0.04^0) grid cell size.

The system is set to continuously collect and pre-process incoming satellite observations throughout the day. The final processing of satellite observations and the snow/ice map generation is performed once a day and incorporates satellite data acquired within the 24-hour time period (0000- 2359UTC). It is set to start several hours past the end of the calendar day to allow for a possible delay in the satellite data delivery. The output daily snow and ice map typically becomes available at 1100-1200UTC the next day.

Particular algorithms applied to derive information on the snow cover from different satellite sensor data and to combine retrievals in one blended product are presented in more detail in the following sections of the document.

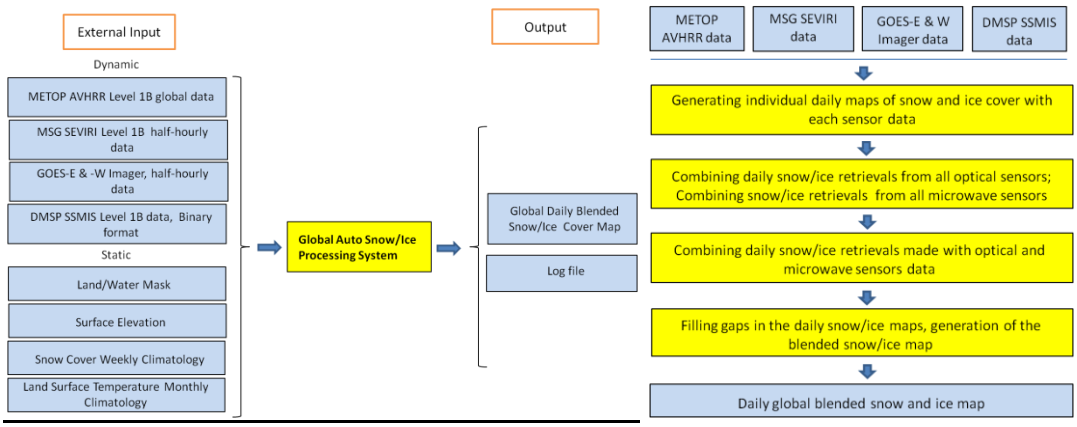

Figure 6.2: System level processing flow of GMASI system (left) and detailed processing line (right).

6.2.1 Snow mapping algorithms (visible/infrared and microwave)

Within GMASI system snow and ice in satellite imagery are identified and mapped using sensor-specific image classification algorithms. These algorithms are presented below.

6.2.1.1 Snow mapping with satellite observations in optical and infrared spectral bands

Snow mapping with satellite observations in the visible and infrared spectral bands is conducted only over geographical areas where a sizeable amount of snow cover may be present and seasonal variations of the snow extent are expected. In the Northern Hemisphere snow cover is mapped north of 25N latitude everywhere in North America (including Greenland), Eurasia and in Africa. In the Southern hemisphere areas where snow cover is mapped include the Western part of South America (west of 60W longitude within 55S to 20N latitudes), the Southern part of Africa (south of 24S latitude) and South-East Australia and New Zealand. The rest of the globe is assumed snow free in all seasons except of the Antarctic continent, which is assumed permanently snow covered. Therefore, snow is not in these latter regions.

The snow mapping algorithm applied to satellite observations in the visible and infrared involves two stages, the preliminary spectral-based image classification and a series of consistency tests to identify and exclude from the further consideration questionable snow retrievals.

The preliminary snow identification algorithm applied to AVHRR data generally follows the line of snow detection algorithms developed earlier for MODIS, AVHRR, MSG SEVIRI, and GOES Imager instrument data (e.g., Hall et al, 2002, Baum and Trepte, 1999, Romanov et al, 1999). It relies on the calculated value of the Normalized Difference Snow Index (NDSI), the Normalized Difference Vegetation Index (NDVI) two Snow Indices expressed as a ratio of reflectances in AVHRR bands 1 and 3a (SI1) and bands 2 and 3a (SI2) along with the observed brightness temperature in band 4 (T4) and reflectances in bands 1,2 and 3a (R1, R2 and R3). High NDSI, high SI1 values along with relatively low infrared brightness temperature in ch.4, low SI2 and low NDVI are the primary indicators of the presence of snow within the instrument field of view.

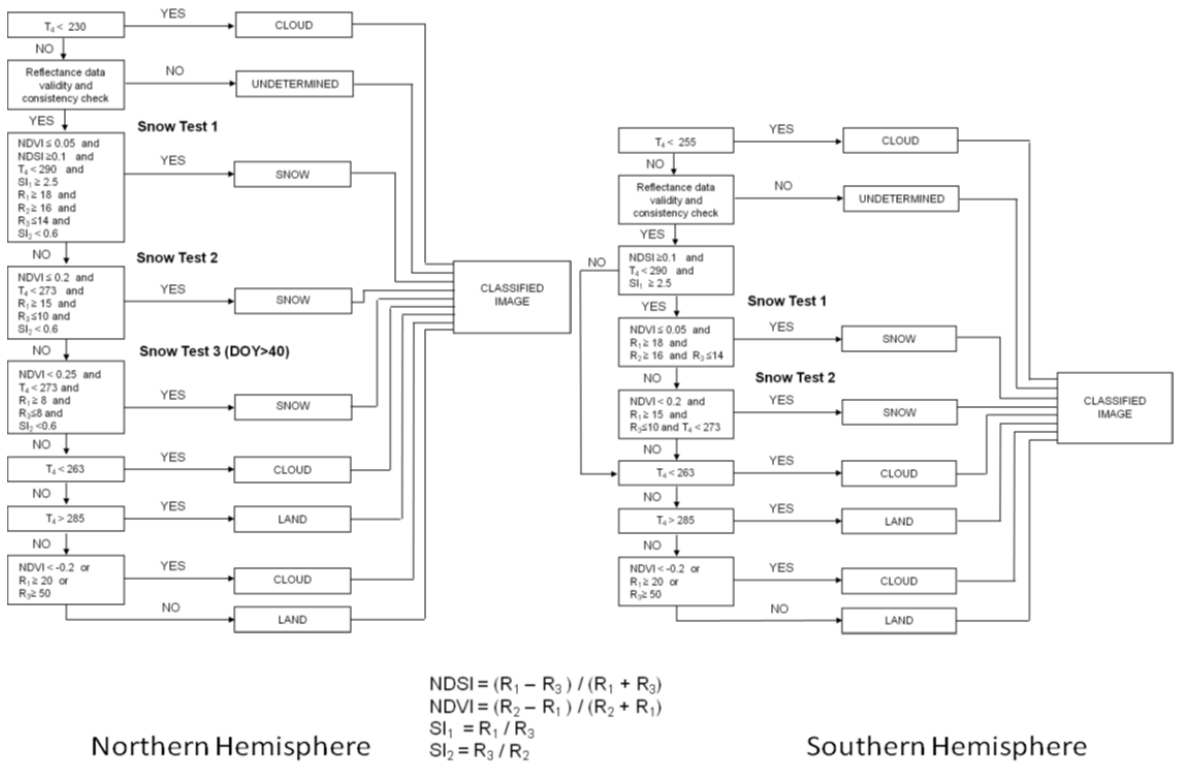

Figure 6.3: Flow chart of the AVHRR spectral-based image classification algorithm over land. Left: Northern Hemisphere, Right: Southern Hemisphere. Threshold values are given in degrees K for the brightness temperature and in percent for the reflectance

The AVHRR image spectral classification algorithm is a threshold-based decision-tree algorithm which is applied on a pixel-by-pixel basis. The algorithm first attempts to identify snow-covered pixels and then labels the remaining pixels as either “snow-free land surface” or “cloud”. Image classification algorithms applied over Northern and Southern Hemisphere are generally similar, but have minor differences accounting for different physio-geographic and climatic characteristics of areas affected by the seasonal snow cover in the two hemispheres. Figure 6.3 shows the flow-chart of AVHRR snow identification algorithm.

Pixels labelled as “Snow covered” by the spectral image classification algorithm are then subjected to a series of additional tests aimed to identify unreliable or possibly spurious snow retrievals. These tests label as “unreliable” (1) snow identified in pixels next clouds, (2) isolated “snow” pixels and (3) small clusters of “snow” pixels in the midst of clouds, (4) “snow” pixels with the infrared brightness temperature much colder than the climatic temperature value for this location and time of the year and (5) “snow” pixels with the infrared brightness temperature much colder than other clear sky pixels in the close proximity. Test (4) and (5) are applied only outside of mountainous areas. Failure to satisfy any of these tests results in the pixel being classified as “unconfirmed snow” and treated in the further processing in the same way as “cloudy” pixels.

Snow mapping algorithms applied to geostationary satellites data utilize all daytime imagery available during the day. Prior to classification and consistency testing all daytime images are composited by retaining in every grid cell observation with the maximum infrared brightness temperature. This compositing helps to reduce the cloud contamination of the imagery and thus to improve the effective area coverage of the snow product. Multiple daytime imagery available from geostationary satellite data is also used to assess temporal variations of the scene spectral response and thus to improve snow/cloud discrimination (Romanov, 2005). The spectral classification algorithm and consistency tests applied to the daily composited images from geostationary satellites are similar to the ones used with AVHRR data.

If snow maps derived from both METOP AVHRR and any geostationary satellite (GOES-E, -W or MSG) over the same area are available, a combined snow map is produced which incorporates all AVHRR-based clear sky retrievals and where clear sky retrievals from geostationary satellites replace “cloudy” grid cells in the AVHRR-based daily snow map. Priority is given to the polar-orbiting satellite retrievals due to their better effective spatial resolution over mid and high-latitude areas and generally better image navigation.

6.2.1.2 Snow mapping with satellite observations in the microwave

Microwave algorithms to identify snow and ice incorporated in the system utilize daily observations from all available SSMIS sensors both at the ascending and descending node. Repeated observations during the day from multiple DMSP satellites allow for more reliable and accurate snow and ice cover mapping. At the time of writing SSMIS observations were provided from four operational DMSP satellites F-16, -17, 18 and -19. Observations from multiple SSMIS and/or older SSM/I instruments were also available for most of the last 15-years time period.

Snow cover in the SSMIS imagery is identified and mapped using the algorithm of Grody and Basist, (1996). The algorithm utilizes SSM/I observations of the brightness temperature at 22, 37 and 85 GHz frequency at vertical polarization and at 19 GHz at both vertical and horizontal polarization. The original threshold values were modified to account for the difference between corresponding SSM/I and SSMIS spectral bands reported by Yan and Weng, (2008). Image classification is applied to SSMIS daily observations brought to a latitude/longitude equal angle projection at 1/3 degree grid cell size. Data collected on the descending and ascending node of each DMSP are processed separately, therefore two daily snow maps become available from each sensor.

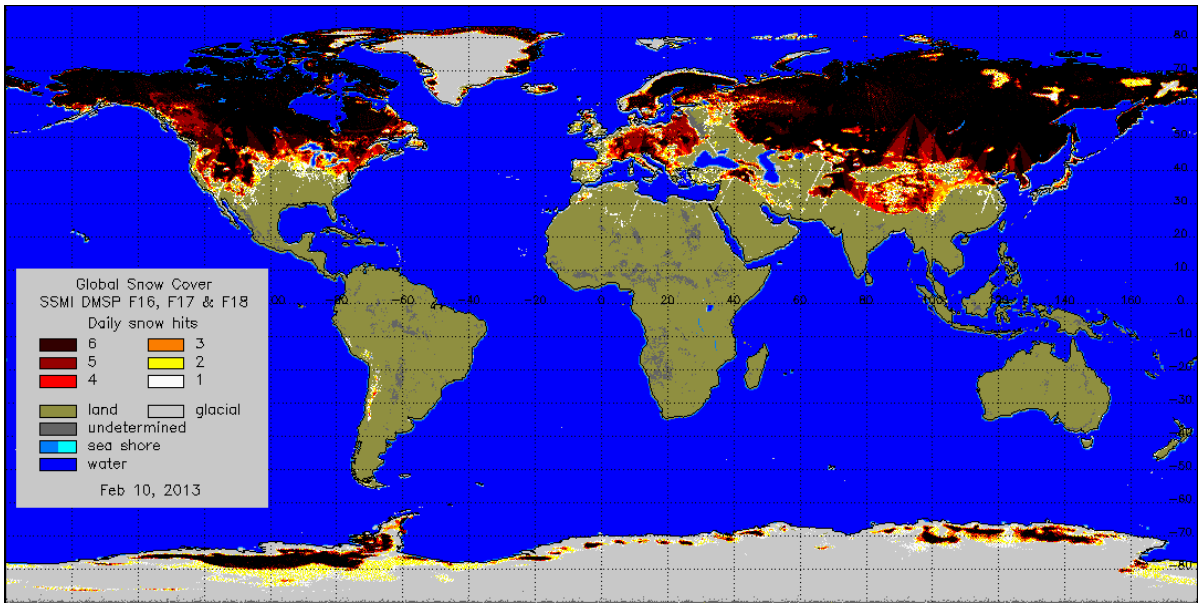

Figure 6.4: Example of the map of the daily number of positive snow identifications (or "snow hits") with SSMIS sensors onboard operational DMSP satellites

Individual snow maps acquired from the data of all SSMIS sensors at two nodes are then combined into one map which presents the number of positive snow identifications ("snow hits") during the day. An example of this map is shown in Figure 6.4. To account for possible snow identification errors due to the instrument noise or atmospheric effects (e.g. undetected precipitating clouds) only snow cover identified in a given grid cell in more than half of all observations or more than 3 times during the day is labelled as "confirmed snow" and is further used in the system.

6.2.2 Blending Approach and Algorithm

At the next stage of the data processing individual daily snow maps based on the data from visible/infrared and microwave sensors are combined. The general approach to combining snow observations utilizes the following basic principles. First, it gives priority to snow retrievals in the visible and infrared as more accurate, reliable and spatially detailed than retrievals from microwave data. A similar approach is also used in the combined MODIS and AMSR-E snow mapping algorithm of Foster et al., (2011). Second, because of known physical limitations of snow remote sensing in the microwave, a cautious approach is adopted with respect to the use of microwave retrievals. In particular, due to the difficulty detecting melting and shallow snow cover, all "no snow" identifications in the SSMIS-based snow map are considered unreliable and are not used in the blended product. Also, in most cases SSMIS observations are not used in the mountains because of their known problem to properly discriminate between snow cover and cold rocky surfaces. Third, the decision on whether to incorporate the snow cover mapped in contributing maps into the blended product depends on the snow cover climatology, surface elevation and vegetation cover type. In particular, a cautious approach to the use of snow cover mapped in both products is followed in regions where the probability of snow cover for the given time of the year was small. On the opposite, snow cover mapped in either contributing product is incorporated in the blended map if snow cover in this region and given time of the year was always observed in the past. Snow cover climatology in the system is characterized by the weekly snow cover probability of occurrence dataset which was derived from historical NOAA interactive snow and ice charts. For details of the developed blending algorithm see the GMASI system ATBD (Romanov, 2014).

It is important that although microwave-based snow retrievals are performed globally, within the system they a set to contribute to the blended snow map only in the Northern Hemisphere. In the Southern Hemisphere snow is mostly confined to mountainous areas, and over plain low-elevation areas it is most often shallow or melting. The performance of microwave snow detection algorithms in

all these cases is not reliable therefore incorporation of microwave retrievals is very likely to bring substantial errors to the blended product.

Due to a cautious use of information derived from microwave sensors and gaps in the area coverage of visible/infrared snow products due to clouds, some grid cells in the daily blended visible/infrared and microwave snow map may not be updated every day and are therefore left undetermined. To fill in these gaps and to achieve the spatial continuity of the daily snow product a recurrent gap-filling approach is applied. Within this approach undetermined grid cells in the daily blended snow map are filled in with the data from the previous-day blended product. This approach clearly brings certain inertia to characterization of changes in the snow and ice cover distribution, but provides a gap free coverage of the area which is very important for numerical model applications.

6.2.3 Input Data

The current input to the system consists of level 1b data (calibrated navigated radiances) of METOP AVHRR along with DMSP F-16, -17, -18, and -19. The system is also capable of processing observations from GOES-E and -W and MSG geostationary satellites and adding snow retrievals from these sensors to the blended product. However, at the time of writing this part of the system was deactivated since it was determined that contribution of geostationary sensors to the system output was disproportionally small compared to efforts needed to maintain geostationary data collection, process the data, provide the retrievals quality control, routinely cross-calibrate the radiances and ensure consistency of snow retrievals from geostationary satellite sensors with polar-orbiting sensors data.

6.2.4 Auxiliary Data Sets

Several auxiliary datasets are used in the algorithm. This includes the land-water mask and the fractional tree cover dataset based on the University of Maryland 1-km land surface cover type classification and forest fraction data (http://www.glcf.umd.edu/data/landcover/), surface elevation dataset based on the United States Geological Survey (USGS) GTOPO30 model (http://eros.usgs.gov/#/Find_Data/Products_and_Data_Available/GTOPO30), monthly land surface temperature climatology dataset based on the data of the International Satellite Cloud Climatology Project (ISCCP) available at ftp://isccp.giss.nasa.gov/pub/data/surface/ and weekly snow cover occurrence climatology derived from NOAA Interactive Snow and Ice charts for the period from 1972 to 1998 (http://nsidc.org/data/docs/noaa/g02156_ims_snow_ice_analysis/).

6.3 Quality and Validation of Product

Validation of GMASI snow cover product is performed routinely via comparison with in situ snow depth observations and with snow charts generated interactively within the NOAA Interactive Multisensor Snow and ice Mapping System (IMS)

6.3.1 Validation with NOAA Interactive Snow Maps (IMS)

Comparison of the automated snow maps with IMS snow products is performed over Northern Hemisphere. For qualitative evaluation of the agreement between the two products an overlay of the two maps is generated. Figure 6.5 shows as an example a GMASI-IMS overlaid snow map. Quantitative evaluation of the automated product is performed by comparing the two maps pixel-by-pixel and aggregating the statistics on a daily basis.

In the last years the yearly mean agreement between the two datasets remains at about 96%. It improves by about 3% in late summer and decreases approximately by the same value in the fall season. This behaviour is seen in the graphs in Figure 6.5 (right) showing the time series of daily estimates of the percent of correspondence and disagreement between GMASI and IMS snow maps over Northern Hemisphere from the end of 2013 to the end of 2014.

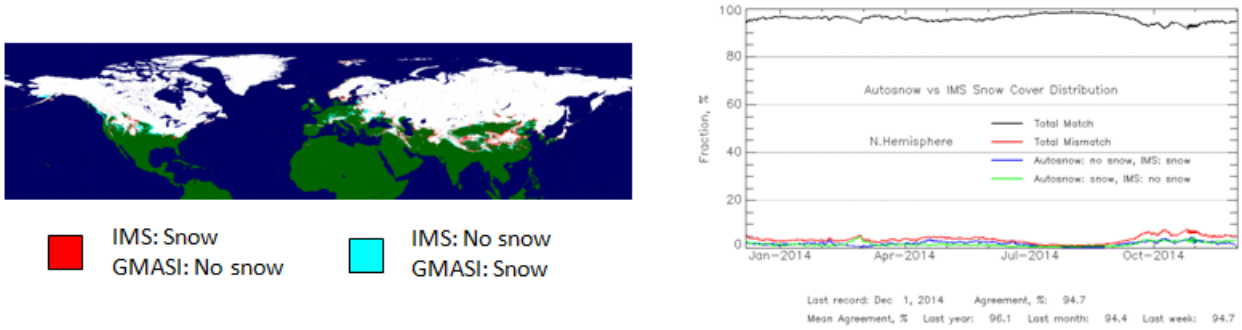

Figure 6.5: Validation of GMASI snow maps with NOAA interactive snow and ice charts (IMS). Left: Example of GMASI daily snow map with IMS snow map overlaid over Northern Hemisphere. Right: Agreement and disagreement statistics between daily GMASI and IMS snow maps during the year of 2014.

Considering IMS product as truth, GMASI commission and omission errors are generally well balanced throughout the year. The only exception presents the month of April when the probability of omission error is about two times larger than commission error. This corresponds to the time of the year when

the snow cover boundary line both in North America and Eurasia is located mostly in the boreal forest zone and thus may be associated with the difficulty of detecting melting snow on the forest floor.

Comparison of the two products also revealed their good agreement with respect to the estimated large-scale snow cover area extent. The mean daily difference in the estimated snow extent both over Eurasia and North America ranges within 3-4% but decreases to about 2% and less than 1.5% for monthly mean and yearly mean values correspondingly.

6.3.2 Validation with in situ snow observations

GMASI snow cover maps are routinely compared to snow cover observations conducted at ground-based meteorological stations. The comparison is limited to the Northern Hemisphere since in the Southern Hemisphere snow cover is observed only at few meteorological station and snow reports are issued quite irregularly. Practically the comparison of GMASI and station data is mostly confined to the Continental US (CONUS) region in North America, which is densely covered by the network of US Cooperative Stations. In contrast to stations under the auspices of the World Meteorological Organization (WMO), US Cooperative stations explicitly report “zero” snow depth when there is no snow on the ground and therefore can be used to produce a full statistics of comparison including the fraction of “true positives”, “true negatives”, “false positives” and “false negatives”.

To allow for an easy qualitative evaluation of the consistency of automated snow maps, the system generates daily satellite snow map images with station data overlaid. An example of the GMASI snow map over Continental US (CONUS) area with overlaid station data on the snow cover is presented in Figure 6.5. Quantitative comparison of the satellite snow product with station data is performed by matching in situ observation data with the status of collocated grid cells in the snow cover map. Since most WMO and US Cooperative stations are located in mid-latitudes, the most consistent estimates of the correspondence between the two datasets are obtained in the middle of the winter season when the portion of stations reporting no snow on the ground and at least some snow on the ground is approximately equal. Estimates made during the last several years show that in the middle of the winter season the agreement between automated snow maps and station data typically ranges within 80%-90%. In late spring, summer, and early fall when the area is mostly snow free the agreement is close to 100%. The yearly mean agreement of automated snow maps to surface observations over CONUS amounts 91.4%, which is about 1% below the accuracy of the IMS snow product.

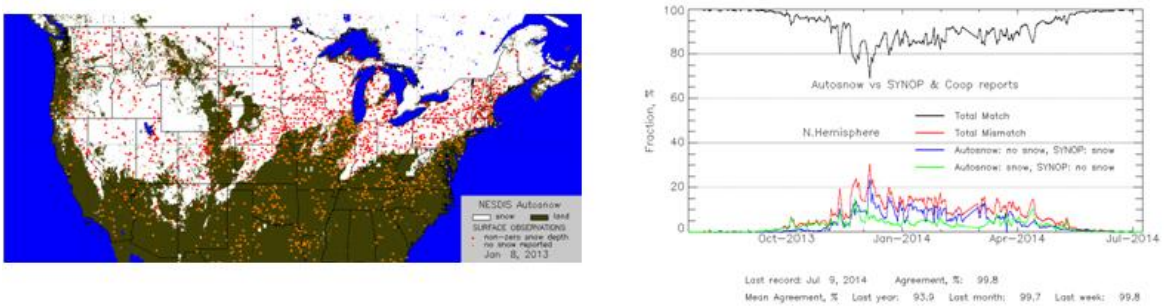

Figure 6.6: Validation of GMASI snow maps with ground-based station data. Left: Example of GMASI daily snow map over Conterminous US (CONUS) with station data overlaid. Right: Agreement and disagreement statistics between daily GMASI and in situ observations in the Northern Hemisphere during the winter season of 2013-2014.

6.4 Strengths and weaknesses of product

The principal strength of the product consists in a spatially continuous characterization of the snow cover distribution combined with high accuracy, daily updates of the map and its high, 4 km nominal spatial resolution. Continuity and daily updates are extremely important for numerical model applications both research and operational. It should be noted that the system is operational and is meant to generate the product routinely in the near-real time mode.

The system is expected to provide a better accuracy of snow identification in cloudy conditions as compared to other existing microwave-based products. This is due to the use of multiple observations per day from several operational DMSP sensors in the GMASI system rather than data from a single instrument and (most often) from a single overpass in other available products.

Improved snow cover characterization by visible/infrared sensors incorporated in the GMASI system is also expected due to the use of the cloud mask specifically tuned for mapping snow cover. This is different from MODIS and current VIIRS data processing systems system where the provided cloud mask is more generic and is developed to fit all derived land surface and atmospheric products.

One of the weaknesses inherent to the product is inertia in reproducing changes in the snow and ice cover distribution. It occurs due to inability of both techniques incorporated in the system to deliver reliable snow retrievals in certain situations (e.g. over precipitating clouds) and due to the use of the recurrent gap-filling approach to ensure a spatially continuous characterization of the snow cover distribution. This inertia may be the cause for both snow cover overestimates and underestimates in the daily product.

It is important that within the adopted blending algorithm possible snow identification errors if occur in the blended daily map may propagate into one or sometimes several subsequent daily products. The use of consistency tests in addition to spectral-based image classification algorithms in snow retrievals from all sensors is meant to reduce the chance of snow identification errors in individual snow products and, hence in the blended snow map, however this possibility cannot be excluded completely.

6.5 Contact

Institution	NOAA/NESDIS Office of Satellite Applications and Research (STAR)
Contact Person	Peter Romanov
Email	Peter.Romanov@noaa.gov
Website for downloading the product:	ftp://ftp.star.nesdis.noaa.gov/pub/smcd/emb/snow/binary/multisensor/global

6.6 References

Baum, B. A., and Q. Trepte, (1999) A grouper threshold approach for scene identification in AVHRR imagery. J. Atmos. OceanicTechnol., 16, 793–800.

Foster, J.L., D.K. Hall, J.B. Eylander, G.A. Riggs, S.V. Nghiem, M. Tedesco, E.J. Kim, P.M. Montesano, R.E.J. Kelly, K.A. Casey and B. Choudhury, (2011) A blended global snow product using visible, passive microwave and scatterometer data, International Journal of Remote Sensing. 32(5):1371-1395. doi.org/10.1080/01431160903548013.

Grody N.C. and A. N. Basist (1996) Global identification of snowcover using SSM/I measurements. IEEE Transactions on Geoscience and Remote Sensing, 34, 237–249.

Hall, D.K., G.A. Riggs, V.V. Salomonson, N. DiGiromamo and K.J. Bayr, 2002: "MODIS Snow-Cover Products," Remote Sensing of Environment, 83:181-194.

Romanov, P., Tarpley, D. (2005) Monitoring snow cover over Europe with Meteosat SEVIRI, in: Proceedings of the 2005 Eumetsat Meteorological Satellite Conference P.46, pp. 282–287, 2005.

Romanov P., D.Tarpley (2003) Automated monitoring of snow cover over South America using GOES Imager data. International Journal of Remote Sensing, 24, 1119-1125.

Romanov P., G. Gutman, and I. Csiszar (2000) Automated monitoring of snow cover over North America with multispectral satellite data, Journal of Applied Meteorology, 39, 1866-1880.

Romanov P. (2014) Global 4km Multisensor Automated Snow/Ice Map (GMASI): Algorithm Theoretical Basis Document. NOAA NESDIS Center for Satellite Applications and Research, September 2014, 60 p., http://www.star.nesdis.noaa.gov/smcd/emb/snow/documents/Global_Auto_Snow-Ice_4km_ATBD.pdf

Yan, B., & Weng, F. (2008). Intercalibration between Special Sensor Microwave Imager/Sounder and Special Sensor Microwave Imager. Geoscience and Remote Sensing, IEEE Transactions on, 46(4), 984-995.

7. NOAA IMS

7.1 Product overview and specification

Documentations of the NOAA IMS products are online available from http://www.natice.noaa.gov/ims/files/ims-hydro-proc-ramsay-1998.pdf and http://www.natice.noaa.gov/ims/files/ramsayESC57.pdf.

7.2 Processing line and algorithm

Processing lines and algorithms of the NOAA IMS products are described in the following publications:

- Helfrich, S. R., M. Li, and C. Kongoli. 2012. Interactive Multisensor Snow and Ice Mapping System Version 3 (IMS V3) Algorithm theoretical basis document version 2.1. Noaa NESDIS Center for Satellite Applications and Research (STAR). 61 pp.
- Helfrich, S. R., D. McNamara, B. H. Ramsay, T. Baldwin, and T. Kasheta. 2007. Enhancements to, and forthcoming developments to the Interactive Multisensor Snow and Ice Mapping System (IMS), *Hydrological Processes* 21: 12, 1576-1586.

Further references and related publications can be found online at http://nsidc.org/data/docs/noaa/g02156_ims_snow_ice_analysis/#references.

7.3 Contact

Institution	NOAA
Contact Person	Sean Helfrich
Email	sean.helfrich@noaa.gov
Website for downloading the product:	http://nsidc.org/data/docs/noaa/g02156_ims_snow_ice_analysis/ www.natice.noaa.gov/ims/

8. CRYOCLIM

Author: Rune Solberg (Norwegian Computing Center, Norway)

8.1 Product Overview and Specification

The snow product was developed by the Norwegian Computing Center (NR) and the Norwegian Meteorological Institute (MET Norway) together, and the service is delivered operationally by MET Norway. The product is based on fusion of optical and passive radiometer data based on a multi-sensor multi-temporal algorithm.

Table 8.1:
Summary on CryoClim snow cover product.

Parameter	***Specification***
Thematic variable	Snow Cover Extent
Thematic resolution	Binary
Thematic range	[0,1] = no snow, 1 snow
Thematic accuracy	~92%
Thematic uncertainty estimate	Under development
Product Quality Map	Under development
Spatial resolution	5 km
Spatial coverage	Global (provided as two maps: Northern Hemisphere and Southern Hemisphere)
Product available since	January 1982
Delivery time period	Full year
Temporal frequency	Daily
Projection/Datum	EASE-Grid 2.0 / WGS 84
Cloud Screening	Bayesian classification in optical component
Invalid / Masked Areas	Open Water (sea, lakes, rivers)
Sensor	AVHRR, SMMR, SSM/I
Satellite data level	Level 1B
File format	NetCDF CF
Developed by	NR and MET Norway
Provider / Generated by	MET Norway
Product available at	http://www.cryoclim.net
Contact	Rune Solberg, NR, rune.solberg@nr.no (algorithm) Service helpdesk: cryoclim@cryoclim.net

The multi-sensor multi-temporal approach is based on a hidden Markov model (HMM) simulating the snow states based on observations with PMR and optical sensors. The basic idea is to simulate the states the snow surface goes through during the snow season with a state model. The states are not directly observable, but the remote sensing observations give data describing the snow conditions, which are related to the snow states. The HMM solution represents not only a multi-sensor model but also a multi-temporal model. The sequence of states over time is required to follow certain optimisation criteria.

The approach for the use of passive microwave radiometer (PMR) data has been based on derivation of a set of features based on the sensor channels and estimation of probability density functions (PDFs) for a set of snow classes further stratified for a set of land cover classes. For SSM/I four snow classes were defined, and for SMMR two classes. For the optical data the three classes snow, snow-free or cloud were applied. The data applied is AVHRR GAC.

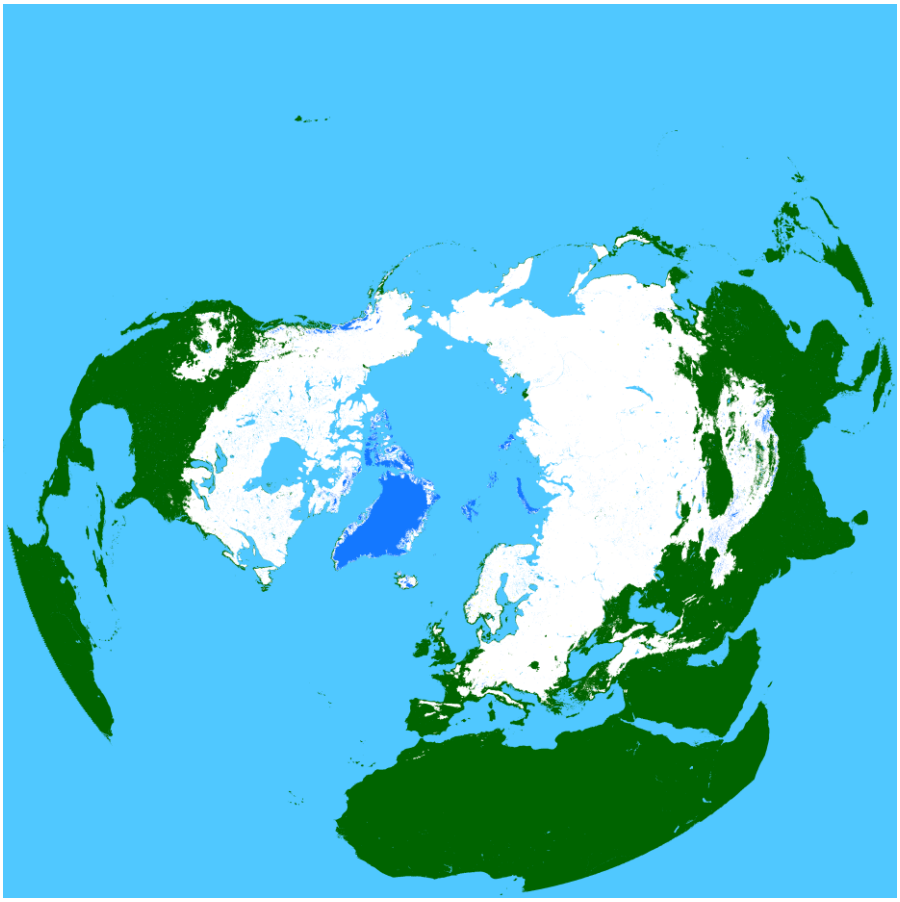

Figure 8.1: CryoClim snow cover product for the Northern Hemisphere, 1 March 2005.

8.2 Processing chain and algorithm

The approach chosen for sensor fusion is inspired from ideas developed by Solberg et al. (2008) where optical and SAR sensor data were fused. The basic idea is to simulate the states the snow surface goes through during the snow season with a state model. The states are not directly observable, but the remote sensing observations give data describing the snow conditions, which are related to the snow states.

8.2.1 Single-sensor algorithms for snow probabilities

The approach for the development of a passive microwave radiometer (PMR) snow cover extent (SCE) algorithm has been based on a Bayesian estimation rule. For SSM/I four snow classes were defined in order to model the SCE: (i) wet snow, (ii) dry snow, (iii) no-snow and (iv) no-snow with a large fraction of nearby water. For SMMR the two snow classes, snow and no-snow, were considered. The algorithm estimates the probability for each snow class given the PMR measurements.

The SSM/I algorithm was trained using SYNOP data on snow depth and temperature, whereas the SMMR algorithm was trained using GHCN-D data on snow depth. To improve the performance of the Bayesian algorithm we used land cover data. This allowed us to construct a Bayesian estimator for each land cover regime, and thereby estimate the snow class probabilities using an estimator consistent with the land cover corresponding to the measurement under investigation.

The optical snow cover algorithm builds on previous development where a framework for probabilistic classification of sea ice using optical satellite data was developed. The methodology builds on Bayes approach combining information from visual and infrared AVHRR channels. Land pixels are assigned to the classes snow, snow-free or cloud. Probabilities for the three independent classes are estimated for all land pixels of the sensor's swath. The cloud masking and the identification of snow cover are thus done in the same operation.

8.2.2 Hidden Markov model algorithm for sensor fusion

We have chosen a hidden Markov model (HMM) to model the snow states and their connection to the observations. HMM is building on statistical theory making it possible to establish a sound probabilistic model derived from observational data (Baum and Petrie, 1966). Note that the HMM solution represents not only a multi-sensor model but also a multi-temporal model. The sequence of states over time is required to follow certain optimisation criteria. Note also that the HMM model is applied per pixel, so each pixel's history through the snow season is modelled.

We model five basic state types in the model: 1) Snow, a seasonal snowpack consisting of a persisting snow layer that will only melt away over a period of time; 2) Temporary snow, a thin snow layer that easily melts away; 3) Wet snow, a state that may occur any time with a snowpack present, only observable with PMR data; 4) Cloud shadow, a moderate reduction of the snow cover as estimated from the optical data only 5) Patchy snow, one or several states with 0% < FSC < 100%, only observable with optical data; and 6) Snow free, only bare ground present.

A HMM is established for each grid cell (pixel) in the snow product. For each time step (day) the whole time sequence of states is recalculated to find the most likely sequence of HMM states (using the Viterbi algorithm) from the start (usually the summer). Single-sensor probabilities for snow based on Bayesian retrieval algorithms go into the HMM scheme as observations.

With HMM, the notion of a class from the classification literature becomes the notion of a model in the HMM formalism. Traditionally, ground-cover classification in a temporal sequence of satellite images is the problem of assigning each pixel in the scene to a class based on this pixel's signal properties (or derived properties). In the HMM case, our aim is to assign each pixel to the model that best explains the observed temporal evolution of the pixel. Solutions to this kind of problem are important in many applications and several algorithms are available. For our problem we have chosen to use the Viterbi algorithm.

The Viterbi algorithm is a dynamic-programming algorithm for finding the most likely sequence of hidden states (the Viterbi path) that result in a sequence of the observables. The Viterbi algorithm was proposed by Viterbi (1967) as a decoding algorithm for convolutional codes over noisy digital communication links. The algorithm requires as input the state probability density functions, the transition probabilities between the different states and the initial probability of each state.

The initial probabilities for each state and the transition probabilities are clearly dependent on the season. For example, the probability of having snow (initial probability) or the probability of changing from bare ground to snow cover (transition probability) are clearly higher in the winter than in the summer. Therefore, we defined a basic time-dependent probability for snow. This is used to experimentally determine the initial probabilities. Furthermore, we defined four basic transition probabilities which are found experimentally.

The state probability density functions are found from the time series of PMR-based snow products. One year of snow probability maps results in a time series of snow probability for each day of the year for each pixel in the map. Such a time series reflects quite well the time dependency of the local snow probability. These time series are however, quite noisy. This is both due to local weather fluctuations

and estimation errors. In order to extract the overall trend reflecting the "seasonal probability" these probabilities are smoothed using a finite impulse response (FIR) filter. The FIR filter is a Savitzky-Golay smoothing filter (Savitsky and Golay, 1964; Schafer, 2011). The approach yields an estimated snow probability for every pixel in the data for every day of the year.

8.2.3 Processing chain

The overall processing flow for constructing the snow cover extent probabilities for PMR consists of importing the SSM/I data and land cover data and reading the PDF parameters for each snow class (Figure 8.2). Then the snow probability of each SSM/I observation is calculated for each SSM/I swath. The snow probability swath data are then averaged and gridded, producing a daily snow probability map.

I

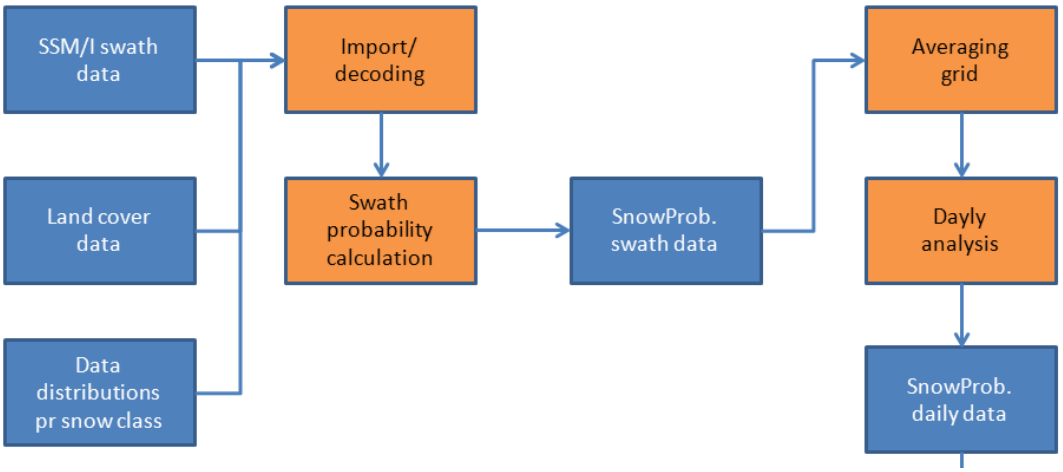

Figure 8.2. Overall processing flow for SSM/I snow probability algorithm.

The following processing steps are carried out:

- Reading input:
  - Histogram of land cover types for each land cover group
  - Feature distributions for snow cover class and land cover group
- For each SSM/I observation:
  - Extract the land-cover types corresponding to a 12.5 x 12.5 km area from a GlobCover map

- Estimate the histogram of land-cover types
- Find the land-cover group (classifier) that has most similar land cover histogram
- Estimate the probability of snow using PDFs of the selected group land cover classes

Input data to the optical snow cover chain is the reprocessed AVHRR GAC dataset from the Satellite Application Facility on Climate Monitoring (CM SAF), together with historical model temperature data from ERA Interim. Based on this, daily optical snow cover products are generated on the 5 km EASE-Grid.

The swath files containing historical AVHRR GAC channel data is applied with the swath algorithm for land pixels that fulfil the demand on solar zenith angle (less than 80°), and for each pixel the probabilities of snow, cloud and snow-free are estimated. The probabilities are stored as internal NetCDF swath files. All available orbits from one day (flexible period) are collected, and swath pixels with a probability of cloud lower than 40% are gridded and averaged into daily data.

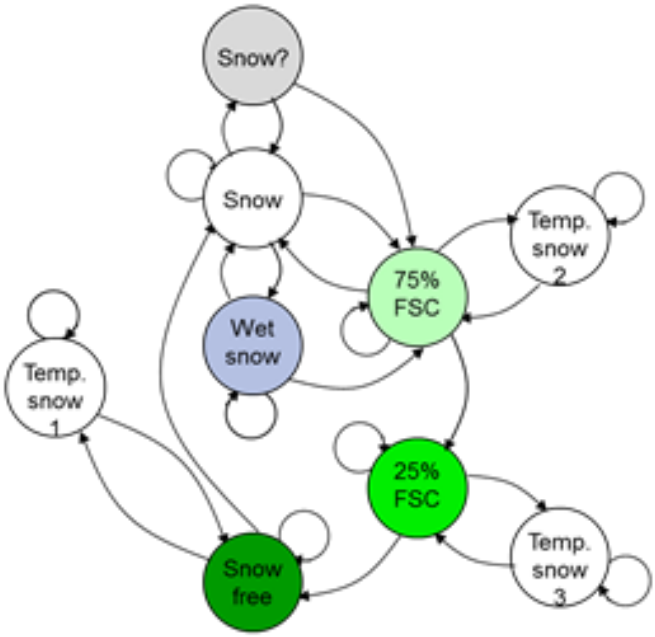

Figure 8.3. The hidden Markov state model applied.

The multi-sensor multi-temporal algorithm is based in the Viterbi algorithm, as explained above. The processing is also, accordingly, based on the steps in this algorithm. Given the observables (the single sensor snow probabilities) the problem is now to determine the sequence of snow states. The Viterbi algorithm finds the most likely sequence of states. It takes as input three sets of probabilities, the initial

probabilities, the transition probabilities and the probabilities of each state given the observations. The Viterbi algorithm consists of four parts in order to find the most likely sequence:

1. *Initialization*: The probabilities for the different states at the first step in the path are derived from the initial probabilities and the observations.
2. *Recursion*: For each following step in the sequence, the probability for each of the states can be found recursively from the existing path of probabilities and transition probabilities.
3. *Termination*: At the final time step the most probable state is selected.
4. *Sequence backtracking*: Finally, the algorithm iterates through the steps backwards and selects the optimal sequence of states from the calculated probabilities.

For the snow maps the sequences corresponding to each pixel are done in parallel. Initialization is done for the first map in the data set, and then the recursion is performed for each following map. At each time step a map containing the most probable state at the previous time step, for each of the possible current states, is written to file. For the last map in the dataset, the termination is performed. The final state with the highest accumulated probability is found. Finally, the backtracking is performed. The algorithm iterates backwards through the dataset, and selects the most likely state for every pixel at each time step. After this processing, a binary snow cover product is created by assigning snow status or bare ground status.

8.3 Quality and Validation of Product

For validation, we have used synoptic weather station data (SYNOP) and snow maps based on Landsat-5 TM and Landsat-7 ETM+ images derived by a combination of classification and photo-interpretation. We collected SYNOP snow depth data records from the Global Historical Climatology Network Daily (GHCN-D) database. To cope with the problem of distinguishing zero snow depths from missing measurements, we applied a data filtering strategy in order to extract which of the missing observations that correspond to zero snow depths. For the Landsat images, the overall approach was to separate sunlit and shaded areas and apply different methodology to the two parts. The sunlit areas were classified into three classes based on the Normalized Difference Snow Index (NDSI). The shaded areas were classified using an unsupervised clustering algorithm as NDSI did not work well for these areas.

The total accuracy was found to be 92.4%. Considering the monthly accuracies (Table 8.2), we see that accuracy is lowest during late autumn/early winter (November–January), and above 90% the rest of the season (except for April).

Table 8.2:
The accuracy of the multi-sensor snow product for each month of the year, when validated against the GHCN-D in-situ dataset. All the available data points in the product are used.

	Jan	***Feb***	***Mar***	***Apr***	***May***	***Jun***	***Jul***	***Aug***	***Sep***	***Oct***	***Nov***	***Dec***
True	0.82	0.90	0.94	0.88	0.93	0.99	1.00	1.00	1.00	0.98	0.78	0.76
False	0.18	0.10	0.06	0.12	0.07	0.01	0.00	0.00	0.00	0.02	0.22	0.24
Total pixels	1298	1318	1385	1008	1254	1437	1488	1488	1427	1225	702	1170

8.4 Strength and weaknesses of product

Strengths:

- Full spatial cover all year independent on cloud cover and polar night
- Generally consistent snow cover mapping even when data are affected by noise

Weaknesses:

- Underestimation of snow cover along coastlines
- Reduced accuracy during polar night when optical data are not contributing for longer periods

8.5 Contact

Institution	Norwegian Computing Center (NR) and Norwegian Meteorological Institute (MET Norway)
Contact Person	Rune Solberg
Email	rune.solberg@nr.no
Website for downloading the product:	http://www.cryoclim.net

8.6 References

Baum, L. E., and Petrie, T. (1966). Statistical Inference for Probabilistic Functions of Finite State Markov Chains. *The Annals of Mathematical Statistics*, 37 (6), 1554–1563.

Savitsky, A., and Golay, M. J. E. (1964). Smoothing and differentiation of data by simplified least squares procedures. *Analytical Chemistry*, 36, 1627-1639.

Schafer, R. W., (2011). What is a Savitsky-Golay filter. *IEEE Signal Processing Magazine* , 111-116, July 2011.

Solberg, R., Huseby, R.B., Koren, H. and Malnes E. (2008). Time-series fusion of optical and SAR data for snow cover area mapping. *Proceedings of EARSeL LIS-SIG Workshop*, Berne, February 11-13 February, 2008.

Solberg, R., Killie, M. A., Andreassen, L. M., and König, M. (2014). *IOP Conf. Series: Earth and Environmental Science* 17, 012008. doi:10.1088/1755-1315/17/1/012008

Viterbi, A. J. (1967). Error bounds for convolutional codes and an asymptotically optimum decoding algorithm. *IEEE Transactions on Information Theory*, 13 (2): 260–269. doi:10.1109/TIT.1967.1054010

9. JASMES MDS10C (JXM10)

Author: Masahiro Hori (JAXA)

9.1 Product overview and specification

This product is cloud and snow cover classification flag on a global scale derived from NASA's MODIS calibrated radiance data. The product has been processed at Japan Aerospace Exploration Agency (JAXA) since 2008 and available through a web site named JASMES (JAXA Satellite Monitoring for Environmental Studies, http://kuroshio.eorc.jaxa.jp/JASMES/index.html). The algorithm employs conventional threshold test technique including temporal filtering to discriminate cloud/clear and snow/non-snow cover classes. Daily, weekly, and semi-monthly products from 2000 to the present have been generated. An example of the product is shown in Figure 9.1.

Table 9.1:
Summary on the JASMES MDS10C snow extent product.

Parameter	***Specification***
Thematic variable	Binary Snow Cover Extent (SEB)
Thematic resolution	100% FSC
Thematic range	[100] SEB
Thematic accuracy	~20%
Thematic uncertainty estimate	Overall accuracy estimated over in-situ snow depth sites
Product Quality Map	NA
Spatial resolution	0.05° × 0.05° (ca 5km)
Spatial coverage	Global: 90°N 0°E – -90°S 0°W
Product available since	Daily products, since February 2000 to the present
Delivery time period	Full Year, daily, weekly, half-monthly (since Dec 2008)
Temporal frequency	Daily, weekly, half-monthly
Projection/Datum	Geographical (lat/lon) / WGS84
Cloud Screening	Threshold tests & Temporal filtering
Invalid / Masked Areas	Open Water (sea, lakes, rivers)
Sensor	Terra MODIS (2000.2-2014) & Aqua MODIS (2002.7-2014)
Satellite data level	Level 1B Swath data (5km resampled data)
File format	GeoTIFF
Developed by	JAXA
Provider / Generated by	JAXA / JAXA
Product available at	http://kuroshio.eorc.jaxa.jp/JASMES/index.html
Contact	Masahiro Hori / JAXA / hori.masahiro@jaxa.jp

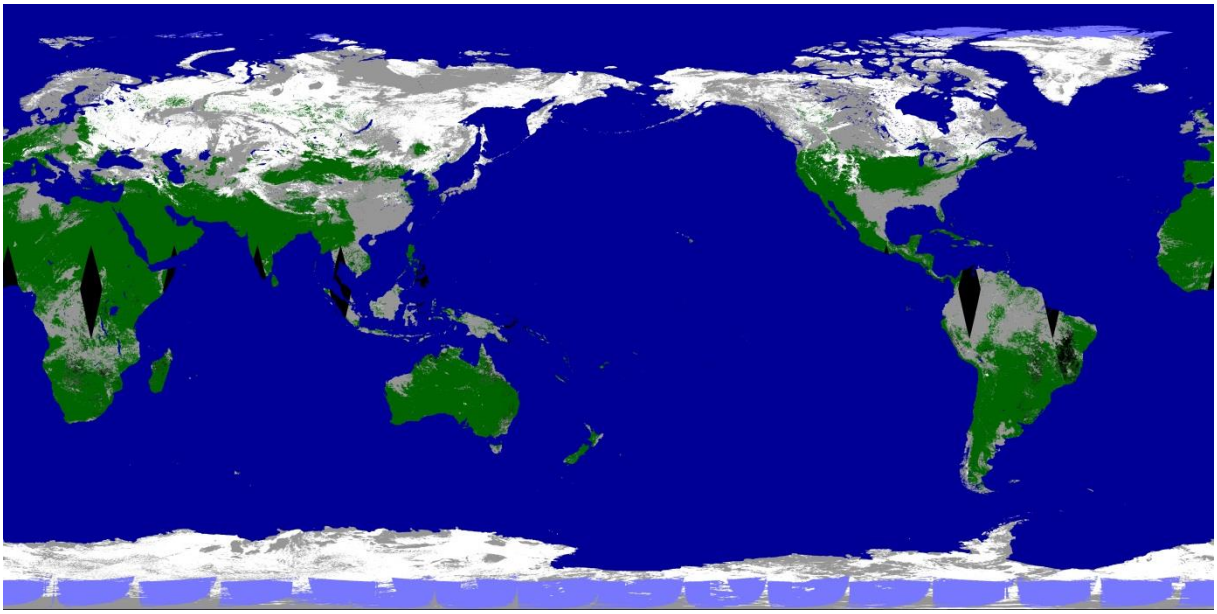

Figure 9.1: Example of JASMES MDS10C daily Binary Snow Extent product, 9 March 2012. (white: snow cover, green: non-snow land, blue: open water, grey: clouds, purple: polar night, black: no data)

9.2 Processing line and algorithm

Figure 9.2 shows the overall processing line of the JASMES MDS10C binary snow extent products from daily flag generation, weekly or semi-monthly aggregation, to monthly aggregation process. Input data are the calibrated radiance data of MODIS onboard NASA's Terra and Aqua satellite (5km resampled MODIS calibrated radiance data: MOD02SSH, MYD02SSH). Spectral bands used in this algorithm are 10 bands (as listed in section 3.2.3) in contrast to GHRM5C that uses only 5 channels.

As auxiliary data we use an elevation data of ETOPO02 and also use land/water flag generated using the Generic Mapping Tools (GMT). Daily process for clear/clouds and snow/non-snow cover discrimination consists of two steps based on the conventional multiple threshold test approach with spectral mixture analysis to consider the difference of underlying land cover type. At the first step, preliminary cloud and snow cover flag (PRCSF) is generated using several reflectances and brightness temperatures data from only single observation day. Next, daily snow cover flag (SNWFG) is determined by temporal filtering method, which uses not only data from the single observation day but also the maximum of reflectances and brightness temperatures during the adjacent 10-days to eliminate residual clouds in the snow pixels of PRCSF.

Then, the daily snow cover flags (SNWFG) during a week (7days) or a half-month (13-16 days) are aggregated to make a weekly or half-monthly temporal composite snow cover data. Finally, monthly snow cover flags (SNWFG) is generated using two half-monthly products.

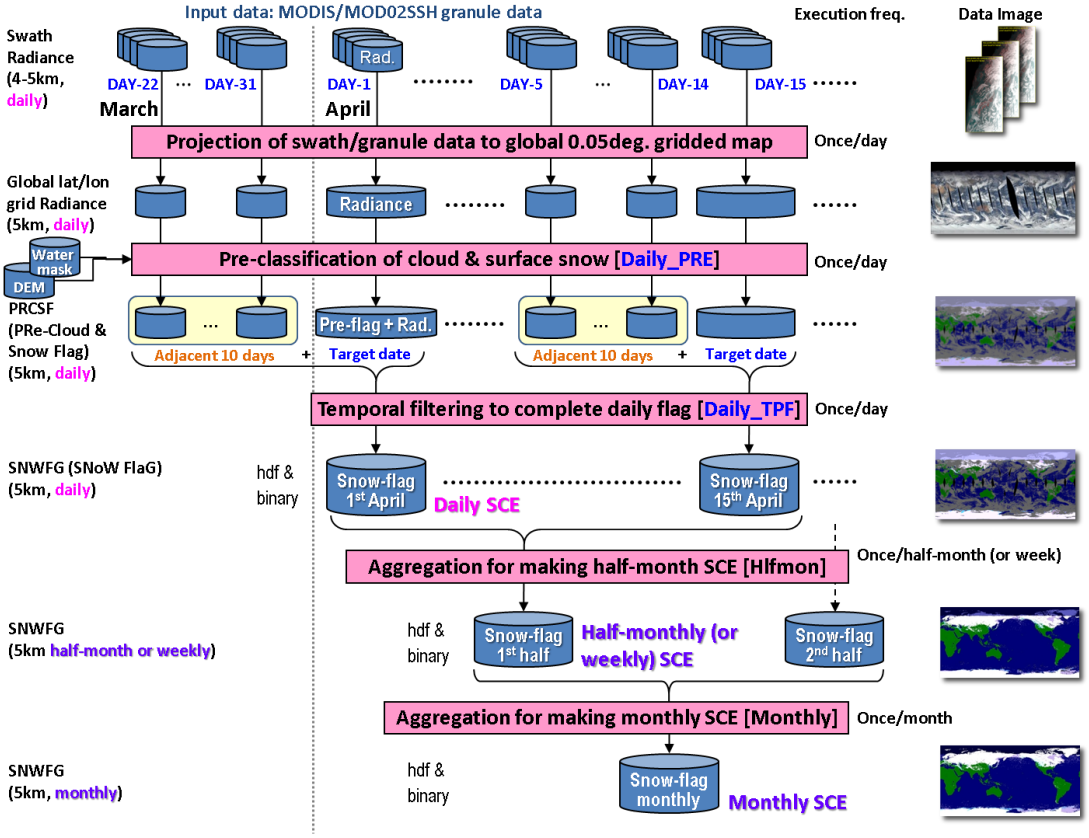

Figure 9.2: Processing line of JASMES MDS10C binary snow extent product.

9.2.1 Snow Mapping Algorithm

The algorithm for cloud/clear and snow/non-snow discrimination is based on the conventional threshold tests including a spectral mixture analysis assuming three typical land cover classes (bare land, vegetation, and snow) (Hori et al., in prep. The algorithm is partly similar to the approach of Stamnes et al., 2007 and Hori et al., 2007, and a spectral mixture analysis (similar to Painter et al., 2009) taking into account the difference in underlying land cover type is implemented. In addition, temporal filtering technique making use of the optical properties of snow cover (i.e., high reflectance in visible wavelengths and low in shortwave and mid-infrared reflectance, for example) is implemented as JXAM5. Threshold tests employed in the algorithm use reflectance (REF) or brightness temperature

(BT) at single channel, difference or ratio between two different channels, normalized difference index such as NDVI and NDSI, difference between REF (or BT) of observation day and average of previous 10days and so on. While most of the threshold tests are selected based on the various previous studies, some of them are newly added to enhance the discrimination ability over cold dry areas. All the threshold values for individual tests are determined and empirically tuned by manual inspection of discrimination results comparing with reflectance images. The algorithm is designed to use visible to shortwave infrared reflectance for discriminating cloud and clear etc. and does not work for night-time data. Thus, we identify the area as “polar night land” in daily and weekly flag. When counting snow cover extent, we assumed that the polar night land is always covered with dry snow and included the area in the SCE.

9.2.2 Cloud Screening

Cloud screening is performed in the same process identifying snow cover as mentioned in the previous section. Algorithm is the conventional threshold techniques with temporal filtering approach.

9.2.3 Input Data

Input data are the calibrated radiance data of MODIS on-board NASA’s Terra and Aqua satellite (5km resampled MODIS calibrated radiance data: MOD02SSH, MYD02SSH). Spectral bands used in this algorithm are the followings; MODIS ch1 (centre wavelength λ = 0.645 μm), 2 (0.858 μm), 5 (1.24 μm), 7 (2.13 μm), 18 (0.936 μm), 19 (0.936 μm), 26 (1.375 μm), 31 (11.03 μm), 32 (12.02 μm), 36 (13.913 μm).

- MODIS L1B calibrated radiance data (MOD02SSH, MYD02SSH)

9.2.4 Auxiliary Data Sets (Static)

- DEM: ETOPO02
- Open water mask (sea, lakes, etc): Land /Water flag generated with GMT

9.2.5 Quality and Validation of Product

Accuracies of snow cover detection were evaluated using in-situ snow depth data taken from meteorological station data through the Global Telecommunication System (GTS).

Producer’s accuracy (PA) was evaluated for the SNWFG of 2008 using the in-situ snow depth data obtained through GTS (user’s accuracy was not evaluated because the in-situ snow depth data used here does not have information of zero mm snow depth thus we cannot estimate commission errors).

Criteria for examining snow cover existence at the in-situ sites is set to 10mm of snow depth. For example, when snow depth is deeper than 10mm at an in-situ site and the pixel class of satellite derived snow cover flag (SNWFG) nearest to the in-situ site is snow cover, then the SNWFG flag is expected to succeed in identifying snow cover at the pixel location.

Comparisons of daily SNWFG with in-situ snow depth (GTS) indicate that PA of SNWFG is about 0.92 exhibiting seasonal variation; high in winter to early spring seasons (Nov. to Apr.) and low in summer and autumn (May. to Oct.) as shown in Figure 9.3.

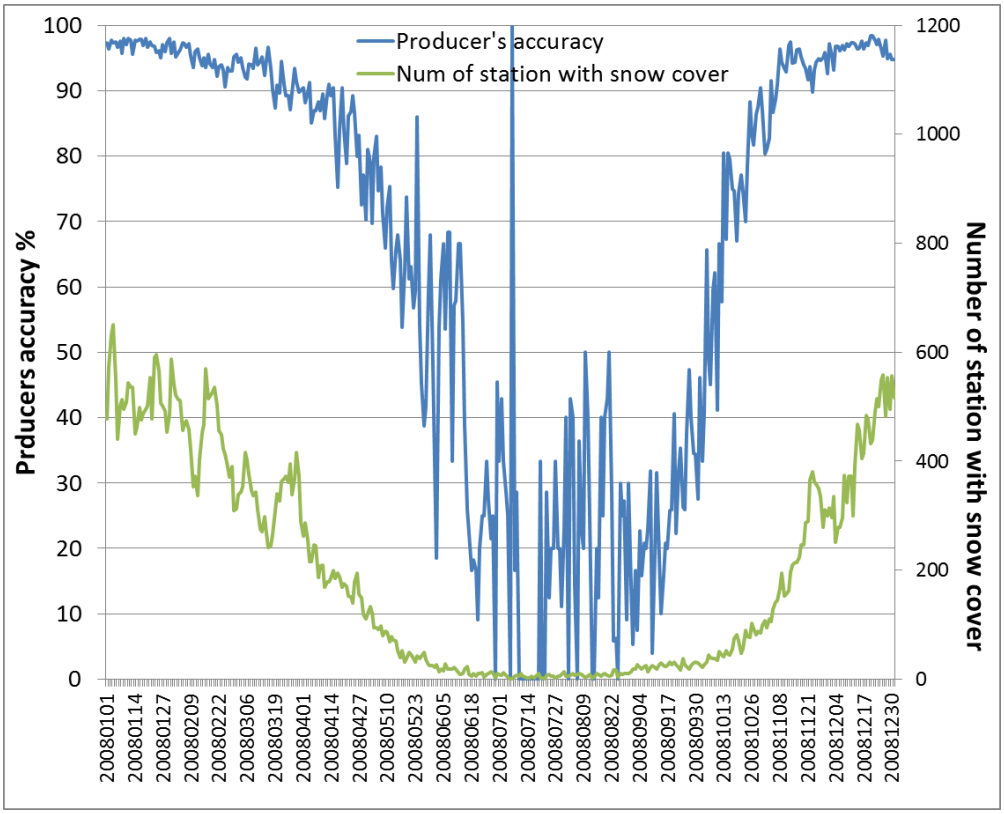

Figure 9.3: Producer's accuracy of daily SNWFG in 2008 (blue line) and the number of meteorological station with snow cover (depth>=10mm)

9.3 Strength and weaknesses of product

The strengths of the product are:

- Higher spatial resolution (5km) compared with NOAA CDR weekly SCE chart
- Long-term data record from 2000 to the present (w/o a half-month period in 2001)

- Discrimination between dry and wet conditions of snow cover (but not included in the SCE data for the SnowPEx inter-comparison)

Identified weaknesses of the products are:

- Still poorer performances possible in dense forest, cold desert, and high mountain areas

9.4 Contact

Institution	Japan Aerospace Exploration Agency
Contact Person	Masahiro Hori
Email	hori.masahiro@jaxa.jp
Website for downloading the product:	http://kuroshio.eorc.jaxa.jp/JASMES/index.html

9.5 References

Hori M, Aoki T., Stamnes K, Li W (2007) ADEOS-II/GLI snow/ice products— Part III: Retrieved results. Remote Sensing of Environment 111:291-336

JASMES (JAXA Satellite Monitoring for Environmental Studies) (2014) JASMES Binary snow cover extent product (GHRM5C), Available at: http://kuroshio.eorc.jaxa.jp/JASMES/index.html

Painter TH, Rittger K, McKenzie C, Slaughter P, Davis RE, Dozier J (2009) Retrieval of subpixel snow covered area, grain size, and albedo from MODIS. Remote Sensing of Environment 113: 868-879

Stamnes K, Li W, Eide H, Aoki T, Hori M, Storvold R (2007) ADEOS-II/GLI snow/ice products—Part I: Scientific basis. Remote Sensing of Environment 111:258-273

10. GHRM5C (JXAM5)

Author: Masahiro Hori (JAXA)

10.1 Product overview and specification

This product is cloud and snow cover classification flag on a global scale derived from AVHRR and MODIS calibrated radiance data. The product has been processed at Japan Aerospace Exploration Agency (JAXA) and will be open to the public soon through a web site named JASMES (JAXA Satellite Monitoring for Environmental Studies, http://kuroshio.eorc.jaxa.jp/JASMES/index.html). The algorithm employs conventional threshold test technique including temporal filtering to discriminate cloud/clear and snow/non-snow cover classes. Daily, weekly, and semi-monthly products from Nov. 1978 to the present (without some months in 1980, 1981, 1994, 1995, 2001) will be available.

Table 10.1:
Summary on JASMES GHRM5C global binary snow cover product.

Parameter	***Specification***
Thematic variable	Binary Snow Cover Extent (SEB)
Thematic resolution	100% FSC
Thematic range	[100] SEB
Thematic accuracy	~20%
Thematic uncertainty estimate	Overall accuracy estimated over in-situ snow depth sites
Product Quality Map	NA
Spatial resolution	0.05° × 0.05° (ca 5km)
Spatial coverage	Global: 90°N 0°E – -90°S 0°W
Product available since	Daily products, since November 1978-the present
Delivery time period	Full Year, daily, weekly, half-monthly (since early 2015)
Temporal frequency	Daily, weekly, half-monthly
Projection/Datum	Geographical (lat/lon) / WGS84
Cloud Screening	Threshold tests & Temporal filtering
Invalid / Masked Areas	Open Water (sea, lakes, rivers) and Antarctic ice sheet
Sensor	AVHRR (1978.11-2000.2), Terra & Aqua MODIS (2000.2-2014)
Satellite data level	Level 1B Swath data (AVHRR: 4km GAC, MODIS: 5km resampled)
File format	GeoTIFF
Developed by	JAXA
Provider / Generated by	JAXA / JAXA
Product available at	http://kuroshio.eorc.jaxa.jp/JASMES/index.html
Contact	Masahiro Hori / JAXA / hori.masahiro@jaxa.jp

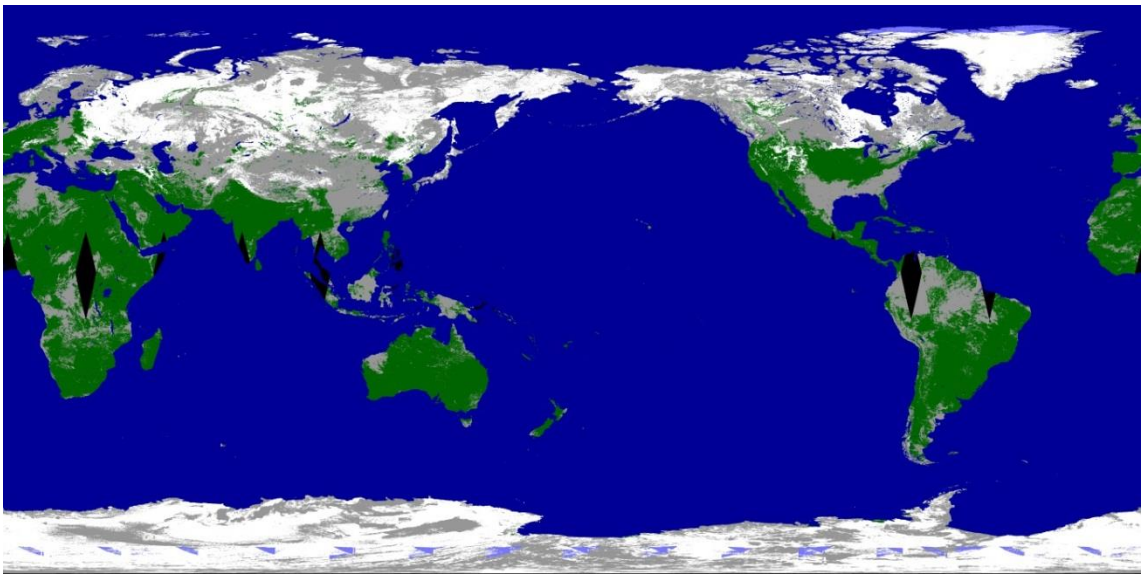

Figure 10.1: Example of JASMES GHRM5C daily Binary Snow Extent product, 9 March 2012. (white: snow cover, green: non-snow land, blue: open water, grey: clouds, purple: polar night, black: no data)

10.2 Processing line and Algorithm

Figure 10.2 shows the overall processing line of the JASMES GHRM5C binary snow extent products from daily flag generation to weekly or semi-monthly aggregation process. Input data are the calibrated radiance data of AVHRR on-board NOAA series satellites (4km resampled calibrated radiance data (GAC)) and MODIS on-board NASA's Terra and Aqua satellite (5km resampled MODIS calibrated radiance data: MOD02SSH, MYD02SSH). Spectral bands used in this algorithm are only the five bands same as the AVHRR channel 1 to 5. The same spectral bands with similar centre wavelengths are selected for the MODIS processing (MODIS channel 1, 2, 20, 31, 32).

As auxiliary data we use an elevation data of ETOPO02 and also use land/water flag generated using the Generic Mapping Tools (GMT).

Daily process for clear/clouds and snow/non-snow cover discrimination consists of two steps based on the conventional multiple threshold test approach. At the first step, preliminary cloud and snow cover flag (PRCSF) is generated using several reflectances and brightness temperatures data from only single observation day as shown in Figure 10.3. Next, daily snow cover flag (SNWFG) is determined by temporal filtering method as shown in Figure 10.4, which uses not only data from the single observation day but also the maximum of reflectances and brightness temperatures during the

adjacent 10-days to eliminate residual clouds in the snow pixels of PRCSF. Finally, the daily snow cover flags (SNWFG) during a week (7days) or a half-month (13-16 days) are aggregated to make a weekly or half-monthly temporal composite snow cover data.

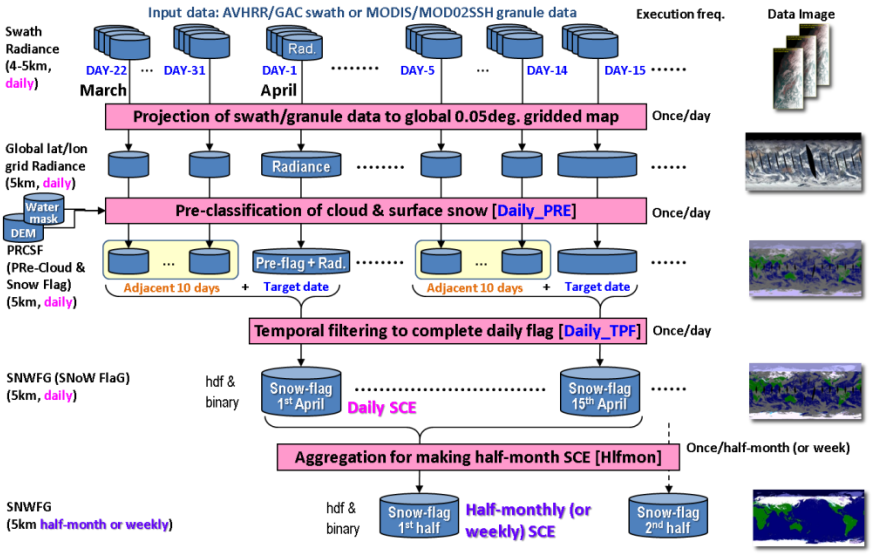

Figure 10.2: Processing line of JASMES GHRM5C binary snow extent product

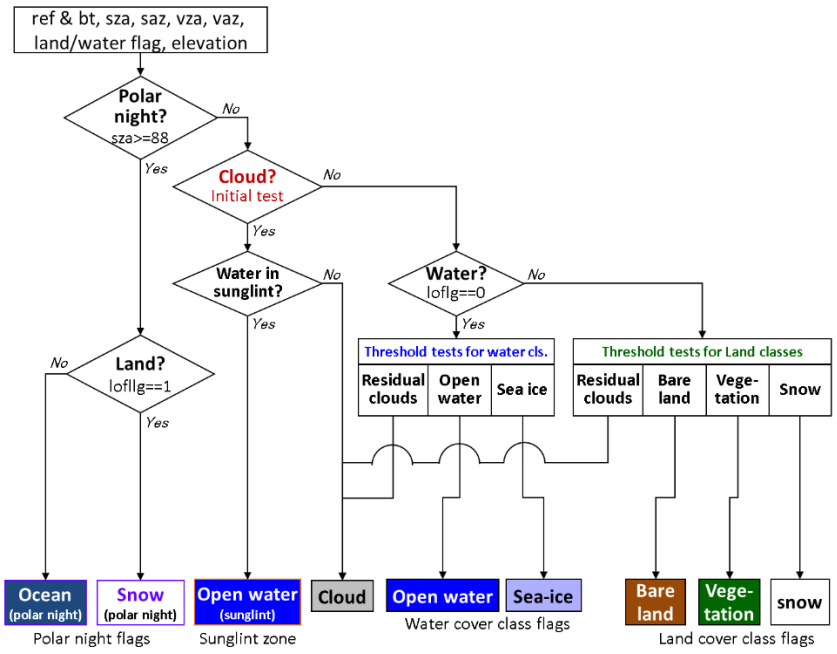

Figure 10.3: Processing line of preliminary daily cloud and snow cover flag (PRCSF)

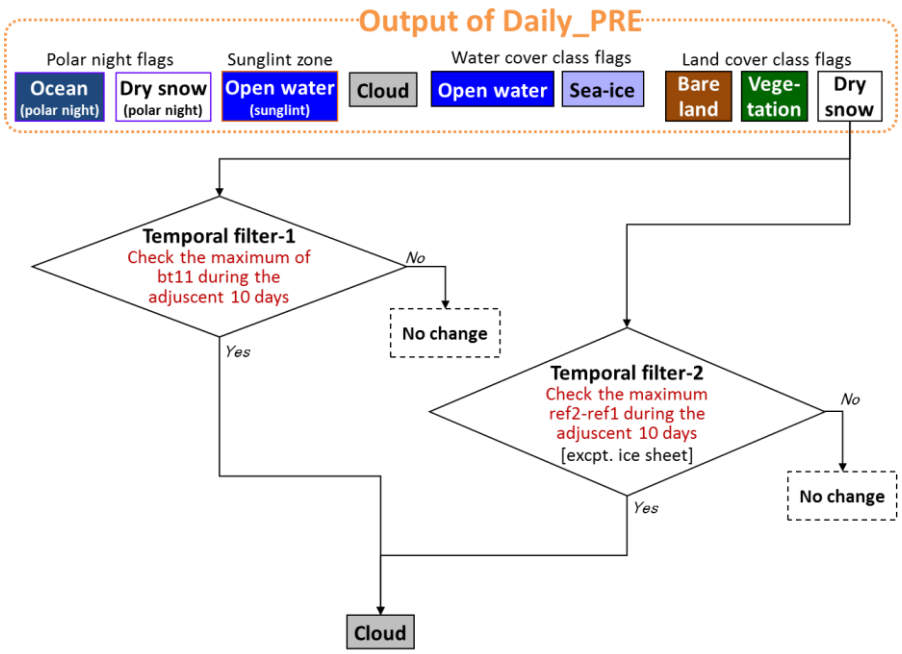

Figure 10.4: Processing line of daily snow cover flag (SNWFG) with temporal filtering

10.2.1 Snow mapping algorithm

The algorithm for cloud/clear and snow/non-snow discrimination is based on the conventional threshold tests as shown in Figure 10.3 (Hori et al., in prep.). The algorithm is similar to the approach of Stamnes et al. (2007) and Hori et al. (2007) but the spectral channels used in the algorithm are confined to only the 5 channels as mentioned above) and temporal filtering techniques which make use of the optical properties of snow cover (i.e., high reflectance in visible wavelengths and low in shortwave and mid-infrared reflectance, for example). Threshold tests employed in the algorithm use reflectance (REF) or brightness temperature (BT) at single channel, difference or ratio between two different channels, normalized difference index such as NDVI and NDSI (reflectance at λ = 3.7μm is used as the shortwave infrared reflectance of NDSI), average of REF or BT difference during the previous 10days and so on. Most of the threshold tests are selected based on the various previous studies. All the threshold values for individual tests are determined and empirically tuned by manual inspection of discrimination results comparing with reflectance images. The algorithm is designed to use visible to near infrared reflectance for discriminating cloud and clear etc. and does not work for night-time data. Thus, we identify the area as “polar night land” in daily and weekly flag. When counting snow cover extent, we assumed that the polar night land is always covered with dry snow and included the area in the SCE.

10.2.2 Cloud screening

Cloud screening is performed in the same process identifying snow cover as mentioned in the previous section. Algorithm is the conventional threshold techniques with temporal filtering approach.

10.2.3 Input data

Input data are the calibrated radiance data of AVHRR on-board NOAA series satellites (4km resampled calibrated radiance data (GAC)) and MODIS on-board NASA's Terra and Aqua satellite (5km resampled MODIS calibrated radiance data: MOD02SSH, MYD02SSH).

- AVHRR L1B GAC (4km resampled calibrated radiance data)
- MODIS L1B calibrated radiance data (MOD02SSH, MYD02SSH)

10.2.4 Auxiliary data sets

The following 2 data sets are required as auxiliary data for generation of the product:

- DEM: ETOPO02
- Open water mask (sea, lakes, etc): Land /Water flag generated with GMT

10.2.5 Quality and validation of product

Accuracies of snow cover detection were evaluated using in-situ snow depth data taken from NOAA/NCDC (DAILY GLOBAL HISTORICAL CLIMATOLOGY NETWORK: GHCN-D, ftp://ftp.ncdc.noaa.gov/pub/data/ghcn/daily).

User's (UA) and Producer's accuracy (PA) are evaluated for the weekly composite of SNWFG during Nov. 1978 to Dec. 2013 using weekly averaged GHCN-D snow depth data. Criteria for examining snow cover existence at the in-situ sites is set to 25mm of snow depth. For example, when snow depth is deeper than 25mm at an in-situ station site and the pixel class of satellite derived snow cover flag (SNWFG) nearest to the in-situ site is snow cover, then the SNWFG flag is expected to succeed in identifying snow cover at the pixel location.

Comparisons of weekly aggregated SNWFG with in-situ snow depth (GHCND) indicate that UA/PA of SNWFG are about 0.84/0.72 exhibiting seasonal variation; high in winter to spring seasons and low in summer and autumn as shown in Figure 10.5.

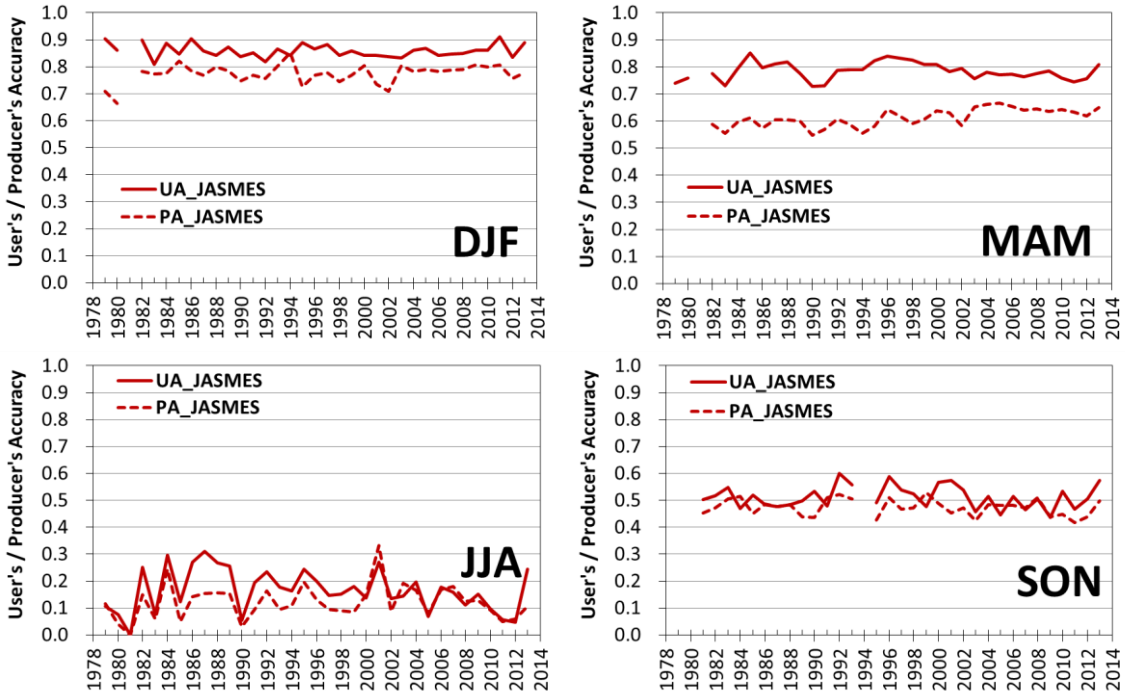

Figure 10.5: User's (UA, solid line) and Producer's accuracy (PA, broken line) of weekly aggregated SNWFG evaluated using GHCN-D (criteria: snow depth>=25mm)

10.3 Strength and weaknesses of product

Strengths

- Higher spatial resolution (5km) compared with the NOAA CDR weekly SCE chart
- Long-term data record from Nov. 1978 to the present (w/o some months in 1980, 1981, 1994, 1995, 2001)
- Continuity of the algorithm and complete automatic reprocessing capability

Weaknesses

- Poorer performances in dense forest, cold desert, and high mountain areas (compared with 10CHs version of our algorithm (JXM10))
- Data gaps as shown above (partly because of snow detection losses due to sensor noises, low solar elevation condition etc.)

10.4 Contact

Institution	Japan Aerospace Exploration Agency
Contact Person	Masahiro Hori
Email	hori.masahiro@jaxa.jp
Website for downloading the product:	http://kuroshio.eorc.jaxa.jp/JASMES/index.html

10.5 References

Hori M, Aoki T., Stamnes K, Li W (2007) ADEOS-II/GLI snow/ice products— Part III: Retrieved results. Remote Sensing of Environment 111:291-336

JASMES (JAXA Satellite Monitoring for Environmental Studies) (2014) JASMES Binary snow cover extent product (GHRM5C), Available at: http://kuroshio.eorc.jaxa.jp/JASMES/index.html

Stamnes K, Li W, Eide H, Aoki T, Hori M, Storvold R (2007) ADEOS-II/GLI snow/ice products—Part I: Scientific basis. Remote Sensing of Environment 111:258-273

11. AVHRR PATHFINDER

Authors: Richard Fernandes and Fuqun Zho (CCRS, Government of Canada)

11.1 Product Overview and Specification – 2 pages

The AVHRR Polar Pathfinder (PATHF) Snow Cover data set consists of 5km EASE-GRID Northern Hemisphere snow extent (SE) derived from twice daily 5km resolution Extended AVHRR Polar Pathfinder (APP-X, Wang and Key 2010a,b) visible and near-infrared top-of-atmosphere reflectance data. The SE is coded as a snow cover fraction (SCF) scaled by 100 although the product itself is intended for detection of snow-free conditions so there is an emphasis on accuracy near SCF=0.

Table 11.1:
Summary on AVHRR snow cover product.

Parameter	***Specification***
Thematic variable	Snow Cover Fraction (FSC)
Thematic resolution	1% FSC
Thematic range	[0, 100]
Thematic accuracy	>80% agreement in BSE for >95% sites
Thematic uncertainty estimate	Comparison over in-situ snow depth sites with BSE >=2m (FCS>20%) or =0cm
Product Quality Map	Not available. Comparison has been performed over 3 sites over NH.
Spatial resolution	5 km × 5 km (EASE-Grid)
Spatial coverage	Northern Hemisphere
Product available since	Daily products, from January 1, 1982–December 31, 2004
Delivery time period	No forward processing
Temporal frequency	Daily, no missing dates due to clouds
Projection/Datum	Lambert Azimuthal Equal Area / WGS84
Cloud Screening	None
Invalid / Masked Areas	Land areas in APP-X Land/Water Mask, permanent ice caps
Sensor	AVHRR
Satellite data level	
File format	NetCDF
Developed by	CCRS. Government of Canada
Provider / Generated by	CCRS. Government of Canada
Product available at	ftp://ftp.ccrs.nrcan.gc.ca/ad/IPY/snowapp/
Contact	Richard Fernandes, CCRS, ricahrd.fernandes@nrcan.gc.ca

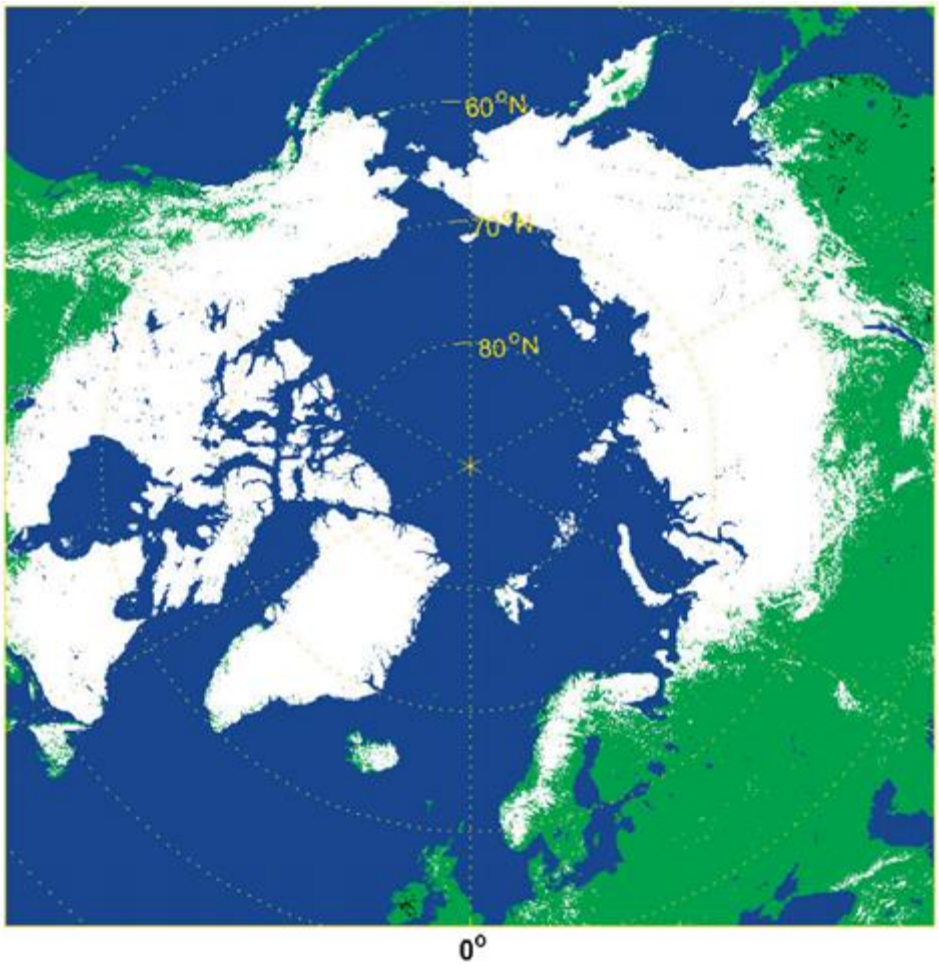

Figure 11.1: Example of AVVHRR snow extent product, 30 April 2002, White correspond to FSC>=20%, green FSC<20%, blue invalid

11.2 Processing line and Algorithm (max 5 pages)

The PATHF product was derived entirely from a full resolution (5km) version of the publically available APP-X satellite dataset (http://stratus.ssec.wisc.edu/products/appx/appx.html). Data processing involved the application of an algorithm originally developed for SC mapping with 1 km resolution AVHRR imagery over Canada. The algorithm is designed to map FSC for snow packs that exhibit a seasonal accumulation and melt pattern in contrast to ephemeral melt and on-set.

11.2.1 Input Data

Input data correspond to top-of-atmosphere (TOA) reflectance of AVHRR Channels 1 (0.58–0.68mm) (CHN1) and 2 (0.725–1.10mm), normalized difference vegetation index (NDVI), derived clear sky surface broadband albedo based on J. R. Key (The Cloud and Surface Parameter Retrieval (CASPR) Version 4.0.3, National Environmental Satellite, Data, and Information Service, 1999), skin temperature (ST), solar zenith angle (SZA), satellite view angle (SVA), sun-satellite relative azimuth angle, and cloud mask. This data set extends poleward from 48.4_N, available from 24 July 1981 through 30 June 2005. Only valid daytime observations corresponding to SZA < 85_ and SVA < 55_ were used to ensure sufficient signal at the detector as well as to reduce the contribution from surfaces outside the nominal pixel.

11.2.2 Data Processing

The algorithm consists of three procedures applied on a grid cell basis to annual daily time series of APP- X measurements: temporal filtering and interpolation, normalization of CHN1 to standard acquisition geometry, and FCS estimation.

The temporal filtering and interpolation stage estimates continuous daily ‘‘clear sky’’ time series of annual CHN1, ST and NDVI measurement time series (CHN1s, STs and NDVIs respectively) on a per-grid cell basis. A series of moving window temporal rank filters, adaptive to local cloud conditions and grid cell wise calibration of snow and snow free end-members, are applied to identify clear sky time series. Cloud shadows are assumed to substantially reduce TOA estimates for CHN1, ST and NDVI in comparison to corresponding clear sky conditions. Then, given an a priori estimate of the probability of clouds and shadows and assuming the clear sky time series is locally monotonic, the rank of a sample within a local time window can be associated with a probability that it is free of cloud or shadow contamination. The a priori cloud probability was estimated by a 30 day moving average frequency of APP cloud flags. A constant cloud shadow probability of 10% was applied on the basis of average statistics derived from AVHRR data processed over Canada that include shadow masks [Latifovic et al., 2005]. Successive passes of the moving window rank filter, with window sizes decreasing from 40 days to 10 days, were applied. The 40-day upper window size was used to limit computational requirements while the lower size corresponded to the smallest window allowing a 0.95 clear sky probability for a priori cloud probability over 0.5.

The Roujean bidirectional reflectance distribution function (BRDF) model [Roujean et al., 1992] was used to normalize the continuous CHN1 measurements to a nominal nadir view at the solar zenith

angle corresponding to the observed overpass time at the local summer solstice. This reference geometry was selected since it minimized the range of solar zenith angles to be normalized at each grid cell. The volume and geometric kernel coefficients were assumed invariant for each calendar year. However, in contrast, grid cell specific coefficients were used to account for land cover variability. At each grid cell, the volume scattering coefficient of the Roujean model was assigned as a function of NDVI on the basis of a relationship fitted using the data from Latifovic et al. [2005]. A relationship between median August NDVI and the geometric kernel coefficient was calibrated using paired CHN1s and in situ snow depth measurements during deep snowpack conditions over Canada between 1985 and 2000. At each site and for each year, the coefficient minimizing the absolute magnitude of the slope of the CHN1sversus solar zenith angle curve was selected.

Our SC detection approach used the CHN1 value corresponding to this discontinuity of the annual CHN1 versus ST curve during the spring melt period, at each grid cell, as the annual CHN1 snow free threshold. Grid cell specific ST thresholds were applied to identify the start (Tmin) and end (Tmax) of a broad interval bracketing the spring melt period (limited to between 1 January and 31 August of each year). The t_o was initially estimated as the point on the CHN1s versus STs curve with minimum projection on the normal to the chord subtending this interval. The interval was then reduced by shrinking the ST thresholds to the halfway point between the current interval boundary and to and the estimation of SC updated until only one other point remained. Dates when CHN1 <= CHN1 (t_o) or with ST > Tmax were mapped as snow free. Dates when CHN1s> CHN1(t_o) or when ST < Tmin were mapped as having snow present. Additionally, a linear mixture model was fitted between the two remaining dates in the fitting interval and applied to the CHN1 annual time series at the grid cell. The fractional value served as an estimate of the precision of the SC detection for other days during the year (Figure 2b).

11.2.3 Output Data Formatting

Daily FSC images using the same input 5-km EASE-GRID projection were generated using unsigned 8-bit layers with a scaling factor of 100 and offset of 0. Invalid regions were coded with a value of 255. These images are currently archived on the CCRS ftp site and catalogued at the International Polar Year Polar Data Catalogue. The images were resampled to EASE-GRID 2.0 and coded in NETCDF format for use within SnowPEx.

11.3 Quality and Validation

Quality control included visual assessment, comparison with in-situ snow depth sites by converting the PATHF product to binary SE, and intercomparison of monthly gridded monthly snow cover duration fraction with other products and model output (Brown et al., 2010).

Visual assessment of daily snow cover maps was performed to identify artefacts due to known issues with the input APP-X data (generally corresponding to coding errors for single dates). In many instances the artefacts were removed by the temporal filtering applied by the PATHF algorithm. However, a list of artefacts in the PATHF product, generally related to prolonged periods of corrupted data, was produced and recoded in an EXCEL file accompanying the dataset.

Comparisons between satellite and in situ SC estimates by applying a 20% FSC threshold to convert FCS to SE and a 2cm depth threshold to snow depth sites, were conducted over the year of 2002 in Canada, and the year of 1993 in the northern Eurasia. During 3-day continuous snow status, the 95 percentile of the total sites exceeds an accuracy of 90% for the full year period during July-August and 80% percentile of Canadian sites exceeds 90% accuracy for the full year (accuracy drops to 80% over Eurasia). The improved melt versus full year accuracy rates indicates that the most frequent disagreements occurred mainly during the snow onset season. This could be due to (1) the temporal filtering and zeroth-order interpolation applied to the satellite measurements, (2) large differences in visible reflectance between fresh snow albedo during onset and the level prior to spring melt used to define the SC end-member in the Snow cover algorithm, and (3) the increase in visible reflectance during fall senescence over vegetated areas resulting in a bias in the snow-free end-member.

11.4 Strength and weaknesses of product

The PATHF product provides some unique aspects in comparison to other SE datasets:

- Nearly continuous temporal coverage.
- Multi-decadal extent.
- Objective data processing nearly independent of AVHRR sensor acquisition conditions (calibration, geometry, atmospheric effects).
- SCF estimation rather than binary SE to allow for improved error analysis.

- Accurate (+/-3days) detection of snow free date over areas with seasonal rather than ephemeral snow melt.
- Performance generally independent of land cover condition or inter-annual land cover changes.

The PATHF product has limitations primarily stemming from its design goal of use for quantification of northern hemisphere springtime snow albedo feedbacks rather than of daily snow cover mapping:

- Ephemeral melt or onset events with temporal length scales of less than 15 months may be undetected.
- SCF estimation assumes winter BRDF correction applies in onset and melt period.
- Snowpack albedo assumed constant when estimating FSC (only one snow free and snow covered endmember applied).
- Linear mixture model assumed for partial FSC conditions.
- Data mapped corresponds to a spatial location that will vary in each 5km grid cell (due to APP-X spatial compositing). This may result in lower precision over grid cells with high spatial variability in FSC or vegetation masking.
- BRDF model assumes flat terrain resulting in low FSC precision over mountainous regions.

In summary, the product is designed to map snow melt conditions outside of ephemeral snow pack melt regimes. The FSC should be used with caution for intermediate values (20%<FSC<80%) or over mountainous or urban regions.

11.5 Contact

Institution	Canada Centre for Remote Sensing, Government of Canada
Contact Person	Richard Fernandes
Email	Richard.fernandes@nrcan.gc.ca
Website for downloading the product:	ftp://ftp.ccrs.nrcan.gc.ca/ad/IPY/snowapp/

11.6 References

Brown, R., C. Derksen, *and* L. Wang *(*2010*),* A multi-data set analysis of variability and change in Arctic spring snow cover extent, 1967–2008, J. Geophys. Res., 115, *D16111, doi:*10.1029/2010JD013975.

Latifovic, R., et al. (2005), Generating historical AVHRR 1 km baseline satellite data records over Canada suitable for climate change studies, Can. J. Rem. Sens., 31(5), 324–364.

Roujean, J. L., M. Leroy, and P. Y. Deschamps (1992), A bidirectional reflectance model of the Earth's surface for the correction of remote sensing data, J. Geophys. Res., 97, 20,455– 20,468.

Wang, X, and J. R. Key. (2010a) Arctic Surface, Cloud, and Radiation Properties Based on the AVHRR Polar Pathfinder Dataset. Part I: Spatial and Temporal Characteristics. Journal of Climate 18:14, 2558-2574.

Wang, X, and J. R. Key. (2010b) Arctic Surface, Cloud, and Radiation Properties Based on the AVHRR Polar Pathfinder Dataset. Part II: Recent Trends. Journal of Climate 18:14, 2575-2593.

Zhao, H., and R. Fernandes (2009), Daily snow cover estimation from Advanced Very High Resolution Radiometer Polar Pathfinder data over Northern Hemisphere land surfaces during 1982–2004, J. Geophys. Res., 114, *D05113, doi:*10.1029/2008JD011272.

12. MEASURES SNOW PRODUCT

Authors: David Robinson (Rutgers University), Dorothy Hall (NASA GSFC), Thomas Mote (University of Georgia).

12.1 Product overview and specification

The MEaSUREs data set consists of 25 km EASE-Grid 2.0 Northern Hemisphere snow extent (SE) derived from three different sources, stored in four different netCDF variables. Three of the snow cover variables are derived from the Interactive Multisensor Snow and Ice Mapping System (IMS), MODIS Cloud Gap Filled (CGF) Snow Cover, and passive microwave (MW) brightness temperatures. The remaining variable merges all three of these source products into a single representation of snow cover.

Table 12.1:
Summary on MEaSUREs maximum snow cover product.

Parameter	***Specification***
Thematic variable	Binary Snow Cover
Thematic resolution	
Thematic range	[0, 1]
Thematic accuracy	Unknown
Thematic uncertainty estimate	
Product Quality Map	
Spatial resolution	25 km × 25 km (EASE-Grid 2.0)
Spatial coverage	Northern Hemisphere
Product available since	Daily products, from January 1, 1999–December 31, 2012
Delivery time period	No forward processing
Temporal frequency	Daily
Projection/Datum	Lambert Azimuthal Equal Area / WGS84
Cloud Screening	5-day CGF (only used for MODIS-derived snow extent)
Invalid / Masked Areas	BU-MODIS LOCI Open Water and Permanent Ice
Sensor	AMSU-B, AVHRR, SSM/I, SSMIS, Terra MODIS, VAS, VIIRS, VISSR
Satellite data level	
File format	NetCDF
Developed by	NASA MEaSUREs Program
Provider / Generated by	Rutgers, The State University of New Jersey
Product available at	https://nsidc.org/data/nsidc-0530
Contact	David Robinson / Rutgers / david.robinson@rutgers.edu

For the purposes of SnowPEx, a maximum SE product was generated using the MEaSUREs product. The merged SE variable was converted into a binary (snow / no snow) representation of snow cover extent by combining values from 10-16 into one value. This means that for each daily file, any pixel indicating snow cover from any source (IMS, CGF or MW) is recorded as snow covered in the SnowPEx output.

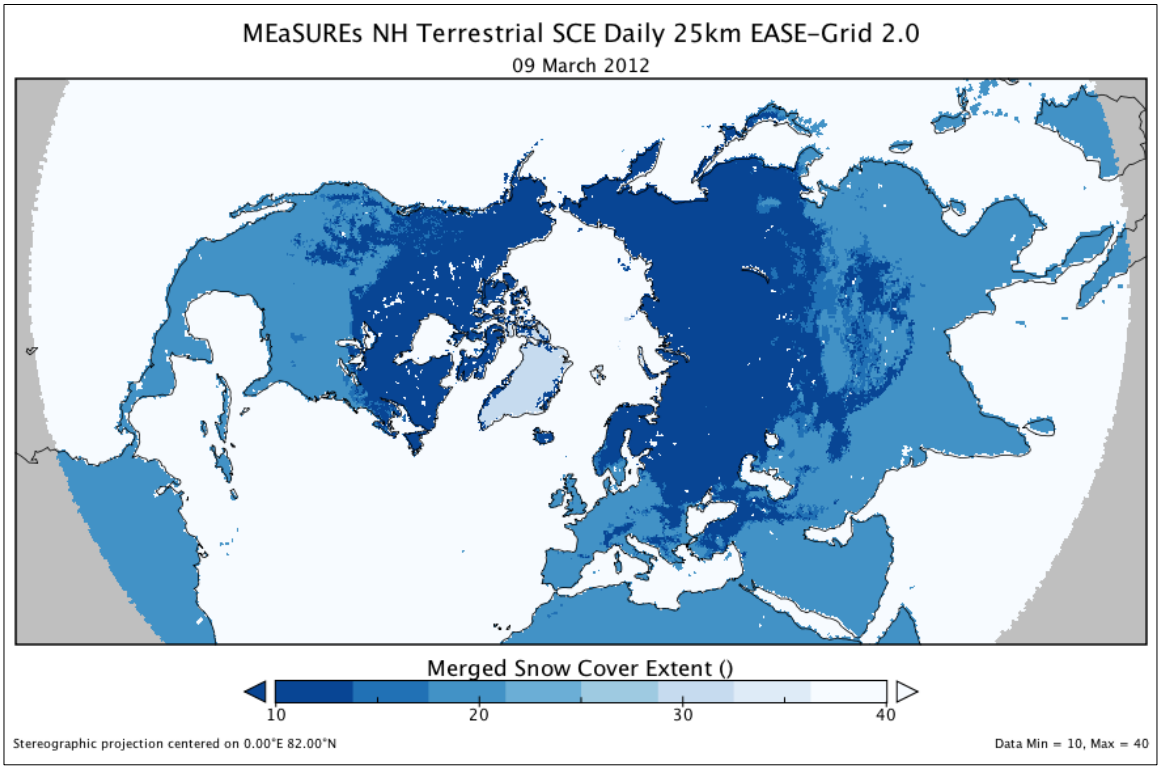

Figure 12.1: Example of MEaSUREs merged snow extent product, 9 March 2012.

12.2 Processing line and algorithm

Original source products used in the creation of the MEaSUREs data set are available via public websites. The following sections describe how each source product was converted into its corresponding SE variable. Much of the information in section 12.2and section 12.3 was originally published by NSIDC on the MEaSUREs product documentation page. For more details see the full NSIDC-0530 documentation here (https://nsidc.org/data/docs/measures/nsidc-0530/index.html).

12.2.1 Conversion of source products

12.2.1.1 IMS

Trained analysts at the National Ice Center (NIC) produce IMS daily 24 km snow maps once per day, using an interactive workstation application to incorporate a wide variety of satellite imagery, derived mapped products, and surface observations. IMS daily ASCII files were acquired from NIC, converted to binary using NCL, and regridded to EASE-Grid 2.0 with the Mapx tool from NSIDC.

IMS data were compared with the BU-MODIS LOCI 25 km mask. In cases where an ocean pixel was converted to land, a 3x3 moving box filter was used to determine snow cover. With the converted cell in the centre, surrounding land cells were examined and if more than 50 percent of the original surrounding land cells were snow covered, the cell was assigned a snow cover value. Otherwise, the cell was determined to be snow-free land.

In cases where an island pixel was created by converting ocean to land, the same 3x3 box filter was utilized to determine the percentage of adjacent cells with IMS values for ice. If more than 50 percent of the surrounding water cells were ice, the new pixel was assigned a snow cover land value.

Once reconciled with BU-MODIS LOCI 25 km mask, the data were written to the IMS snow cover extent variable.

12.2.1.2 CGF

MODIS Cloud Gap Filled Snow Cover (CGF) data are derived from MOD10C1, the MODIS/Terra Snow Cover Daily L3 Global 0.05Deg CMG fractional snow cover product. MODIS snow-cover products are inherently limited by cloud cover, which obscures the sensor's view of the ground and introduces gaps into the daily snow cover maps. The cloud-gap-filled daily snow cover maps are produced using a simple algorithm that fills cloud-obscured grid cells with a previous day's observation of the ground.

If the cloud cover in a cell is greater than or equal to 80 percent, according to the MODIS cloud mask, the last view of the ground is retained as the observation for the current day. To ensure that users are aware of the age of each observation on a per-grid cell basis, the number of days of cloud cover preceding the image date is tracked and updated daily for every grid cell. These data are written to a separate variable known as the Cloud-Persistence Count (CPC). When a view of the surface is re-acquired after one or more days of cloud cover, the CPC is reset to zero for that grid cell.

The MODIS CGF source product input to this data set was generated at NASA Goddard Space Flight Center (GSFC). Observations were limited to five or fewer days (CPC ≤ 5) and the resulting cloud-gap-

filled snow cover maps were re-gridded to EASE-Grid 2.0 using nearest neighbour interpolation. These data were then delivered to Rutgers University.

At Rutgers, fractional snow cover greater than or equal to 40 percent was set as the threshold for snow-covered land. The data were compared with the BU-MODIS LOCI 25 km mask and ocean pixels that were converted to land were evaluated in the same manner as the IMS product. With the converted cell in the center, a 3x3 moving box filter was used to examine the surrounding land cells. If more than 50 percent of the source data land cells were snow covered, the cell was assigned as snow covered land. Otherwise the cell was determined to be snow-free land. Once reconciled with the BU-MODIS LOCI 25 km mask, the data were written to the *modis_cloud_gap_filled_snow_cover_extent* variable.

12.2.1.3 MW

Snow cover extent was derived from passive microwave brightness temperatures using the *DMSP SSM/I-SSMIS Pathfinder Daily EASE-Grid Brightness Temperatures*, Version 2 data set. In a series of ongoing missions, the Defense Meteorological Satellite Program (DMSP) has been acquiring brightness temperature data since 09 July 1987 with the Special Sensor Microwave/Imager (SSM/I) and Special Sensor Microwave Imager/Sounder (SSMIS) instruments onboard DSMP satellites F8, F11, F13, F17.

The following steps were used to convert brightness temperatures into snow cover:

1. SSMIS F17 brightness temperatures were converted to SSM/I F13 based on the methodology in Meier et al., 2011. Ascending and descending passes were averaged into daily average brightness temperatures.
2. The presence of snow was identified where the 19/37 GHz and 22/85 GHz (91 GHz for SSMIS) vertical polarization frequency gradients exceed minimum thresholds. Additionally, the brightness temperature for the 37 GHz channels (horizontal and vertical polarization) and 85GHz (vertical polarization) must not exceed a maximum threshold. The approach is conceptually similar and uses the same frequency gradients and channels as the AMSR-E Snow Water Equivalent Algorithm (Chang and Rango, 2000). Thresholds were set to achieve a 60 percent probability of detecting snow, determined by: hemispheric comparison with IMS snow; snow depth observations from available stations including the Global Historical Climatology Network, cooperative stations, and the Meteorological Service of Canada; and daily average brightness temperatures during the 2005-2006 snow season.

3. At locations where the elevation exceeds 1500 meters above mean sea level, the 19/37 GHz and 22/85 GHz frequency gradients were reduced by 0.001 K and 0.002 K per meter elevation, respectively. This correction was applied because passive microwave snow retrievals overestimate snow-covered area in high elevation locations, and in particular the Tibetan Plateau, because the decrease in atmospheric thickness increases the spectral gradient (see Savoie et al., 2009). The coefficients were determined by a comparison with high elevation (>1500 m) locations in the same manner discussed in Step 2.

4. In regions with a maximum snow-covered albedo ≤58 percent, the 19/37 GHz and 22/85 GHz frequency gradients were increased by 3 K and 4K, respectively. Because snow that falls through the canopy may not be apparent when on the ground (for example, see Foster et al. 1991), passive microwave snow retrievals underestimate snow covered area in densely forested locations such as the boreal forests. To account for this effect, a maximum snow covered albedo data set (Robinson et al., 1985) was re-gridded to EASE Grid 2.0 and used to identify regions in which snow cover is spectrally masked by vegetation. Coefficients were determined by comparing areas with maximum snow covered albedo ≤58% in the same manner discussed in step 2.

5. The criteria described in Step 2, as modified in steps 3 and 4, were applied to the daily average brightness temperatures to determine the presence or absence of snow. Internally, separate codes were used to track cells with snow cover identified by only the 19 GHz and 37 GHz channels or the 85 (91) GHz channels.

6. Areas of missing data were reduced by employing a six-day gap fill. If data were missing for a given date, the most recent previous date with valid data (up to five days prior) was retained as the observation for the current day.

7. The resulting gap-filled snow cover map was re-gridded to EASE-Grid 2.0 using Mapx.

8. Areas of permanent ice and ocean were masked using the BU-MODIS LOCI 25 km mask. A maximum snow cover extent mask was also applied based on all cells with IMS data that indicated snow on any date during a given month.

9. Intermediate, daily two-byte flat binary files in EASE-Grid 2.0 were created for the microwave snow layer. The data were then written to the *passive_microwave_gap_filled_snow_cover_extent* variable.

12.2.2 Merged snow extent product

Once all snow cover variables were reconciled with the BU-MODIS LOCI 25 km mask, the merged SE variable was generated as follows:

- BU-MODIS LOCI 25 km mask ocean and land pixels were written to an array.
- Values for snow covered land and ocean converted to snow covered land were written to the array.
- BU-MODIS LOCI 25 km mask permanent ice values were written to the array.
- The data were written to the *merged_snow_cover_extent* variable.

12.2.3 MEaSUREs maximum SE for SnowPEx

A maximum SE product was generated at ENVEO using the Merged SE variable in the MEaSUREs product. These values were converted into a binary (snow / no snow) representation of snow cover extent by combining coded values from 10-16 into one value. For each daily file, any pixel indicating snow cover from any source (IMS, CGF or MW) is recorded as snow covered in the SnowPEx output.

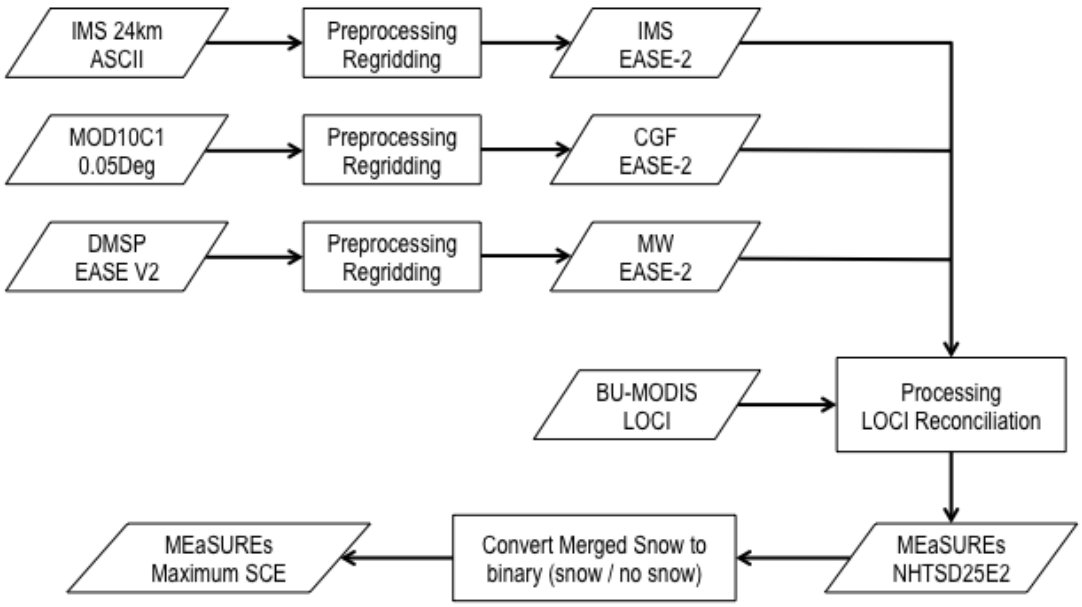

Figure 12.2 shows the overall processing line of the MEaSUREs maximum snow extent product.

12.2.4 Snow mapping algorithm

See Processing line and Algorithm (section 3.2) above for snow mapping details.

12.2.5 Cloud screening

See Processing line and Algorithm, CGF in section 3.2 above. The MODIS cloud-gap-filled daily snow cover maps are produced using a simple algorithm that fills cloud-obscured grid cells with a previous day's observation of the ground.

12.2.6 Input data

The Measures product aggregates the following data sets:

- IMS sourced from NIC (http://www.natice.noaa.gov/ims/) and processed at Rutgers University
- CGF sourced from MOD10C1 (https://nsidc.org/data/mod10c1) and processed at NASA GSFC
- MW sourced from DMSP SSMI SSMI/S brightness temperatures (https://nsidc.org/data/nsidc-0032/) and processed at the University of Georgia

12.2.7 Auxiliary data sets

The MEaSUREs SE product uses an EASE-Grid 2.0, 25 km Land-Ocean-Coast-Ice (LOCI) mask derived from the Boston University MOD12Q1 V004 Land Cover Product (BU-MODIS). For more information about the BU-MODIS LOCI 25 km mask, see EASE-Grid 2.0 Land-Ocean-Coastline-Ice Masks Derived from Boston University MODIS/Terra Land Cover Data. The LOCI mask can be retrieved from https://nsidc.org/data/nsidc-0609

12.3 Quality and validation of product

Missing data represents the biggest impact to data quality, as all of the input products lack some daily files during the period of record. The IMS SE maps are not constructed according to a formal algorithm, but instead rely on the expertise of trained analysts using the IMS workstation. Because the IMS workstation software is continually being evaluated and improved, changes in mapping methodologies have occurred over time. Error sources in the MODIS CGF product are discussed in Hall et al., 2010. For the passive microwave derived SE, errors in the input data may carry through to the output. For details about potential errors in passive microwave brightness temperatures, see the Error Sources section (https://nsidc.org/data/docs/daac/nsidc0032_ssmi_ease_tbs.gd.html#errorsource) of the DMSP SSM/I-SSMIS Pathfinder Daily EASE-Grid Brightness Temperatures, Version 2 documentation.

12.4 Strength and weaknesses of product

The product has the following strengths:

- Combination of three snow products:
    - a) two utilizing the visible portion of the spectrum, one the microwave portion,
    - b) one visible product is fully automated, the other involves human interpretation,
    - c) strengths of one approach can compensate for weaknesses in the others to best determine the presence of snow.

  The three contributing products are presented at uniform spatial and temporal resolution.
- All have the same land/water mask applied.
- All are available in a common format.

The identified weaknesses of the product are:

- Only snow extent, not depth or SWE is mapped.
- Spatial and temporal resolutions vary amongst the original three products.
- Mapping snow extent in each spectral region has well known issues.
- Spatial and temporal resolutions are not as fine as some might like. However, this is a function of a user's needs.

12.5 Contact

Institution	Rutgers, The State University of New Jersey
Contact Person	David Robinson
Email	david.robinson@rutgers.edu
Website for downloading the product:	https://nsidc.org/data/nsidc-0530

12.6 References

Abdalati, W., K. Steffen, C. Otto, and K. C. Jezek. 1995. Comparison of Brightness Temperatures from SSMI Instruments on the DMSP F8 and F11 Satellites for Antarctica and the Greenland Ice Sheet. International Journal of Remote Sensing, 16, 1223-1229. doi:10.1080/01431169508954473.

Brodzik, M. J., B. Billingsley, T. Haran, B. Raup, and M. H. Savoie. 2012. EASE-Grid 2.0: Incremental but Significant Improvements for Earth-Gridded Data Sets. ISPRS International Journal of Geo-Information, 1(1):32-45, doi:10.3390/ijgi1010032

Brodzik, M. J., B. Billingsley, T. Haran, B. Raup, and M. H. Savoie. 2014. Correction: Brodzik, M. J. et al. EASE-Grid 2.0: Incremental but Significant Improvements for Earth-Gridded Data Sets. ISPRS International Journal of Geo-Information 2012, 1, 32-45. ISPRS International Journal of Geo-Information, 3(3):1154-1156, doi:10.3390/ijgi3031154

Chang, Alfred T. C., and Albert Rango. 2000. Algorithm Theoretical Basis Document for the AMSR-E Snow Water Equivalent Algorithm, Version 3.1. Greenbelt, Maryland USA: NASA Goddard Space Flight Center. (PDF, 300 KB)

Foster, J., A. Chang, D. Hall, and A. Rango. 1991. Derivation of Snow Water Equivalent in Boreal Forests using Microwave Radiometry, Arctic, 44 (Supp. 1), 147-152.

Hall, D.K., G.A. Riggs, J.L. Foster, and S.V. Kumar. 2010. Development and Evaluation of a Cloud-Gap-Filled Modis Daily Snow-Cover Product. Remote Sensing of the Environment, 114, 496-503. doi:10.1016/j.rse.2009.10.007

Helfrich, S. R., D. McNamara, B.H. Ramsay, T. Baldwin, and T. Kasheta. 2007. Enhancements to, and Forthcoming Developments in the Interactive Multisensor Snow and Ice Mapping System (IMS). Hydrological Processes, 21:1576-1586. doi:10.1002/hyp.6720

Jezek, K. C., C. Merry, D. Cavalieri, S. Grace, J. Bedner, D. Wilson, and D. Lampkin. 1991. Comparison Between SMMR and SSM/I Passive Microwave Data Collected Over the Antarctic Ice Sheet. Byrd Polar Research Center Technical Report, no. 91-03. The Ohio State University.

Meier, Walt N., Siri Jodha Singh Khalsa, and Matt Savoie. 2011. Intersensor Calibration between F-13 SSM/I and F-17 SSMIS Near-Real-Time Sea Ice Estimates. IEEE Trans. Geosci. Rem. Sens. 49(9), 3343-3349.

Ramsay, B. H. 1998. The Interactive Multisensor Snow and Ice Mapping System. Hydrological Processes, 12:1537-1546. doi:10.1002/(SICI)1099-1085(199808/09)12:10/11<1537::AID-HYP679>3.0.CO;2-A

Robinson, D. A., and G. Kukla. 1985. Maximum Surface Albedo of Seasonally Snow-Covered Lands in the Northern Hemisphere. Journal of Climate and Applied Meteorology, 24, 402-411.

Robinson, D. A., D. K. Hall, and T. L. Mote. 2014. MEaSUREs Northern Hemisphere Terrestrial Snow Cover Extent Daily 25km EASE-Grid 2.0. Boulder, Colorado USA: NASA DAAC at the National Snow and Ice Data Center. doi: 10.5067/MEASURES/CRYOSPHERE/nsidc-0530.001.

Savoie, M., R. Armstrong, M. Brodzik, and J. Wang. 2009. Atmospheric Corrections for Improved Satellite Passive Microwave Snow Cover Retrievals over the Tibet Plateau. Remote Sensing of Environment, 113, 2661-2669. doi:10.1016/j.rse.2009.08.006

Stroeve, J., J. Maslanik, and L. Xiaoming. 1998. An Intercomparison of DMSP F11- and F13-Derived Sea Ice Products. Remote Sensing of Environment, 64, 132-152. doi:10.1016/S0034-4257(97)00174-0

13. CRYOLAND FSC (CRYOL)

Authors: Gabriele Bippus, Thomas Nagler, Elisabeth Ripper (ENVEO), Sari Metsämäki (SYKE)

13.1 Product Overview and Specification

The pan-European snow cover service provides a homogeneous fractional snow cover product (0 % - 100 % FSC) for the area extending from 72°N/11°W to 35°N/50°E. The algorithm compensates for the effects of the forest and estimates the below-tree FSC. The product, and associated accuracy estimation (root mean square error) per pixel, is provided daily with 0.005° spatial resolution (approx. 500 m). The product is based on medium resolution optical satellite data from Terra MODIS (in the future Sentinel-3) distributed by NASA.

Table 13.1:
Summary on CryoLand pan-European fractional snow cover product.

Parameter	***Specification***
Thematic variable	Fractional Snow Cover (SCF)
Thematic resolution	1% FSC
Thematic range	[1, 100] FSC
Thematic accuracy	~20%
Thematic uncertainty estimate	RMSE per pixel;
Product Quality Map	Uncertainty map calculated and attached to daily products
Spatial resolution	0.005° × 0.005° (ca 500m)
Spatial coverage	Pan-European region: 72°N 11°W – 35°N 50°E
Product available since	Daily products, since November 2000
Delivery time period	Full Year, daily (since Dec 2013 in Near Real Time)
Temporal frequency	Daily
Projection/Datum	Geographical (lat/lon) / WGS84
Cloud Screening	MODIS Cloud Product
Invalid / Masked Areas	Open Water (sea, lakes, rivers)
Sensor	Terra MODIS
Satellite data level	Level 1B Swath data
File format	GeoTIFF
Developed by	CryoLand
Provider / Generated by	ENVEO / SYKE
Product available at	https://www.cryoland.eu
Contact	Thomas Nagler / ENVEO / thomas.nagler@enveo.at

The final product is provided to the users daily in the late afternoon via FTP and the CryoLand web service (http://neso.cryoland.enveo.at/cryoclient/), only a few hours after the last image acquisition over the area of interest. In Table 13.1 the specifications of the CryoLand FSC product are summarized.

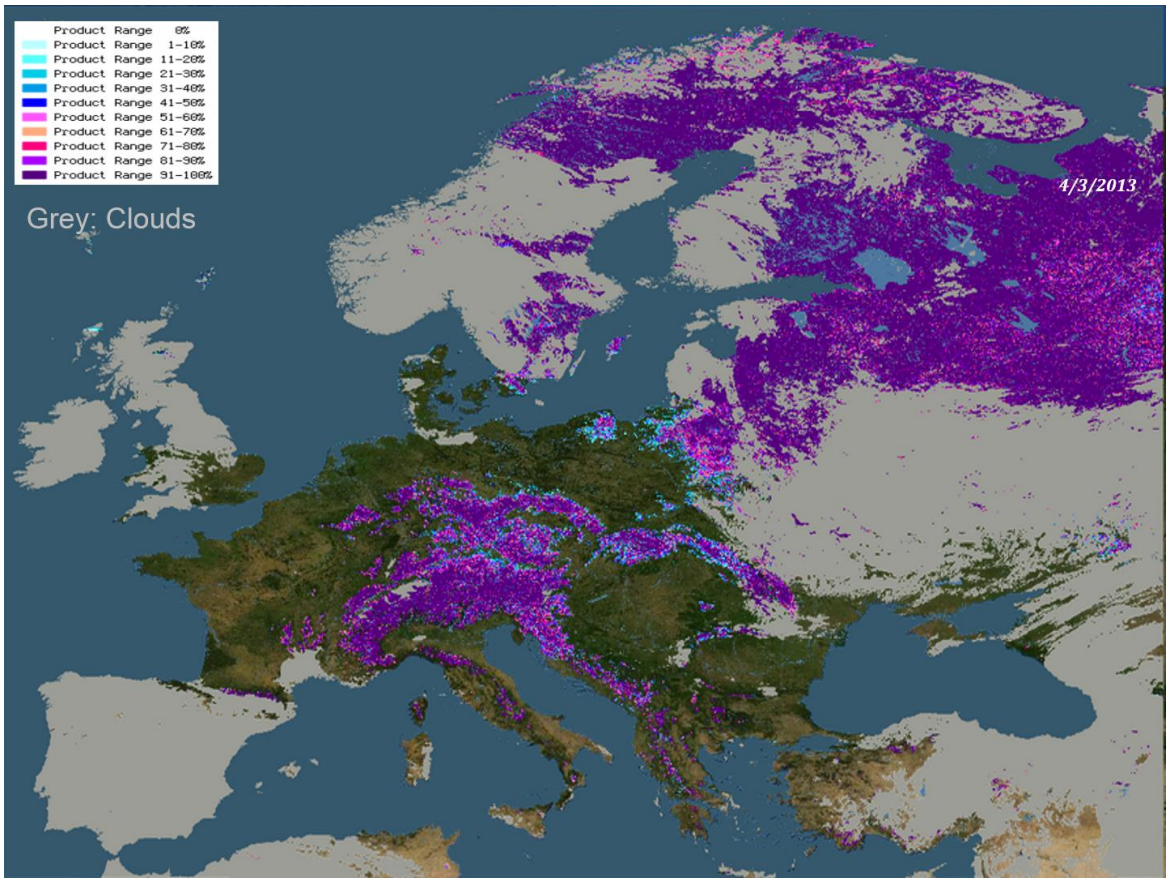

Figure 13.1: CryoLand Fractional Snow Extent product from MODIS data, 9 March 2012.

13.2 Processing line and Algorithm

Figure 13.2 shows the overall processing line of the CryoLand fractional snow extent products. Input data are optical satellite data from MODIS / TERRA.

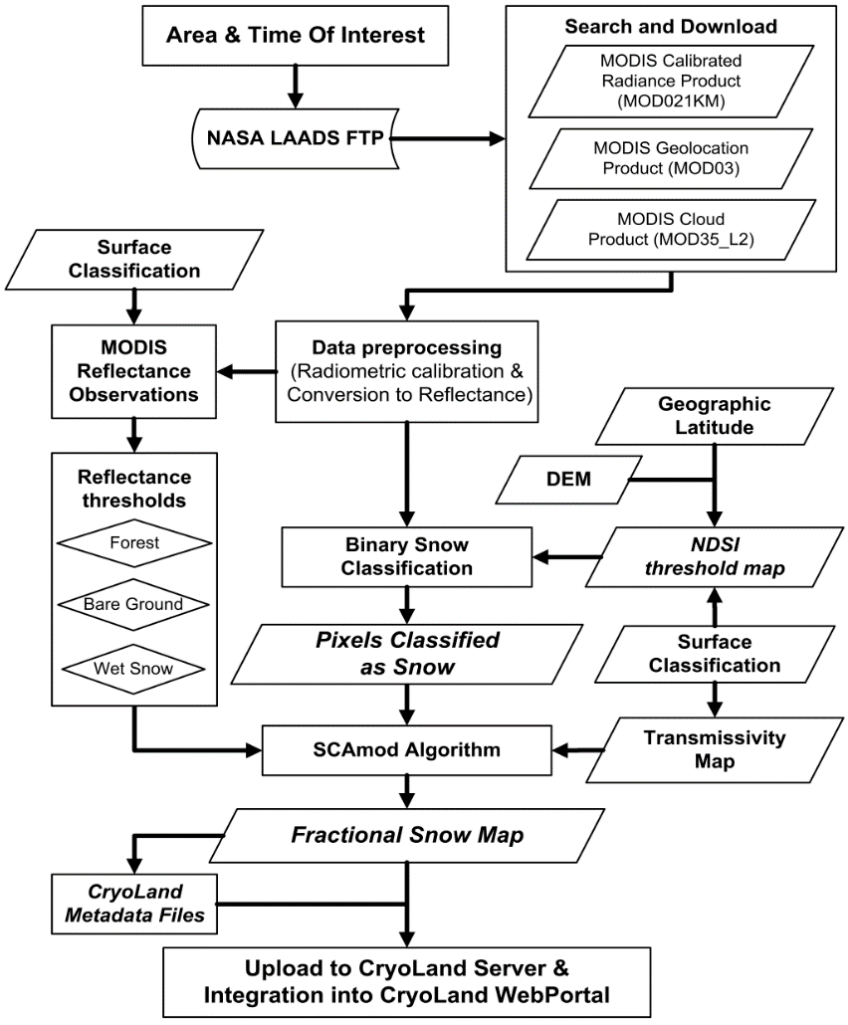

Figure 13.2: Processing line of CryoLand Pan European fractional snow extent product.

13.2.1 Snow Mapping Algorithm

Based on the top of atmosphere reflectances generated from MODIS bands, a strict binary snow pre-classification is made using the Normalized Difference Snow Index (NDSI), which is based on the different reflectivity of snow and other surfaces in the visible and mid-infrared wavelengths (Hall et al., 2002). A NDSI threshold map changing with the geographic latitudes and with terrain elevation is used for the strict preliminary binary snow classification.

In order to avoid misclassifications of pixels located in small cloud gaps, the information of a brightness temperature (TB) band is used. As the land surface is usually warmer than cloud temperature, and misclassifications of snow in pixels surrounded by clouds were mainly observed when the land surface

temperature was already far above freezing temperatures, the following classification rule is applied on the emissive MODIS band 31 (10.780 µm - 11.280 µm) with 1 km grid size:

$$IF\ (T_B(11\mu m) >= 283.0\ K)\ THEN\ FSC = 0 \qquad (Equ.\ 13.1)$$

In a second step the SCAmod algorithm (Metsämäki et al., 2012), described in detail in section 5.2 is applied on all pixels classified as snow by the pre-classification using the NDSI and the additional threshold on the brightness temperature.

Pre-defined typical reflectance values for forested areas, bare ground and wet snow are needed for the SCAmod algorithm. According to Metsämäki et al. (2012) these reflectance values are set as 0.65 for wet snow, 0.08 for forest canopy, and 0.10 for snow-free ground.

The snow classification is applied on each of the MODIS scenes needed for a complete coverage of the pan-European area. As soon as the generation of the particular snow maps is completed, the product is merged to one large snow map. For overlapping snow-free pixels on image boundaries the pixels with the steepest local sensor incidence angle are used for the merged product in order to get the best available information. If a pixel of the overlapping image part is classified as cloud in one scene, and as any other class in another scene, the classification of the cloud-free pixel is used.

During the polar night a snow classification is not possible in the northern latitudes of the pan-European area. All pixels with solar zenith angle greater than 84° are classified as “polar night”.

13.2.2 Cloud Screening

The daily MODIS cloud mask (MOD35) is used for the CryoLand FSC. The MODIS cloud product (http://modis.gsfc.nasa.gov/data/dataprod/dataproducts.php?MOD_NUMBER=35) is automatically downloaded for the area of interest as soon as the data are available on the server.

Of the MODIS cloud product with 500 m pixel size all classes with probable occurrence of clouds are used for the cloud mask. Only confident clear pixels are excluded. The MODIS cloud product is checked for data gaps, which are filled by averaging neighbouring pixels. No other filter or pre-processing operation is applied on the MODIS cloud product. The reliability of the MODIS cloud product is partly limited, especially in case of clouds over snow covered areas. Therefore, the NDSI pre-classification described before is useful for distinguishing between snow and cloud pixels.

13.2.3 Input Data

The CryoLand FSC product is based on Terra MODIS (Version 5) data, retrieved from the FTP sites LAADS (Level 1 and Atmosphere Archive and Distribution System) Web and LANCE (Land Atmosphere Near Real-time Capability for EOS) hosted by NASA. The following MODIS products are automatically downloaded daily for the area of interest as soon as the data are available on the server:

- Level-1B calibrated radiance product with 1 km and 500 m spatial resolution (MOD02)
- geo-location product (MOD03)
- MODIS cloud product (MOD35_L2)

13.2.4 Auxiliary Data Sets (Static)

The following auxiliary data sets are used for the CryoLand FSC product generation:

- Digital Elevation Model (EU-DEM, SRTM V4, ASTER GDEM V2)
- Surface classification (CORINE Land Cover 2006, GLOBCOVER 2009)
- Transmissivity map
- NDSI threshold map

Over European countries, the digital elevation model EU-DEM is used for the processing of the pan-European snow map. The EU-DEM has been generated by the Initial GMES Service for Geospatial Reference Data Access (GSGRDA) from ASTER GDEM, corrected with data from SRTM, NEXTMap, Landsat and other data sets. For the remaining areas, a combined DEM based on elevation data from SRTM (Shuttle Radar Topography Mission, Version 4; Jarvis, Reuter, Nelson, & Guevara, 2008) for the latitude range 60°N – 35°N, and on the ASTER GDEM V2, a joint product of METI and NASA, for the northern latitudes, between 60°N and 72°N is used.

For the surface classification the CORINE Land Cover 2006 (CLC2006) data set, Version 16, published by the European Environment Agency (EEA) in April 2012 is used over large areas in Europe. For regions not covered by the CLC2006 product, the GlobCover 2009, Version 2.3, released by the DUE GlobCover project of ESA in December 2010, is used. The GlobCover product has a lower spatial resolution compared to the CLC2006 data set, but is available globally. Based on the land-cover classification a homogeneous surface mask using CryoLand coding was generated, including the classes water (differentiating sea, lake and river), bare ground, glacier, forest and urban area.

The transmissivity describes the transparency of the forest canopy and is related to crown coverage. The generation of the mandatory transmissivity map from MODIS and GlobCover data is described in Section 5.2.4. For the CryoLand FSC product generation the transmissivity map has been upgraded to 500 m pixel size for the Pan-European area.

The NDSI threshold map is used for a binary snow pre-classification. By default, the NDSI threshold north of 58°N is set to a minimum of -0.10. A linear gradient is applied on the NDSI threshold to change between 58°N and 38°N from -0.10 to +0.50. South of 38°N, the NDSI threshold is set constant to +0.50. A NDSI threshold of +0.70 is allotted to areas classified in the CORINE Land Cover 2006 (CLC2006, EEA, 2012) data set as rice fields, permanent irrigated lands, salt marshes, salines, or intertidal flats in order to avoid misclassifications due to very-high reflectivity of these areas. Additionally with the geographic latitude the NDSI thresholds change with the surface elevation derived from the digital elevation model. For altitudes above 500 m a.s.l. the NDSI threshold decreases linearly about 0.01 per 100 m elevation interval. Thus, for example high altitudes in the main alpine mountain ridge have also the minimum NDSI threshold of -0.10.

13.3 Quality and Validation of Product

For evaluating the CryoLand Pan-European FSC product, a set of 59 Landsat scenes, 39 SPOT-5 scenes, 4 WorldView-1/-2 and 1 Quickbird scenes were used, assuming that these very high and high resolution optical satellite data represent the ground truth. Only reference data with clear sky conditions, acquired between 2000 and 2014 are used.

Binary and fractional snow cover maps are derived from the Landsat scenes applying the algorithms of Dozier and Painter (2004), Klein et al. (1998), Salomonson and Appel (2006) and a multi-spectral unmixing approach developed by ENVEO (only for non-forested areas). ENVEO's approach is only applied on 20 Landsat scenes, as the algorithm is tailored to non-forested high-alpine terrain. Snow maps from the very high resolution optical satellite data were mapped manually. The resulting (very) high resolution snow maps are resampled to the spatial resolution of the CryoLand FSC product, calculating the associated fractional snow cover for the coarse resolution based on the high resolution snow information. The CryoLand and the reference snow maps are then intercompared pixel by pixel, calculating statistical measures Correlation Coefficient, Root Mean Square Error (RMSE), unbiased RMSE and Bias for assessing the quality of the CryoLand product.

The mean unbiased RMSE for all Landsat snow maps generated with the algorithms of Dozier, Klein and Salomonson compared with the CryoLand FSC product is about 16 %, with mean Bias ranging

between about -2 % and +3 %. The mean unbiased RMSE derived for the intercomparison with the very high resolution snow maps is slightly better, with about 15 %, and for Landsat scenes the ENVEO algorithm was applied on it is about 11 %.

In Table 13.2 the detailed statistical results for the intercomparison of the CryoLand FSC product with the reference snow maps are provided.

Table 13.2:
Results of CryoLand pan-European FSC product evaluation with snow maps generated with different algorithms from Landsat data and manually mapped from very high resolution optical satellite data (SPOT-5, WorldView-1/-2, Quickbird).

MEASURE		Landsat scenes				VHR scenes
		Dozier	Klein	Salomonson	ENVEO	Manual mapping
Number of scenes		59	59	59	20	44
unbiased RMSE	MIN	3,00	3,14	2,63	2,26	0,00
	MAX	25,96	26,17	25,01	17,29	38,75
	AVERAGE	15,93	15,86	15,76	11,08	15,36
	1st QUARTILE	11,46	11,87	12,45	8,63	9,22
	3rd QUARTILE	19,69	19,83	19,61	12,84	22,42
BIAS	MIN	-12,91	-5,28	-20,14	-2,64	-13,45
	MAX	6,64	12,21	7,01	5,92	44,64
	AVERAGE	-0,70	2,78	-1,89	0,27	3,02
	1st QUARTILE	-2,07	0,43	-3,64	-1,72	-0,26
	3rd QUARTILE	1,36	5,26	1,29	1,14	5,52
RMSE	MIN	3,00	3,17	2,64	2,28	0,00
	MAX	28,98	28,88	27,87	17,49	59,11
	AVERAGE	16,27	16,42	16,48	11,26	16,85
	1st QUARTILE	11,52	12,21	12,58	8,70	9,51
	3rd QUARTILE	20,58	20,46	20,01	13,38	23,49
Correlation Coefficient	MIN	0,00	0,00	0,07	0,52	-0,05
	MAX	0,97	0,96	0,97	0,99	0,92
	AVERAGE	0,75	0,74	0,75	0,88	0,74
	1st QUARTILE	0,61	0,63	0,61	0,87	0,69
	3rd QUARTILE	0,93	0,92	0,92	0,96	0,86

13.4 Strengths and weaknesses of product

Strengths:

- Daily product generation in near-real time (latency time: ca 6 hours)
- Continuous time series available since winter 2000/01
- Daily uncertainty measure (RMSE) is provided per pixel
- Product is provided with 500 m pixel size
- SCAmod reflectance model compensates the forest canopy effect on the observed reflectance and thus allows more accurate SCF retrieval in forested areas

Weaknesses:

- Product extends only the Pan-European area
- Misclassifications occur sometimes along the margins of cloud masks and inland water bodies masks
- The used transmissivity map is static, and does not correct for changes in forest density or coverage

13.5 Contact

Institution	ENVEO IT GmbH
Contact Person	Dr. Thomas Nagler
Email	Thomas.nagler@enveo.at
Website for downloading the product:	http://www.cryoland.eu

13.6 References

Dozier J, Painter TH (2004) Multispectral and hyperspectral remote sensing of alpine snow properties. Annu. Rev. Earth Planet. Sci. 32:465 – 494

Hall DK, Riggs GA, Salomonson V V., DiGiromamo N, Bayr KJ (2002) MODIS snow-cover products. Remote Sensing of Environment 83:181–194.

Jarvis A, Reuter HI, Nelson A, Guevara E (2008) Hole-filled SRTM for the globe Version 4, available from the CGIAR-CSI SRTM 90m Database. Available at: http://srtm.csi.cgiar.org

Klein AG, Hall DK, Riggs GA (1998) Improving snow cover mapping in forests through the use of a canopy reflectance model. Hydrol. Process. 12:1723–1744

Metsämäki S, Mattila O-P, Pulliainen J, Niemi K, Luojus K, Böttcher K (2012) An optical reflectance model-based method for fractional snow cover mapping applicable to continental scale. Remote Sensing of Environment 123:508–521

Salomonson V., Appel I (2004) Estimating fractional snow cover from MODIS using the normalized difference snow index. Remote Sens. Environ. 89:351–360 Available at: http://linkinghub.elsevier.com/retrieve/pii/S0034425703002864 [Accessed January 21, 2014].

Salomonson VV, Appel I (2006) Development of the Aqua MODIS NDSI fractional snow cover algorithm and validation results. IEEE Trans. Geosci. Remote Sens. 44:1747–1756 Available at: http://ieeexplore.ieee.org/lpdocs/epic03/wrapper.htm?arnumber=1645275.

14. H-SAF10 / H-SAF31 SNOW EXTENT PRODUCT

Authors: Mathias Takala (FMI)

14.1 Product Overview and Specification

EUMETSAT H-SAF Snow products H10 and H31 differentiate whether pixel is snow covered or bare ground. Flat areas are derived from LSA SAF product H31 and Turkish State Meteorological Service (TSMS) provides mountainous areas. FMI merges these two areas to single product. Product is generated for SEVIRI (Spinning Enhanced Visible Infra-Red Imager) images of Meteosat-satellite series in the native projection. Also cloud, water, dark and no data pixels are flagged.

Table 14.1:
Summary on pan-European binary snow product H10 and H31.

Parameter	***Specification***
Thematic variable	Binary
Thematic resolution	Status Flag
Thematic range	No data, Dark, Water, Bare ground, Cloud, Snow
Thematic accuracy	-
Thematic uncertainty estimate	-
Product Quality Map	None provided
Spatial resolution	depends on geometry, (ca 8 km)
Spatial coverage	Pan-European region: 75°N 25°W – 25°N 45°E
Product available since	Since 2009 (H-SAF10), since 2008 (H-SAF31)
Delivery time period	Full Year
Temporal frequency	Daily
Projection/Datum	Seviri disk
Cloud Screening	Cloud screening is part of the H10/H31 algorithm
Invalid / Masked Areas	No data, Dark, Water, Cloud
Sensor	Spinning Enhanced Visible Infra-Red Imager (SEVIRI)
Satellite data level	
File format	HDF 5
Developed by	EUMETSAT H-SAF
Provider / Generated by	FMI / TSMS
Product available at	http://hsaf.meteoam.it
Contact	Panu Lahtinen / FMI / panu.lahtinen@fmi.fi; Niilo Siljamo / FMI / niilo.siljamo@fmi.fi

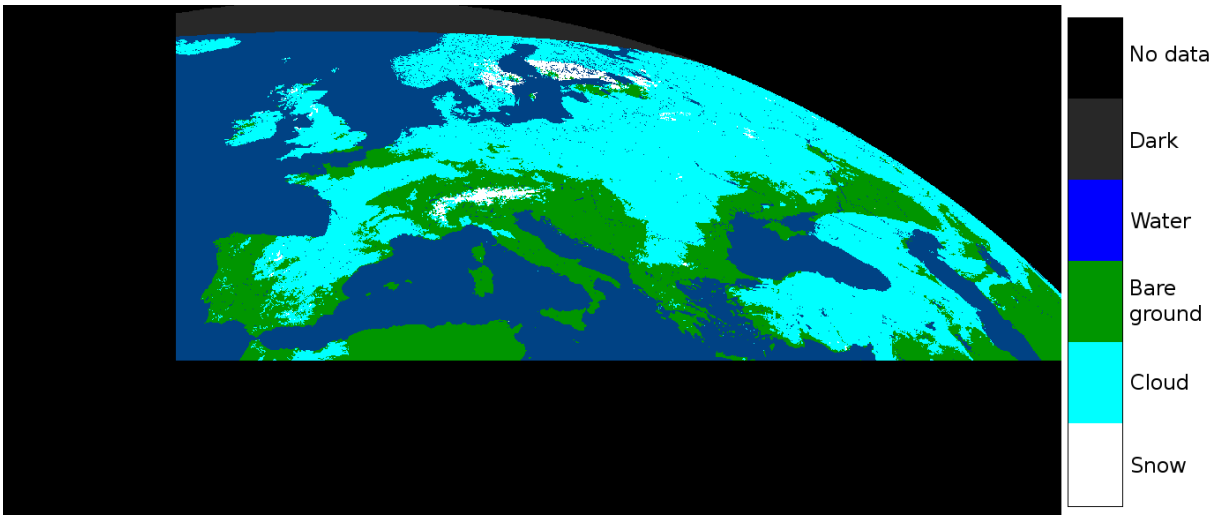

Figure 14.1: Example of H10 snow product, 9 March 2012.

14.2 Processing line and Algorithm

The processing line for SC on flat lands (operations are made by LSA SAF in Portugal), developed by the Finnish Meteorological Institute (FMI), consists of two separate units (Figure 14.2). Unit 1 refers to production of instantaneous snow cover maps from 15- minutely imagery. Unit 2 combines these 96 images from latest 24 hours to a single daily product [ATBD]. The corresponding block diagram for mountainous areas, developed by the Middle East Technical University (METU) and the Turkish State Meteorological Service (TSMS) is shown in Figure 14.3.

The following text and figures are from the ATBD:

For flat and forested areas, the LSA-SAF snow cover algorithm is basically a thresholding method based on the different properties of the snow covered and snow free surfaces and clouds. The LSA-SAF snow cover is a daily product, but it is produced in two separate phases. Phase 1 is the SC1 snow cover product which is based on one cycle of SEVIRI images (every 15 minutes). All of the SC1 products are used to produce the daily LSA-SAF snow cover product (SC2).

The classification starts by setting all the pixels as unclassified. Then several tests are applied one by one until all the rules have been applied. As a result, each pixel is classified to one of the snow cover (or snow free) classes or remains unclassified. Usually the pixel is unclassified if it is too dark, cloudy or in the area where satellite elevation angle is too low. There are also rules which remove obvious misclassifications such as pixels where the land surface is too warm to contain snow.

The class of partial or in some sense probable snow is used if the pixel is both snow free and snow covered during the same day or if the snow cover in the pixel is patchy or otherwise partial. This class is not yet well defined, because there are only a very limited number of reliable surface observations which could be used to estimate the accuracy of this classification.

Once per day the daily Snow Cover (SC2) product is calculated using the SC1 products of the day. Again the system classifies each pixel as snow free, partially snow covered or totally snow covered. For the daily LSA-SAF snow cover product, all snow cover maps which are produced every 15 minutes are combined. The algorithm counts the number of different classifications for each pixel and then determines the final daily classification if there has been reasonable amount of cloud free observations during the day.

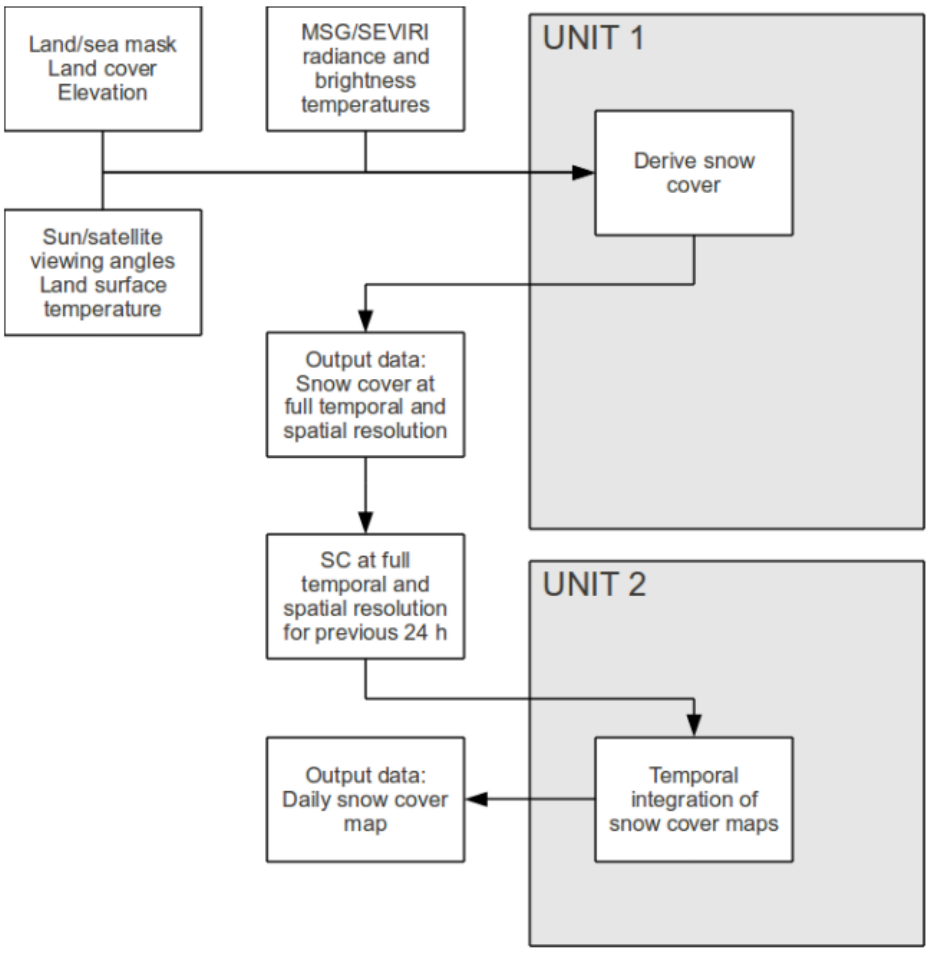

Figure 14.2: Overall processing line of the EUMETSAT H-SAF product for flat areas [ATBD].

For mountainous areas the algorithm is based on a spectral thresholding method applied on sub-pixel scale of MSG-SEVIRI images. No atmospheric correction was applied for the images and top of the atmosphere (TOA) values were used in the algorithm. The different spectral characteristics of cloud, snow and land determines the structure of the algorithm. The threshold values for the mountainous areas were collected from the RGB composite images where channel 1 (centered at 0.64 µm), channel 3 (centered at 1.64 µm), channel 4 (centered at 3.9 µm) and channel 9 (centered at 10.8 µm) were used.

Daily snow cover map is obtained from the snow cover maps obtained for each individual 15 minutes image by accepting pixels having at least 3 snow hits among 32 images during a day. Finally, a daily thematic map has been produced which is consisting of 4 different classes: snow, cloud, water and bare ground.

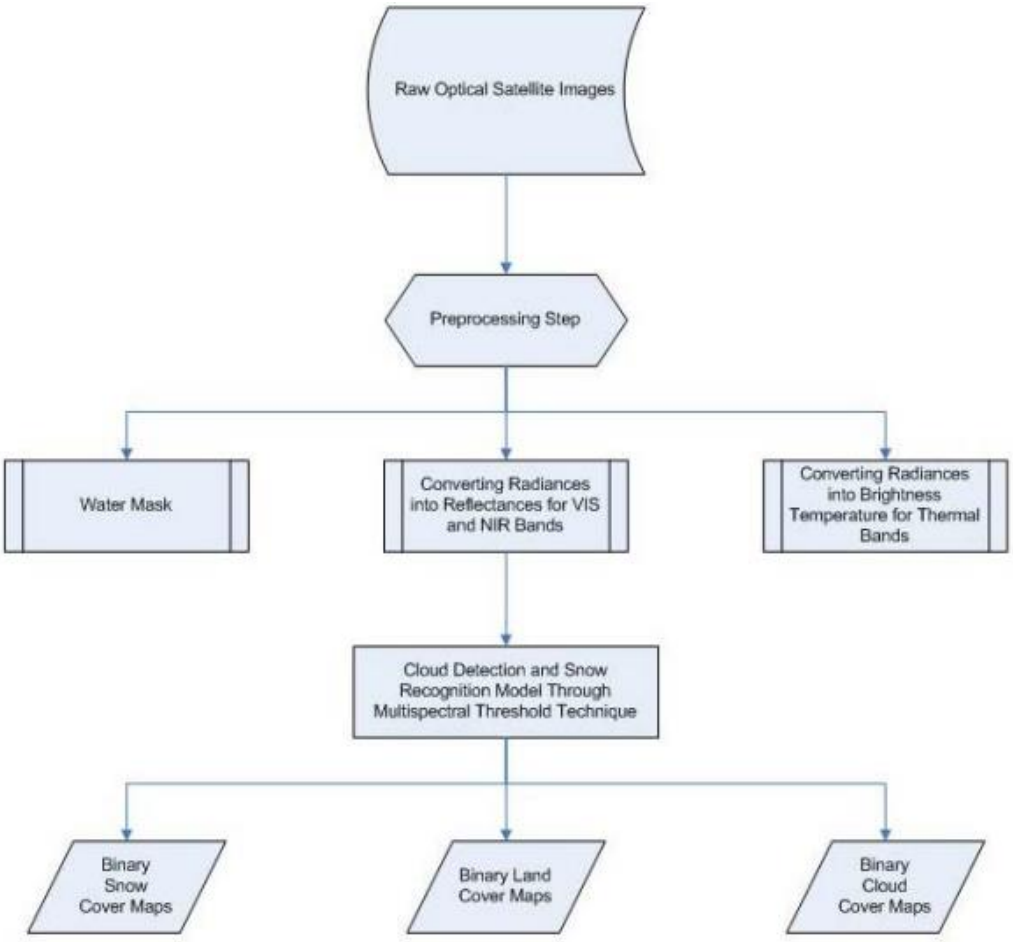

Figure 14.3: Overall processing line of the EUMETSAT H-SAF product for mountainous areas [ATBD].

Although the products for flat/forested areas and for mountainous areas generated by FMI and TSMS cover the full H-SAF area, their quality differs in different areas, the product from FMI being tuned for flat/forested areas, that one from TSMS being tuned for mountainous areas. However, a single product is distributed to the users, obtained by merging the two products in such a way that in flat/forested areas the FMI product is captured, and in mountainous areas the TSMS product is captured. The distinction is determined by the "mountain mask", that was defined by METU.

The products from the institutes have different projections and nearest neighbourhood approach was selected for data co-location. The main idea of the merging algorithm is to minimize projection errors and try to reflect the strengths of the two algorithms in the final merged product. A mask based on digital elevation model (DEM) was used to separate the mountainous pixels from flat/forested areas.

The merging algorithm finds the exact location of the non-mountainous pixels using this mask. These values are then replaced with the ones from the product for flat and forested areas.

14.3 Cloud Screening

Discriminating cloud and snow pixels is the challenging part in snow cover mapping. In order to get rid of cloud covered pixels, cloud mask (CMa) and cloud type (CT) products of Nowcasting Satellite Application Facilities (SAFNWC) (SAF/NWC/IOP/MFL/SCI/SUM/01 2007: the User Manual for the Cloud Products of the SAFNWC/MSG) have been used. After detailed analysis on CMa and CT products of SAFNWC, a combination of these products in order to integrate into the proposed snow recognition algorithm as the cloud recognition part has been generated. As cloud mask (CMa) cloud filled class (pixel value class 3), indicating the opaque clouds completely filling the IFOV, was used. As cloud types; high opaque and stratiform, very high opaque and stratiform and high semitransparent thick clouds were used. These cloud mask class and cloud types were obtained through intensive visual interpretation of the SEVIRI images for the winter season in 2007. If the cloud mask and cloud type products of SAFNWC were not available, clouds were determined based on thresholds for channel 1, channel 3, channel 4 and channel 9. Snow cover maps using MSG-SEVIRI data have been produced for each 15 minutes cycle between 8:00-15:45 UTC that makes 32 individual images a day. All individual 15 minute images acquired during a day are subjected to a series of thresholding tests based on spectral signatures and temporal stability criteria. First, the high visible reflectance of snow was considered and pixels having reflectance values higher than 0.30 were collected. The classification algorithm uses the snow index (SI), obtained by dividing NIR1.6 to VIS0.6. The idea of using the ratio of the visible to the middle-infrared or short-wave infrared reflectance to identify snow in satellite

images was proposed by Bunting and d'Entremont 1982. Due to a low reflectance of the snow cover in the middle infrared and a high reflectance in the visible, the snow index enhances the difference of the spectral response of the snow cover from the response of other surfaces. The pixels having NIR1.6 / VIS0.6 values lower than a fixed threshold value of 0.80 have been collected. To establish channel 1 T and channel 3 T and the model approximating the land surface reflectance anisotropy in the visible and in the shortwave infrared, the statistics of MSG cloud-clear observations accumulated during snow-free periods of the first 6 months of 2007 were used.

Then, pixels having low sun zenith angle (SZA) were discarded by a filter accepting pixels having sun zenith angle higher than 5°. A final test for covering all cold pixels below freezing point has been applied and pixels having temperature lower than 288 K on channel-9 (IR10.8) were accepted considering that the temperature of snow cannot exceed the freezing point (Romanov et al. 2003).

14.4 Contact

Institution	Finnish Meteorological Institute
Contact Person	Panu Lahtinen, Matias Takala, Niilo Siljamo
Email	panu.lahtinen@fmi.fi, matias.takala@fmi.fi; niilo.siljamo@fmi.fi
Website for downloading the product:	http://hsaf.meteoam.it; http://landsaf.meteo.pt/

14.5 References

Algorithm Theoretical Baseline Document (ATBD) for product H10, version 1.1 16 May 2011. http://hsaf.meteoam.it/documents/ATDD/SAF_HSAF_ATBD-10_1_1.pdf

Algorithm Theoretical Baseline Document (ATBD) for product H31, version 0.3, 26 May 2010. http://landsaf.meteo.pt/GetDocument.do?id=279

Bunting J.T. and R.P. d'Entremont, 1982: "Improved cloud detection utilizing defense meteorological satellite program near infrared measurements". Air Force Geophysics Laboratory, Hanscom AFB, MA, AFGL-TR-82-0027, Environmental Research Papers, No. 765, 91 pp.

Romanov P., D. Tarpley, G. Gutman and T.R. Carroll, 2003: "Mapping and monitoring of the snow cover fraction over North America". Journal of Geophysical Research, 108:D16:8619.

15. EURACSNOW – BINARY SNOW EXTENT PRODUCT

Authors: Claudia Notarnicola, Bartolomeo Ventura/EURAC, Bolzano, Italy

15.1 Product overview and specification

The EURAC snow product provides information on the snow extent (binary) at 250 m resolution. The maps are produced daily and from 2009 thanks to the EURAC receiving station are provided in near real time (within the same day of the image acquisition) to the Civil Protection of the Autonomous Province of Bolzano (Italy).

Table 15.1:
Summary on EURACSnow snow cover product.

Parameter	***Specification***
Thematic variable	Snow cover Binary
Thematic resolution	Binary
Thematic range	[0,1] = no snow, 1 snow
Thematic accuracy	~90% based on ground data and LANDSAT images
Thematic uncertainty estimate	
Product Quality Map	Not available in the actual file, can be available on request
Spatial resolution	0.0025° × 0.0025° (ca 250m)
Spatial coverage	Alpine areas: 43°-48° N / 5°-15°E
Product available since	Daily products, since January 2002
Delivery time period	Full Year, daily (since Nov 2009 in Near Real Time)
Temporal frequency	Daily
Projection/Datum	UTM / WGS84
Cloud Screening	MODIS Cloud Product
Invalid / Masked Areas	Open Water (sea, lakes, rivers)
Sensor	Terra MODIS
Satellite data level	Level 2G Grid data
File format	GeoTIFF
Developed by	EURAC
Provider / Generated by	EURAC
Product available at	http://webgis.eurac.edu/snowalps/
Contact	Claudia Notarnicola / EURAC / claudia.notarnicola@eurac.edu (algorithm part) Bartolomeo Ventura /EURAC / bartolomeo.ventura@eurac.edu (data delivery & processing chain)

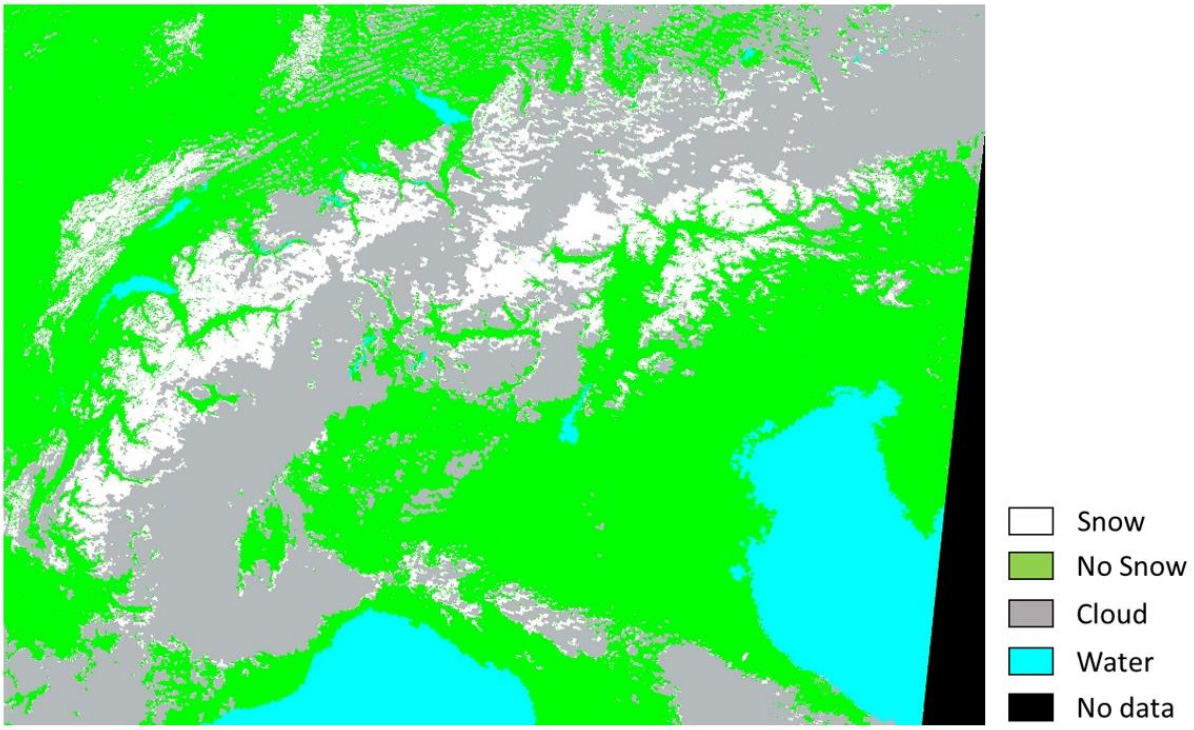

Figure 15.1: Example of EURAC snow product (binary snow cover), 9 March 2012.

15.2 Processing line and algorithm

15.2.1 Snow mapping algorithm

The overall processing line is given in Figure 15.2. It is divided into three major parts. In the first part, the input data, is prepared for the classification (re-projection, calibration, water body masking). The second part of the algorithm is mainly devoted to snow cover is composed of two modules. The first module is dedicated to snow detection based on the 250 m resolution MODIS bands and on Normalized Difference Vegetation Index (NDVI). The second module is related to the detection of snow in forest (Figure 15.2).

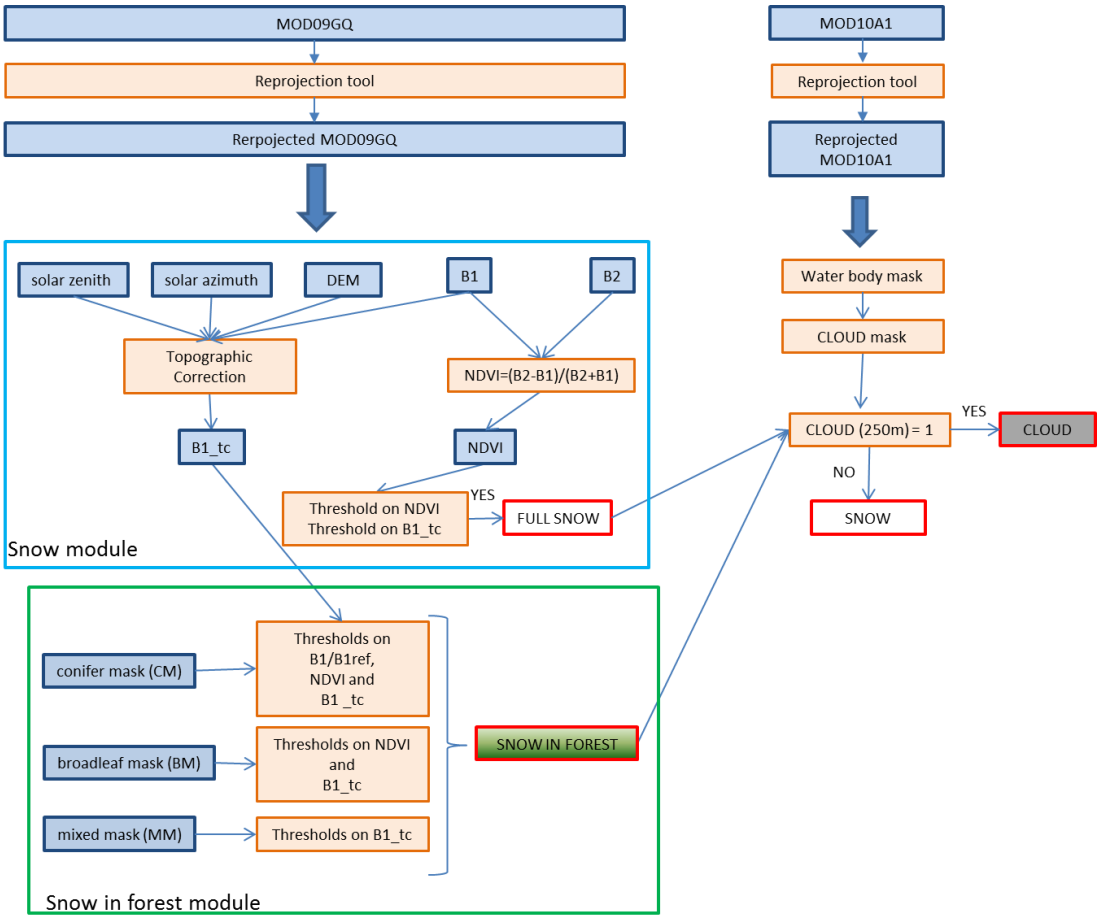

Figure 15.2: Processing line of EURAC snow extent product (adapted from Notarnicola et al., 2013a)

15.2.1.1 Pre-processing of MODIS data

All pre-processing steps were conceived to work both with MODIS data downloadable from NASA websites and with MODIS data received in near real-time from operating receiving stations. For this reason, part of the processing was tailored to work with the antenna facilities. In fact, the data are processed at EURAC's processing and archiving facility conceived to deal with near real-time images, directly received through the EURAC receiving station located at Renon Peak (2,230 m). This allows ingesting the data directly from the antenna into the snow algorithm.

The re-projection tool is organized in order to be adjusted to the processing chain of the receiving station. This processor is designed to re-project all MODIS bands that are necessary to compute the SCA map over the defined area of interest into in UTM WGS824 (other projects can be used based on requests).

As topography can have a high influence on the reflectance, band 1, mainly used for snow detection, also underwent a topographic correction. This procedure is fundamental, as it reduces the effect of topography on the signal. When single bands are used, the topographic correction has to be performed in order to reduce the shadowing effects and their changes due to the seasonal cycle. This operation converts the reflectance to normalized reflectance, as if the surface was fully horizontal. The topographic correction is a modified cosine correction, where some coefficients are empirically evaluated in order to reduce the typical over- and underestimation of the standard cosine approach (Civco, 1980). Details are available in Notarnicola et al., 2013a.

15.2.1.2 Snow module

The resolution of 250 m provides the possibility to detect smaller snow covered surfaces, especially in mountainous areas that are characterized by extreme heterogeneous landscapes. The MODIS 250 m resolution bands are the red and the near-infrared channels, named in the following B1 and B2, respectively. To maintain the 250 m resolution, the methodology proposed here is adapted from Metsämäki et al. 2002 and Malcher et al. 2003 and is based on the rationale that B1 and B2 reflectances are, in general, very high with respect to other natural objects (rocks, bare ground, forest) even though they change according to different snow conditions.

For the pure snow detection, the NDVI is calculated from the two bands of MODIS 250 m (either MOD09GQ or MYD09GQ) products. Pixels are classified as “snow” after application of thresholds to NDVI and reflectance values of B1, mainly for detection of snow in forested areas (snow detection in the forest module). As a main difference, the NASA standard algorithm uses the NDSI at 500 m resolution for both, pure snow detection along with NDVI to better constrain the detection of snow in a forested area (Hall et al., 2002). The thresholds are determined on a statistical base by using numerous images from different years and different seasons within one year in order to take into account the changing reflectance variability of different types of snow.

Snow is detected for NDVI values below 0.10. Furthermore, it has been proved that the use of NDVI avoids the overestimation of the snow cover area due to increased reflectance from seasonal vegetation, especially at the end of the winter season (Metsämäki et al., 2002).

15.2.1.3 Module for snow detection in forest

For the detection of snow in forested areas, a multi-temporal approach is used, exploiting for B1 the ratio between the image to be classified and a snow-free reference image. As a reference image, an

average of ten eight-day composite images is considered to have stable reference and to avoid the daily fluctuations of the reflectance.

Pixels with ratio values above a certain threshold, which is different for the different forest types, are classified as snow covered. For mapping purposes, the forest standings are divided in pure coniferous standings (evergreen), pure broad-leaved standings (deciduous) and mixed forest, as each class can interact with snow differently, based on its own proper characteristics.

Conifer: Soon after a snowfall, snow may lie on the tree crown or branches for a short time. If B1 reflectance values are very high, in case of dense forest stands (NDVI values over a certain threshold), the presence of snow on the conifer trees can also be detected. Afterwards, the snow falls below the tree crown due to wind action, the snow weight itself, and can also disappear due to melting. Therefore, the radiometric contribution of the snow under the trees is partially masked by the tree canopy. The pure coniferous standings cover the snow beneath and hinder its detection with the optical sensors. In this case, the NDVI value and the ratio between the actual image (snow) and the reference image are considered. The approach is adapted after Klein et al. 1998, but exploits only the NDVI variation in the multi-temporal comparison. Three thresholds are defined for the following values:

- NDVI is lower for forest in winter with respect to summer with values around 0.2–0.4 (Civco, 1980);
- B1 reflectance tc (topographically correct) values higher than 0.10–0.15 indicates the presence of snow due to the high value of snow reflectance even if mixed with forest reflectance;
- B1/B1ref indicates a difference with respect to the summer image in order to avoid misclassification in the evaluation of B1 reflectance due to problem of mixed pixels and the contribution of tree reflectance. Ratio values higher than 1.2–1.4 may indicate the presence of snow.

Broadleaf: In the case of broadleaf forest, the presence of snow is less influenced by the presence of trees as the leaves are lost in fall. In the forest stands, a further subdivision is considered between dense and sparse forest to take into account the different tree density. This discrimination is performed based on NDVI thresholds, generally for values lower than 0.2. We have validated this discrimination in some selected areas by using Land Cover Classification Maps. Subsequently, the distinction of snow covered and snow-free areas is performed using the threshold on B1 band (for values higher than 0.10–0.25 based on the forest density).

Mixed: in case of mixed forest, a threshold on B1 reflectance is considered. The mixed forest is quite complicated to be detected and the evaluation of the algorithm outputs is also very difficult. For this reason, only the threshold on B1 reflectance is considered (for values higher than 0.10–0.15).

15.2.2 Cloud screening

The cloud cover masks derive from MODIS snow cover products MOD10A1.

15.2.3 Input data

The following MODIS products are used to produce the SCA maps at 250 m resolution:

- MOD09GQ and MOD09GA (Terra): atmospherically corrected surface reflectance product at 250 m–500 m resolution. The 250 m resolution bands, band 1 (0.62–0.67 µm) and 2 (0.841–0.876 µm), are used to detect snow and snow in forested areas. The bands at 500m are used to derive the NDSI and to determine a correction factor for the detection of snow in forest through a downscaling procedure with NDVI values.
- Cloud masks derived from MOD10A1 products.

15.2.4 Auxiliary data sets

Static auxiliary data are the following:

- DEM from Shuttle Radar Topography Mission (SRTM) (90 m resolution)
- maps for broadleaf, coniferous and mixed forest are extracted from CORINE Land Cover 2006 (http://sia.eionet.europa.eu/CLC2006/). For Switzerland, a forest mask developed by the Joint Research Centre (JRC) was adopted (http://forest.jrc.ec.europa.eu/forest-mapping).
- For detection of snow in the forest, another input data is a summer reference image for band 1. To avoid biases, which can derive from the selection of a single image, an average of ten eight-day composite images is used. Lake and sea masks derived from MOD10A1 products.

15.3 Quality and validation of product

The validation is carried out in the following ways (Notarnicola et al., 2013b):

- A comparison with high resolution SCA maps derived from Landsat 7 ETM+ images;

- A comparison with the NASA standard SCA products, MOD10A1 (MYD10A1). This validation was carried out on the same area and for the same dates of the comparison with Landsat 7 ETM+ images to have an overall accuracy assessment of the proposed snow algorithm.
- A validation with snow depth measured from ground stations in selected test sites in Austria, Slovakia, Germany and Italy

The results of the comparison with Landsat/ETM+ images indicate a mean overall accuracy of around 88.1%. The accuracy depends strongly on forest coverage, while in open areas, the accuracy is the highest with 93.6%. The detection of snow in forest is more reliable when also the NDSI is used as indicated in Klein et al. 1998. The same behaviour was found in the comparison with NASA MODIS SCA, where the accuracy is 90.2% and drops to 85.4% in forested areas. In the comparison with ground measurements, the EURAC snow cover maps (SCA) maps have reached an accuracy of around 93.7%. In some cases, in very rugged terrain with northern exposition, the accuracy decreases to around 82.4%, mainly due to the low values of reflectances, which make the snow detection very difficult based only on the 250 m bands.

15.4 Strength and weaknesses of the product

The strengths of the product are:

- Improved resolution 250 m useful for mountain areas
- Improved topographic correction for MODIS bands

The identified weaknesses are:

- Some limitations in detecting snow in forested areas
- Some misclassification snow-cloud especially in summer season.

15.5 Contact

Institution	EURAC
Contact Person	Claudia Notarnicola
Email	claudia.notarnicola@eurac.edu
Website for downloading the product:	http://webgis.eurac.edu/snowalps/ (Data can be requested through this WebGIS but they will have an EURAC internal naming convention and coding different from the ones used for the SnowPEx project).

15.6 References

Civco, D.L. Topographic normalization of Landsat Thematic Mapper digital imagery. Photogramm. Eng. Remote Sensing 1980, 46, 1191–1200.

Hall, D.K.; Riggs, G.; Salomonson, V.V.; DiGirolamo, N.E.; Bayr, K.J. MODIS snow-cover products. Remote Sens. Environ. 2002, 83, 181–194.

Klein, A.G.; Hall, D.K.; Riggs, G.A. Improving snow-cover mapping in forests through the use of a canopy reflectance model. Hydrol. Process. 1998, 12, 1723–1744.

Metsämäki, S.; Vepsäläinen, J.; Pulliainen, J.; Sucksdorff, Y. Improved linear interpolation method for the estimation of snow-covered area from optical data. Remote Sens. Environ. 2002, 82, 64–78.

Malcher, P.; Floricioiu, D.; Rott, H. Snow Mapping in Alpine Areas Using Medium Resolution Spectrometric Sensors. In Proceedings of IEEE International Geoscience and Remote Sensing Symposium, Toulouse, France, 21–25 July 2003; Volume 4, pp. 2835–2837.

Notarnicola, C.; Duguay, M.; Moelg, N.; Schellenberger, T.; Tetzlaff, A.; Monsorno, R.; Costa, A.; Steurer, C.; Zebisch, M. Snow Cover Maps from MODIS Images at 250 m Resolution, Part 1: Algorithm Description. Remote Sens. 2013a, 5, 110-126.

Notarnicola, C.; Duguay, M.; Moelg, N.; Schellenberger, T.; Tetzlaff, A.; Monsorno, R.; Costa, A.; Steurer, C.; Zebisch, M. Snow Cover Maps from MODIS Images at 250 m Resolution, Part 2: Validation. Remote Sens. 2013b, 5, 1568-1587.

Thirel G., C. Notarnicola, M. Kalas, M. Zebisc, T.Schellenberger, A. Tetzlaff, M. Duguay, N.Mölg, P.Burek, A. de Roo, Assessing the quality of a real-time Snow Cover Area product for hydrological applications, Remote Sensing of Environment, Volume 127, December 2012, Pages 271–287.

16. SNOW WATER EQUIVALENT ALGORITHMS AND PRODUCTS

By Chris Derksen (Environment Canada, Canada)

16.1 Overview

Satellite passive microwave data are commonly used for the retrieval of snow information because of a wide swath, all-weather imaging capabilities, and multi-frequency response to the presence of snow on land. The emission detected from a dry snowpack originates largely from the underlying ground, with frequency dependant scatter occurring in the snowpack (Figure 16.1). The total scatter is governed by the combined interaction of snow depth, density and grain size (i.e. the scattering particles). As microwaves pass through a snowpack, extinction losses occur through both absorption and volume scattering processes. When the radii of snow grains approach a few hundredths of the wavelength, volume scattering by the individual ice particles significantly decreases microwave emission. At frequencies above 20 GHz, therefore, scattering becomes the dominant component of the total extinction loss (Ulaby et al., 1986) with larger grains contributing greater scatter (Hall, 1987). At lower microwave frequencies the snow grains are not large enough to produce scatter, and thus absorption becomes the dominant extinction process. In a dry snowpack, however, very little absorption occurs, therefore the emission undergoes almost no extinction processes and snow is largely 'invisible' to longer wavelength microwave frequencies.

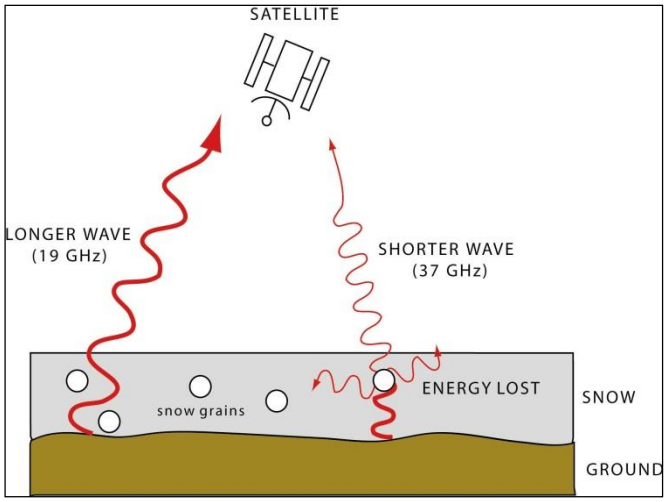

Figure 16.1: The scattering influence of terrestrial snow.

Most passive microwave SWE retrieval algorithms exploit the negative spectral gradient between a measurement frequency sensitive to snow grain volume scattering (~37 GHz) and a measurement frequency considered insensitive to snow (~19 GHz). The larger the difference between these two measurements, the higher the estimate of SWE. The combined use of these two frequencies reduces diurnal temperature and day-to-day atmospheric effects on measured brightness temperature (T_B) with the added benefit of measurement continuity at these frequencies through the satellite record (1978 to present), even as the measurement characteristics of various sensors have evolved (see Table 16.1).

Table 16.1:
Overview of space-borne passive microwave radiometers.

Satellite & Launch Year	Sensor	Scanner Type	Frequency (GHz)	Swath Width (km)	Incident Angle (degrees)	Polarization	Instantaneous Field of View (km)
Nimbus - 5 (1972)	ESMR	Electronically Scanned Phased Array	19.35	3000	+/- 50	Horizontal	25 x 25 to 160 x 45
Nimbus-6 (1975)			37	1300		Dual Polarization	20 x 43
Nimbus-7 (1978) Seasat (1978)	SMMR	Conical Scanner	6.6 10.69 18.0 21.0 37.0	800	50.3	Dual Polarization	95 x 148 70 x 109 43 x 68 36 x 56 18 x 27
DMSP-F8 to F15 (excluding F9) (1987)	SSM/I	Conical Scanner	19.35 22.235 37.00 85.50	1400	53	Dual Polarization	45 x 70 40 x 60 30 x 38 14 x 16
Aqua (2002)	AMSR- E	Conical Scanner	6.925 10.65 18.70 23.80 36.50 89.00	1445	54.8	Dual Polarization	43 x 75 29 x 51 16 x 27 18 x 32 8.2 x 14 3.5 x 5.9

The theoretical relationship between SWE and T_B is complicated by a number of landscape and snowpack state variables that are present at a range of scales. Because of the relatively low levels of naturally emitted microwave energy, grid cell dimensions for re-sampled spaceborne passive microwave T_B's are large: typically 25 km. A single passive microwave-derived SWE estimate therefore represents an integration of multiple land and snow cover conditions within the 625 km^2 grid cell. The physical parameters that influence T_B over snow covered land include:

Deep snow: Volume scatter at 37 GHz increases only to a threshold SWE value, after which there is a slope reversal in the SWE versus TB relationship (Ulaby et al., 1986). For regions that receive high amounts of snowfall, this means the same TB can be theoretically associated with two magnitudes of

SWE (early in the season during shallow snow cover and later in the season during deep snow cover) separated by 100 to 200 mm (Schanda et al., 1983). The exact slope transition point is dependent on local conditions, but has been documented between 120 and 180 mm (De Seve et al., 1997; Matzler et al., 1982; Matzler, 1994). The cause of this transition is the diminished scattering influence of large faceted and depth hoar grains found at the base of typical shallow snow packs, as surface layers of fine-grained new snow crystals accumulate and metamorphose slowly. Assuming a snow density of 0.2 g/cm3, a 120 mm SWE threshold is reached at a relatively modest snow depth of 60 cm. With a typical depth range of 30-120 cm for the taiga (as identified by Sturm et al., 1995) measurements at 37 GHz over deep boreal snow packs will typically be influenced by ambiguity in the SWE versus TB relationship. The mean snowpack grain size will also influence the depth at which the 36.5 GHz slope reversal will occur. Kelly et al. (2003) used radiative transfer model results to show a greater range in TB response with larger mean grain radii. Direct measurements (with ground based microwave radiometers) of the transition of a taiga snowpack from volume scatter to emission are provided in Sturm et al. (1993). Their measurements identified volume scatter to a critical snow depth of 31 cm; depths above this threshold produced an increase in the effective emissivity at 37 GHz. A second challenge related to deep snow is that beyond a critical snow depth volume scatter becomes detectable at 19 GHz (Markus et al., 2006). Analysis of airborne data by Lemmetyinen et al (2008) showed both 19 and 37 GHz TB decreased with increasing SWE above 100 mm, with the relationship more tightly constrained at 19 than at 37 GHz. This was an unexpected result since 19 GHz TB's were generally considered insensitive to the snowpack volume scatter that occurs at 37 GHz. These results illustrated that when SWE exceeds approximately 100 mm, volume scatter also influences 19 GHz measurements. Combined with microwave emission at 37 GHz, this volume scatter at 19 GHz reduces the 37-19 TB difference even as the snowpack continues to deepen, exacerbating systematic SWE underestimation across deep snow regions.

Snow wetness: Wet snow approaches black body behaviour so the T_B gradient between frequencies degrades, snow cover becomes 'invisible', and SWE cannot be estimated (Stiles and Ulaby, 1980; Walker and Goodison, 1993).

Snow grain size: Microwave scatter increases as the grain size approaches the size of the wavelength. This increased scattering can artificially lower the T_B of the snowpack relative to the SWE, contributing to systematic overestimation in regions with pronounced depth hoar layers (Hall, 1983).

Snow density: The density of snow varies over time and space, and is dependent on the amount of air in the interstices between individual snow crystals, which is a function of the temperature and wind

during and after a snowfall event. Density also tends to increase over time due to snowpack settlement and compaction. The larger the interstices between snow crystals (lower density) the less scattering of microwave energy occurs, hence the scattering signal from freshly fallen snow is typically difficult to detect compared to a mature snowpack.

Snow stratigraphy: The layering of the snowpack can add a significant level of complexity in interpreting passive microwave T_B when the emitting wavelength is comparable to snow layer thickness, or when there are notable dielectric contrasts between different snow layers (Colbeck, 1991).

Ice lenses: Ice layers in the snowpack (either from melt/refreeze or rain-on-snow events) alters absorption and emission characteristics, and increases emissivity at high frequencies relative to low frequencies. The ice lens influence is particularly pronounced with H-pol T_B's (Rees et al., 2010).

Vegetation: In general, there is a latitudinal evolution from closed canopy boreal forest in the south, to open canopy forest near the northern treeline. This vegetation gradient will influence the efficiency of snowfall interception and retention at the surface (Hedstrom and Pomeroy, 1998), and influence TB measurements (De Roo et al., 2007). Numerous studies have linked forest cover properties with uncertainty in passive microwave SWE retrievals (Derksen et al., 2005; Foster et al., 2005). Standing vegetation is a strong microwave absorber at 37 GHz, so the scattering signal from the underlying snowpack can be overwhelmed by upwelling microwave radiation from the stems and canopy. High resolution airborne measurements over forested areas have provided evidence of systematic relationships between TB and forest inventory variables (such as stem volume and canopy closure), and increased TB sensitivity to physical temperature changes in comparison to open environments (Derksen et al., 2007; Kurvonen and Hallikainen, 1997; Chang et al., 1997). In general, open environment airborne SWE retrievals are too high, and the forest environment retrievals are too low (Derksen et al., 2005; Lemmetyinen et al., 2008). These results suggest that the degree of openness within a grid cell is essential for producing sufficiently high SWE retrievals in forested areas, and explains why consistent SWE underestimation from spaceborne passive microwave data is a serious problem in areas with high stem volume and canopy closure. To further complicate the issue, forest cover fraction or land cover information cannot be used as a systematic adjustment for SWE underestimation because the statistical relationship between forest fraction and SWE retrieval underestimation can be ambiguous at the satellite scale (Derksen et al., 2005). Forest inventory variables such as stem volume and canopy closure are more likely to impact microwave emission, and therefore be statistically related to SWE underestimation, but these data are not typically available for large areas of the northern boreal forest in Eurasia and Canada.

Topography: Surface elevation influences the atmospheric contribution to spaceborne measurements (Savoie et al., 2009). Additionally, emission from complex terrain (variable sub-grid topography) cannot be resolved within coarse resolution satellite footprints. MacKay et al. (2003) showed that empirically derived SWE retrievals above 800 m elevation in the Mackenzie basin of Northwest Canada were strongly biased, which necessitates a more complex approach to SWE retrievals in alpine regions (such as the neural network approach presented in Tong et al., 2009).

Lakes: To understand and potentially exploit microwave TB response across lake-rich tundra environments, the seasonally-evolving influence of the snowpack must be separated from the seasonally evolving influence of lake ice across the range of satellite measurement frequencies. Because liquid water has a very low emissivity compared to ice (Hall et al., 1978), a frozen water body with liquid water below the ice will have much lower microwave emission at longer wavelengths and subsequently lower TB compared to adjacent land surfaces. Over the course of the ice growth season, an increase ice thickness increases the TB (Swift et al. 1980) because the thicker ice reduces the influence of the lower emissivity liquid water below the ice. The passive microwave frequencies traditionally used to retrieve SWE (~19 and 37 GHz) therefore have penetration depths that are strongly influenced by water beneath the ice for part of the season, but are also influenced by the ice and overlying snowpack by the end of the season. The timing of this shift in the primary emission source is different at 19 versus 37 GHz, due to wavelength specific variations in penetration depth (Derksen et al., 2009). Low frequency measurements are controlled by emission below the ice layer; higher frequency measurements are influenced by the water when the snow and ice are thin, but the combined snow and ice thickness will eventually exceed the penetration depth.

16.2 Common Approaches

Operational SWE products, all of which are constrained by low spatial resolution (25 km), utilize spectral T_B differences (typically at 37 and 19 GHz) to estimate SWE or snow depth; only the assimilation algorithm of Pulliainen (2006) considers other sources of information. The algorithm originally proposed by Chang et al. (1987) estimated snow depth from horizontal polarization Scanning Multichannel Microwave Radiometer (SMMR) measurements. The algorithm has a physical basis - the parameterisation was based on forward simulations with a radiative transfer model. This algorithm has been widely adopted for estimating SWE from different space-borne microwave radiometers (Armstrong and Brodzik, 2001) including modifications to account for variable surface and snowpack characteristics (Tait, 1998; Foster et al, 1991; 1997). Armstrong and Brodzik (2002) compared the

performance of several traditional algorithms (Chang et. al, 1987, Goodison, 1989; Rott et al., 1991; Nagler and Rott, 1992) and found large errors at the hemispheric scale when compared to available in situ data with a general tendency for the algorithms to underestimate SWE, especially under deep snow conditions. Large errors (approaching 100%) were reported in the hemispheric application of T_B difference algorithms by Kelly et al. (2003).

A different approach is the use of theoretical or semi-empirical radiative transfer models for snow cover, coupled with atmospheric and vegetation models, to simulate microwave emission and inversely calculate snow characteristics from satellite measurements (e.g. Pulliainen et al., 1999, Wiesmann and Matzler, 1999). The more complicated models are computationally expensive and require precise ancillary data in order to give accurate predictions (i.e. Durand et al., 2008). These factors restrict their operational applicability on a global scale. Simpler models, while being more easily applied to larger areas, may not be able to accurately simulate natural snowpacks (Tedesco and Kim, 2006).

Improving the performance of passive microwave retrieval algorithms by means of data assimilation has also been investigated. Assimilation can include other remotely sensed data, such as optical or radar imagery, or available ground information. Pulliainen (2006) presents an assimilation technique which weighs passive microwave data driving a semi-empirical radiative transfer model, and prior snow information from ground measurements, with their respective statistical uncertainties. The study indicates that the assimilation technique can address effects of saturation related to high values of SWE, as well as reduce systematic errors related to satellite only based SWE retrievals. In studies by Pulliainen and Hallikainen (2001) and Pulliainen (2006) unbiased RMSE values of 15 to 40 mm were achieved when compared to in situ data. The method is currently used in the production of the northern hemisphere SWE data record produced within the GlobSnow project (Takala et al., 2011).

16.3 References

Armstrong, R. L., and M. J. Brodzik. 2001. Recent Northern Hemisphere snow extent: a comparison of data derived from visible and microwave sensors. Geophysical Research Letters28 (19): 3673-3676.

Armstrong, R. L., and M. J. Brodzik. 2002. Hemispheric-scale comparison and evaluation of passive microwave snow algorithms. Annals of Glaciology 34: 38-44, doi:10.3189/172756402781817428.)

Chang, A., J. Foster, and D. Hall, 1987. Nimbus-7 SMMR derived global snow cover parameters. Ann. Glaciol., 9, 39-44.

Chang, A., J. Foster, D. Hall, B. Goodison, A. Walker, J. Metcalfe, and A. Harby. 1997. Snow parameters derived from microwave measurements during the BOREAS winter field campaign. Journal of Geophysical Research. 102(D24): 29 663-29 671.

Colbeck, S. 1991. The layered character of snow covers. Reviews of Geophysics. 29(1): 81-96.

De Roo, R., A. Chang, and A. England. 2007. Radiobrightness at 6.7-, 19-, and 37-GHz downwelling from mature evergreen trees observed during the Cold Land Processes Experiment in Colorado. IEEE Transactions on Geoscience and Remote Sensing. 45(10): 3224-3229.

De Seve, D., M. Bernier, J.-P. Fortin, and A. Walker. 1997. Preliminary analysis of snow microwave radiometry using the SSM/I passive-microwave data: the case of La Grande River watershed (Quebec). Annals of Glaciology. 25: 353-361.

Derksen, C., A. Walker, and B. Goodison. 2005. Evaluation of passive microwave snow water equivalent retrievals across the boreal forest/tundra transition of western Canada. Remote Sensing of Environment. 96(3/4): 315-327.

Derksen, C., A. Walker, and P. Toose. 2007. Estimating snow water equivalent in northern regions from satellite passive microwave data. In Woo, M-K (ed.). Cold Region Atmospheric and Hydrologic Studies, The Mackenzie GEWEX Experience. Volume I: Atmospheric Dynamics. Springer. pp. 195-212.

Derksen, C., M. Sturm, G. Liston, J. Holmgren, H. Huntington, A. Silis, and D. Solie. 2009. Northwest Territories and Nunavut snow characteristics from a sub-Arctic traverse: Implications for passive microwave remote sensing. Journal of Hydrometeorology. 10(2): 448-463.

Foster, J. A. Chang, D. Hall, 1997. Comparison of snow mass estimates from a prototype passive microwave snow algorithm, a revised algorithm and a snow depth climatology. Remote Sens. Environ., 62: 132-142.

Foster, J., A. Chang, D. Hall, and A. Rango, 1991. Derivation of snow water equivalent in boreal forests using microwave radiometry. Arctic, 44, 147-152.

Foster, J., C. Sun, J. Walker, R. Kelly, A. Chang, J. Dong, and H. Powell. 2005. Quantifying uncertainty in passive microwave snow water equivalent observations. Remote Sensing of Environment. 94(2): 187-203.

Goodison, B. 1989. Determination of areal snow water equivalent on the Canadian Prairies using passive microwave satellite data. In Proceedings, IGARSS'89, Vancouver. 3:1243-1246.

Hall, D.K., J.L. Foster, A. Rango, A.T.C. Chang. 1978. Passive microwave studies of frozen lakes. Proceedings of the American Society of Photogrammetry: Fall Technical Meeting. pp 195-207

Hall, D.K. 1987. Influence of depth hoar on microwave emission from snow in northern Alaska. Cold Regions Science and Technology. 13: 225-231.

Hedstrom, N., and J. Pomeroy. 1998. Measurements and modelling of snow interception in the boreal forest. Hydrological Processes. 12: 1611-1625.

Kelly, R., A. Chang, L.Tsang, and J. Foster. 2003. A prototype AMSR-E global snow area and snow depth algorithm. IEEE Transactions on Geoscience and Remote Sensing. 41(2): 230-242.

Kurvonen, L., and M. Hallikainen. 1997. Influence of land-cover category on brightness temperature of snow. IEEE Transactions on Geoscience and Remote Sensing. 35(2): 367-377.

Lemmetyinen, J., C. Derksen, J. Pulliainen, W. Strapp, P. Toose, A. Walker, S. Tauriainen, J. Pihlflyckt, J-P Kärnä, and Martti Hallikainen. 2009. A comparison of airborne microwave brightness temperatures and snowpack properties across the boreal forests of Finland and western Canada. IEEE Transactions on Geoscience and Remote Sensing. 47(3): 965-978.

MacKay, M., F. Seglenieks, D. Verseghy, E. Soulis, K. Snelgrove, A. Walker, and K. Szeto. 2003. Modeling Mackenzie Basin surface water balance during CAGES with the Canadian Regional Climate Model. Journal of Hydrometeorology. 4(4): 748-767.

Markus, T., D. Powell, and J. Wang. 2006. Sensitivity of passive microwave snow depth retrievals to weather effects and snow evolution. IEEE Transactions on Geoscience and Remote Sensing. 44(1): 68-77.

Mätzler, C., E. Schanda, and W. Good, 1982. Towards the definition of optimum sensor specifications for microwave remote sensing of snow. IEEE Trans. Geosci. Remote Sens., GE-20, 57-66.

Mätzler, C., 1994. Passive microwave signatures of landscapes in winter. Meteorology and Atmospheric Physics. 54: 241-260.

Nagler and Rott, 1992. Development and intercomparison of snow mapping algorithms based on SSM/I data. Proc. IGARSS'92. IEEE:812-814.

Pulliainen, J. 2006. Mapping of snow water equivalent and snow depth in boreal and sub-arctic zones by assimilating space-borne microwave radiometer data and ground-based observations. Remote Sensing of Environment. 101(2): 257-269.

Pulliainen, J., and M. Hallikainen. 2001. Retrieval of regional snow water equivalent from space-borne passive microwave observations. Remote Sensing of Environment. 75: 76-85.

Pulliainen, J., Grandell, J., & Hallikainen, M., 1999. HUT snow emission model and its applicability to snow water equivalent retrieval. IEEE Trans. Geosci. Remote Sens., 37, 1378−1390.

Pulliainen, J., Grandell, J., & Hallikainen, M., 1999. HUT snow emission model and its applicability to snow water equivalent retrieval. IEEE Trans. Geosci. Remote Sens., 37, 1378−1390.

Rott, H., T. Nagler, and J. Aschbacher. 1991. Algorithm development for monitoring the global snow cover by spaceborne microwave radiometry. Proceedings, 11th EARSel Symposium, Graz, Austria, July, 1991, pp. 58-69.

Savoie, M., R. Armstrong, M-J Brodzik, and J. Wang. 2009. Atmospheric corrections for improved satellite passive microwave snow cover retrievals over the Tibet Plateau. Remote Sensing of Environment. 113: 2661–2669.

Schanda, E., C. Matzler, and K. Kunzi. 1983. Microwave remote sensing of snow cover. International Journal of Remote Sensing. 4(1): 149-158.

Stiles, W., and F. Ulaby. 1980. The active and passive microwave response to snow parameters. 1. Wetness. Journal of Geophysical Research. 22(C2): 1037-1044.

Sturm, M., T. Grenfell, and D. Perovich. 1993. Passive microwave measurements of tundra and taiga snow covers in Alaska, U.S.A. Annals of Glaciology. 17: 125-130.

Sturm, M., J. Holmgren, and G. Liston. 1995. A seasonal snow cover classification system for local to global applications. Journal of Climate. 8: 1261-1283.

Swift, C.T., W.L. Jones, Jr., R.F. Harrington. 1980. Microwave radar and radiometric remote sensing measurements of lake ice. Geophysical Research Letters. 7: pp 243-246

Tait, 1998. Estimtion of snow water equivalent using passive microwave radiation data. Remote Sensing of Environment, 64:286-191.

Takala, M., K. Luojus, J. Pulliainen, C. Derksen, J. Lemmetyinen, J-P Kärnä, and J. Koskinen. 2011. Estimating northern hemisphere snow water equivalent for climate research through assimilation of space-borne radiometer data and ground-based measurements. Remote Sensing of Environment. 115: 3517–3529, doi:10.1016/j.rse.2011.08.014.

Tedesco, M., and E. Kim. 2006. Intercomparison of electromagnetic models for passive microwave remote sensing of snow. IEEE Transactions on Geoscience and Remote Sensing. 44(10): 2654-2666.

Tong, J., S. Dery, P. Jackson, and C. Derksen. 2009. Testing snow water equivalent retrieval algorithms for passive microwave remote sensing in an alpine watershed of western Canada. Canadian Journal of Remote Sensing.

Ulaby, F., R. Moore, and A. Fung. 1986. Microwave Remote Sensing, Active and Passive, Vol. III: From theory to applications. Reading: Addison-Wesley Publishing.

Walker, A. and B. Goodison. 1993. Discrimination of a wet snow cover using passive microwave satellite data. Annals of Glaciology. 17: 307-311.3

Wiesmann, A., and C. Mätzler, 1999. Microwave emission model of layered snowpacks. Remote Sens. Environ., 70(3) 307 - 316.

17. GLOBSNOW SWE PRODUCT

By Kari Luojus (Finnish Meteorological Institute, Finland)

17.1 Algorithm

The European Space Agency 'GlobSnow' SWE product, based on a method first described in Pulliainen (2006) is produced from a combination of two snow depth estimates: (1) climate station snow depth observations kriged to form a continuous field, and (2) snow depth estimates derived from satellite passive microwave measurements using two iterations (one to estimate grain size, the second to estimate snow depth) of forward microwave emission model simulations (Takala et al., 2011). Figure 17.1 provides an overview of the GlobSnow SWE processing chain.

Snow Depth (SD) observations from synoptic weather stations are obtained for the northern hemisphere from the European Centre for Medium-Range Weather Forecasts (ECMWF; this dataset is described further below). An 'observed snow depth' field is produced from the synoptic weather station observations by ordinary kriging interpolation to the 25 km EASEGrid. The available synoptic weather station measurements of snow depth are used as input to forward model simulations of brightness temperature (TB) using the single layer HUT snow emission model. The model is fit to satellite observed TB values at the locations of weather stations by optimizing the value of effective snow grain size. The HUT model describes TB as a function of SWE, snow density and snow grain size. Snow density is treated with a constant value of 0.24 g/cm3, and snow depth is taken from the weather station measurements. At each synoptic station location, the final estimate of the grain size (and its standard deviation λ) is obtained by averaging values obtained for the ensemble of the nearest stations. A spatially continuous background field of the effective snow grain size (including a variance field) is then interpolated using a kriging technique from the snow grain size estimates produced at the weather station locations.

A map of spatially continuous 'assimilated SWE' is produced through forward simulations with the HUT model using the interpolated effective grain size and land cover information (dataset described below). The simulations are compared with spaceborne radiometer measurements via a cost function at each grid cell. The cost function also considers the background snow depth field. Model estimates are matched to observations numerically by fluctuating the SWE value. The cost function constrains the grain size value according to the predicted background grain size and the estimated variance. Thus, the assimilation adaptively weighs the space-borne brightness temperature observations and the

'observed snow depth' field) to estimate a final SWE and a measure of statistical uncertainty (in the form of a variance estimate) on a grid cell by grid cell basis. The higher the estimated sensitivity of TB to SWE, the higher the weight given to the radiometer data. Thus, the weight of the radiometer data varies both temporally and spatially in order to provide a maximum likelihood estimate of SWE.

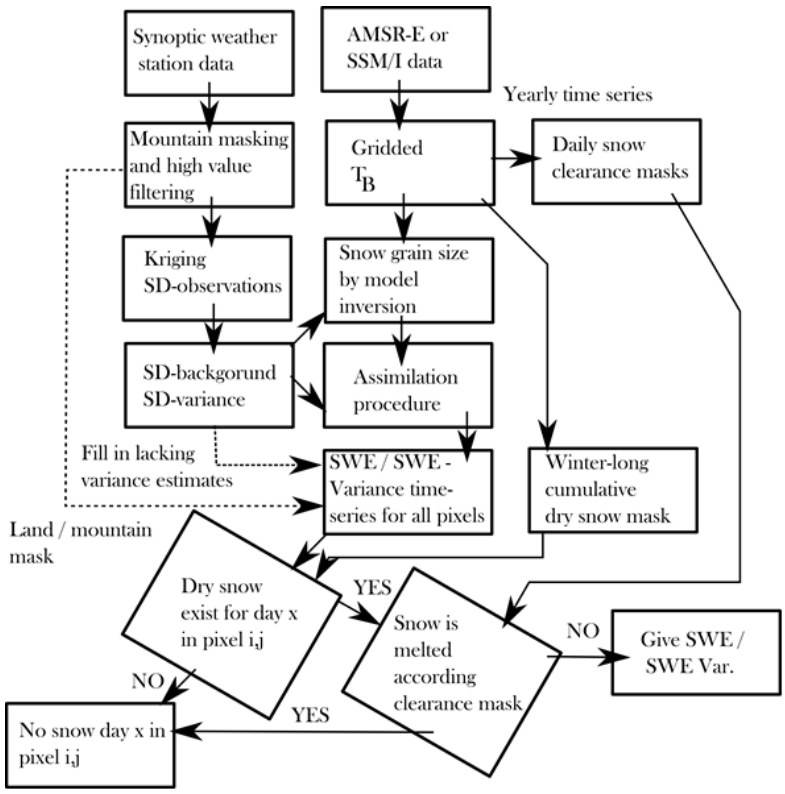

Figure 17.1: GlobSnow SWE processing chain.

In order to provide a hemispheric SWE map for the region of seasonal snow cover, it is also necessary to produce a cumulative dry snow mask for each snow cover season (beginning September 1). For this purpose, the dry snow detection algorithm of Hall et al. (2002) is applied to satellite radiometer data. From satellite passive microwave measurements, the date of snow clearance can also be estimated using the algorithm of Takala et al. (2009). If the cumulative dry snow mask shows that a grid cell in question for a particular date has never been marked as dry snow it is labelled as snow free through the winter. If the cumulative dry snow mask suggests that the pixel has had dry snow conditions, but is already snow free according to the snow clearance algorithm, the pixel is marked as snow free. An estimate of the SWE and SWE variance is given for grid cells for which dry snow cover has been

detected and for which snow melt has not yet been indicated (note that for wet snow cover the algorithm inherently assesses the weight of radiometer data to approach zero). If a grid cell is in a mountainous area it is flagged as such and no SWE is retrieved due to the uncertainty of microwave measurements in complex, snow covered alpine terrain.

Further information on GlobSnow and access to the products is available at www.globsnow.info.

17.2 Input and Auxiliary Data

Satellite radiometer data used for the GlobSnow product come from the Level 3 brightness temperature archive at the National Snow and Ice Data Center (NSIDC). For the years 1978–1987, the Scanning Multichannel Microwave Radiometer (SMMR; Knowles et al., 2002) data from Nimbus 7 are used. Since 1987, data from the sequence of Special Sensor Microwave/Imager (SSM/I) and Special Sensor Microwave Imager/Sounder (SSMIS; Armstrong et al., 1994) instruments on-board the Defense Meteorological Satellite Program (DMSP) F-8, F-11, F-13, and F-17 platforms are used.

Parallel retrievals for the years 2002–2010 were performed using the Advanced Microwave Scanning Radiometer (AMSR-E; Knowles et al., 2006) on-board the Aqua satellite, but the baseline GlobSnow record is based on the SSM/I and SSMIS time series. No adjustments for inter-sensor bias in the satellite time series are performed. This may introduce some small biases from one instrument to another, however, this is mitigated by the assimilation approach used to produce the SWE retrievals.

The space-borne brightness temperature measurements are in the EASE-Grid north azimuthal equal-area projection with a nominal resolution of 25 km × 25 km (Armstrong et al., 1994). The local overpass time varies but the difference is less than 2 h. The descending orbit measurements correspond to the early morning (0500 to 0700 local time) and ascending orbit measurements correspond late afternoon (1500–1700 local time), although in the case of SSM/I the local overpass time (ascending vs. descending) depends on which DSMP satellite the instrument was on-board. Night time orbits form the basis of the GlobSnow record, with daytime passes applied only to fill gaps between night time passes. This enhances the spatial coverage without deteriorating the overall accuracy. The most important frequencies for snow detection and SWE retrieval are 19 and 37 GHz. Channels at these frequencies are available from all instruments, although with different native footprint dimensions. These differences in swath level resolution are removed through brightness temperature re-sampling to the EASE-Grid as described in Armstrong et al. (1994). Some data gaps exist both in time and space within the satellite passive microwave data record. SMMR had a narrow swath width (600 km) and was de-activated every other day due to power constraints.

Daily SD background fields are generated from observations at synoptic weather stations acquired from ECMWF. For each measurement, a WMO station identifier, date of measurement, and snow depth (SD) are given. The snow depth is traditionally manually measured with a rod or ruler, although in the 1990s there was a transition to automated snow depth sensors in many countries. The ECMWF SD data are enhanced with the inclusion of the INTAS-SCCONE snow depth dataset which improves the density of surface observations across the former Soviet Union. Manual SD measurements are available for 223 different locations. In addition to information on WMO station identifier, date of measurement and SD, a qualitative estimate of the snow covered area and a status flag value are given. Uncertainty in the point snow depth measurements is derived by assigning a land cover specific variance of to the observations (based on comparison of pointwise data with coincident snow course measurements from Finland and Canada).

The Global Land Cover 2000 was used as land use information for the GlobSnow algorithm (http://bioval.jrc.ec.europa.eu/products/glc2000/glc2000.php). The dataset covers the whole globe at a resolution of 1 km with 23 land cover classes. Areal fractions of two basic land cover categories are calculated for each EASE-Grid cell and input to the forward Tb model in the assimilation scheme. The two applied land cover classes are (a) forest and (b) all other land cover classes. Grid cells with major lakes are masked if the areal fraction of open water exceeds 50%. The approximate forest biomass (stem volume) was assigned to the forest fraction of each grid cell. For North America, a mean forest stem volume value of 80 m^3/ha is used to characterize the effect of forest cover based on FAO statistics (http://www.fao.org/forestry/32042/en/). While this is a very generalized approach, estimation of effective grain size greatly reduces the sensitivity of the algorithm to forest biomass allowing a constant value to be adopted. For northern Eurasia, a spatially varying stem volume value is assigned to the forest fraction of each grid cell based on a digital forest map described in Bartalev et al. (2004).

Topographic information for the masking of complex terrain was derived from ETOPO5 (National Geophysical Data, 1988) data. This dataset contains global elevation information at a resolution of 5 arc minutes, an appropriate resolution given the scale of the 25 km EASE-Grid.

17.3 Product Specs

The SWE product is projected to Equal-Area Scalable Earth Grid (EASE-Grid) and provides the whole Northern Hemisphere (lambert's equal-area azimuthal – projection) in a single data field. The nominal resolution of single pixel is 25 km x 25 km and the geometry of the pixels varies. The data field has the

size of 721 x 721 (rows x columns). Although the EASE-Grid can represent data almost to the equator the product is limited between latitudes 35° and 85° for physical reasons.

There are three available GlobSnow SWE products (all in the EASE-Grid):

- Daily Snow Water Equivalent (Daily L3A SWE), snow water equivalent (mm) for each grid cell for all evaluated land areas of the Northern Hemisphere.
- Weekly Aggregated Snow Water Equivalent (Weekly L3B SWE), calculated for each day based on a 7-day sliding time window aggregation of the daily SWE product.
- Monthly Aggregated Snow Water Equivalent (Monthly L3B SWE) a single product for each calendar month providing the average and maximum SWE, calculated from the weekly aggregated SWE product.

In addition to the information on snow water equivalent, the SWE product includes information on the overall extent of snow cover. The information on snow extent is included in the product by utilizing the following coding for the SWE product:

- 0 mm denote snow-free areas (Snow Extent 0%)
- 0.001 mm denote areas with melting snow (Snow Extent between 0% - 100%)
- >0.001 mm denote areas with full snow cover (Snow Extent 100%)

The areas that have been flagged as snow-free or melted are identified using a time series melt detection approach described in Takala et al. (2009). The areas that are identified as wet snow or have no SWE retrieval, but are identified as snow covered with the time-series melt detection approach are denoted with a SWE value of 0.001 mm. The areas that are determined as snow-free or melted by the melt detection approach are denoted with a SWE value of 0 mm. All the other areas show a retrieved SWE value (that is in all cases greater than 0.001 mm).

The weekly (7-days) aggregated product is calculated using sliding window averaging: the SWE estimate for the current day is calculated as a mean of the samples from the previous 6 days and the current day SWE (for each grid cell). The monthly aggregate, a single product for each month, is calculated by determining the mean and the maximum of the weekly SWE samples.

The SWE product file includes two data fields:

- The SWE estimate [mm]
- The variance of the SWE estimates [mm] (i.e. the accuracy information for each SWE sample).

The data type of both data fields is a 32 bit floating point 'float 32'. Positive values and zero are reserved for SWE and negative values for flags. The physical values of SWE are in millimetres. Negative values mean that the pixel is masked out due to water, mountains or no data (value of -1 is used for water bodies and -2 for mountains). The mountainous areas of Northern Hemisphere are masked out from the SWE product. The mountain mask applied is derived from 4 minute averaged ETOPO2 data set which includes the Global elevation and bathymetry on 2x2 minute grid from the National Geophysical Data Center (NGDC). The dataset was original published in September 2001 and was revised to include correction to Caspian Sea area in April 2006. It contains improvements that include the blending of satellite altimetry with ocean soundings and new land elevation data from the Global Land One-km Base Elevations (GLOBE) project. SWE estimates for wet snow areas (where retrieval using the radiometer data is not feasible) are determined solely from the weather station data using kriging interpolation.

17.4 Validation

A sequence of GlobSnow prototype and full product sets (v0.9, v1.0, v1.2, v1.3, v2.0) were subjected to standardized validation in order to facilitate inter-version comparisons. These evaluations are all documented in technical reports produced for ESA, and available via the GlobSnow website (www.globsnow.info). Validation of full product set v1.0 is also described in Takala et al (2011) which represents the primary peer reviewed article describing the GlobSnow SWE algorithm and validation.

Three datasets were used for GlobSnow validation:

17.4.1 INTAS-SCCONE snow course data

The former Soviet Union operated an extensive network of snow observation sites, covering most of the Eurasian landmass. The snow transect data used for SWE validation are available via the website of All-Russian Research Institute of Hydrometeorological Information - World Data Center (RIHMI-WDC) on the following website: (http://meteo.ru/english/climate/snow1.php). The data has been freely available for all interested users, containing data from 517 snow transect locations spanning 1966 to 2009. Note that the validation described in Takala et al (2011) used only measurements from 1978 to 2000, but this was extended to 2009 for later product versions. The snow transect sites are concentrated strongly south of the 70°N parallel. Distances between individual snow survey sites can be up to hundreds of kilometres. Data from snow survey sites are typically available several times per month, depending on the year and site. There are 3 types of snow transects depending on the landscape. In forests, the length of snow path is 500 m, with snow depth measured every 10 m, and

snow density every 100 m. In forested regions with openings the length of the snow path is 1000 m. In steppes, the length of snow path is 2000 m. For these longer transects, snow depth is measured every 20 m, and snow density every 200 m (in some cases every 100 m). Obtained snow depths and snow densities are then averaged along the path and snow water equivalent is calculated.

17.4.2 Finnish snow course data

The snow course network managed by the Finnish Environment Institute (SYKE) has a heritage from the beginning of 20th century. The network consists of ~160 snow courses which are visited monthly. Each snow course is a 2-4 km long transect going through different landscapes; the observer registers the snow information typically at 80 locations along the transect. The observations include snow depth, snow density (measured with a snow tube), and fraction (%) of snow-free ground (visually estimated for an area within 25m radius from the observer's location).

The route of each snow course by SYKE is individually planned so that it should represent the locality of few square kilometres. The trail goes through different landscapes in order to capture the local differences in snow conditions; the prevailing landscape is assigned to each measurement location. For GlobSnow validation, a snow course SWE value refers to the average value of all SWE observations along that transect. Snow courses are visited once a month, the typical observation day is 16th of each month during the snow season (November – May). The currently available snow course dataset spanned the years 2006-2011, with the years of 2006, 2007 and 2008 utilized for the assessment of GlobSnow retrieval accuracy (Takala et al., 2011).

17.4.3 Canadian Reference Data

In order to evaluate coarse resolution satellite retrievals and climate model simulations, Environment Canada has augmented the sparse Canadian national snow survey network with field measurement campaigns designed to provide regionally representative snow measurements. Various field campaigns have provided measurements across the northern boreal forest of Manitoba and the Northwest Territories between 2004 and 2008. Intensive tundra snow surveys were performed in the Daring–Exeter– Yamba watershed of the Upper Coppermine River Basin in the Northwest Territories Canada near the timing of peak SWE, April 2004 through 2010. A stratified sampling approach was utilized to determine slope, aspect, and land cover controls on snow properties. During April 2007, a coordinated series of snow measurements were made across the Northwest Territories and Nunavut, Canada during a snowmobile traverse from Fairbanks, Alaska to Baker Lake, Nunavut.

Hourly snow depth measured at sites representative of old growth boreal forest (aspen, black spruce, jack pine), a chrono-sequence of harvested sites (1975, 1994, 2002), fire disturbed stands (1977, 1989, 1998), and a boreal fen were provided by the Boreal Ecosystem Research and Monitoring Sites (BERMS) program for 2003 through 2009. These automated point measurements were augmented with bi-weekly snow course measurements at the BERMS sites, and similar forest cover types in the same region of central Saskatchewan. Bi-weekly snow surveys at open prairie sites south of the boreal forest are also available from Environment Canada. These prairie measurements take into account different agricultural land use (i.e. fallow vs. stubble fields) through multiple sampling transects.

Table 17.1:
Seasonal summary of SWE assimilation algorithm performance over Eurasia, 1980-2000 (fall: September-December; winter: September-March; spring: April-May). In parenthesis are the values for cases with reference SWE < 150 mm. R is significant at 99 % level in all cases.

Season	*RMSE (mm)*	*bias(mm)*	*Corr. coeff*	*Samples*
Fall	23.0 (21.7)	5.8 (6.5)	0.69 (0.70)	35 197 (34 943)
Winter	37.7 (28.9)	1.7 (7.7)	0.72 (0.72)	165 784 (150 405)
Spring	72.5 (47.3)	-37.6 (-19.3)	0.53 (0.47)	42 843 (33 189)

Details on validation of the GlobSnow SWE product are provided in Takala et al (2011). A comparison of SWE estimates produced from the assimilation algorithm with INTAS-SCCONE snow course observations was performed from 1980 to 2000 (Table 17.1). The RMS error and bias fluctuate from season to season, but across a relatively narrow range (RMSE of about 30 to 40 mm; and a bias ranging from −3 to +9 mm when SWE <150 mm indicating that a small bias is possible). When all snow course measurements are considered the RMS error increases to 45 mm and a bias of −5 mm is observed, which indicates a tendency of SWE underestimation for deep snow packs. Similar results were found using the Finnish snow course data for 2006-2008: the RMS errors remained below 40 mm for all months except April 2007.

A summary of the evaluation with Canadian reference data is provided in Table 17.2. Evaluation statistics were also calculated for each land cover category given the unique characteristics of the reference measurements available for each region. Retrieval uncertainty was relatively high for deep boreal forest snow, consistent with the evaluation for Finland and Eurasia. This is the only Canadian region under investigation for which SWE regularly exceeds the 150 mm threshold. When the statistics were re-computed using a 150 mm threshold, algorithm performance improved appreciably with the RMSE value decreasing from 40 mm to 21 mm. The daily automated measurements from the BERMS

sites showed there is a tendency for early season shallow snow to be missed by the assimilation scheme, and the retrievals to drop too rapidly in the spring. The relatively high uncertainty over tundra regions is likely driven by the extremely sparse network of surface climate stations across the Canadian sub-Arctic, the complex microwave emission from lake rich snow covered tundra (see Derksen et al., 2009), and the extremely heterogeneous tundra snow cover which complicates the determination of 'ground-truth' SWE at coarse spatial resolutions.

Table 17.2:
Summary of SWE assimilation algorithm performance over Canada, 2005/06 – 2007/08.

Land Cover	*Reference Dataset*	*Year*	*n*	*Mean SWE (mm)*	*RMSE (mm)*	*R*	*R Significant at 95% level*	*R Significant at 99% level*	*Mean Bias*
Tundra	Intensive Sites; SnowSTAR 2007	2005-2007	28	120	47	0.05	No	No	-36
Northern Boreal	EC Snow Surveys	2006-2007 SWE <150 mm	105 73	134 101	70 21	0.00 0.52	No Yes	No Yes	-32 3
Southern Boreal	EC Snow Surveys	2005-2007	57	75	28	0.43	Yes	Yes	-8
Southern Boreal	BERMS	All	468	70	25	0.87	Yes	Yes	-3
Prairie	EC Snow Surveys	All	41	47	21	0.51	Yes	Yes	6

The validation results in Takala et al (2011) were focussed on the GlobSnow full product set v1.0. Validation with subsequent GlobSnow versions, including the most recent v2.0 show very little change in the statistical validation results (Figure 17.2 and Figure 17.3).

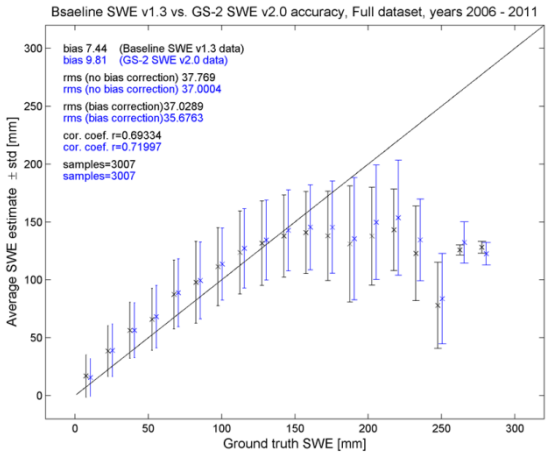

Figure 17.2: Comparison of ground reference SWE from Finnish snow courses with GlobSnow v1.3 and v2.0 retrievals.

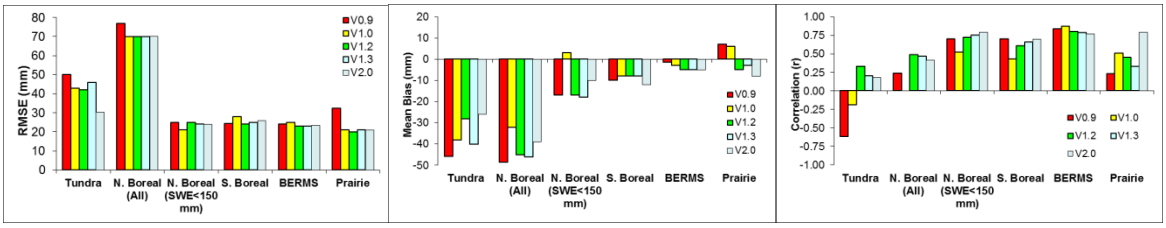

Figure 17.3: Change in RMSE, bias, and correlation for the series of GlobSnow product versions for Canadian reference data.

17.5 References

Armstrong, R. L., K. W. Knowles, M. J. Brodzik and M. A. Hardman. 1994. DMSP SSM/I Pathfinder daily EASE-Grid brightness temperatures, Jan 1987 – Jul 2008. Boulder, Colorado USA: National Snow and Ice Data Center. Digital media.

Bartalev, S., D. Ershov, A. Isaev, P. Potapov, S. Turubanova, A. Yaroshenko, 2004. Russia's Forests. TerraNorte Information System. RAS Space Research Institute. (http://terranorte.iki.rssi.ru).

Derksen, C., M. Sturm, G. Liston, J. Holmgren, H. Huntington, A. Silis, and D. Solie. 2009. Northwest Territories and Nunavut snow characteristics from a sub-Arctic traverse: Implications for passive microwave remote sensing. Journal of Hydrometeorology. 10(2): 448-463.

Hall, D., R. E. J. Kelly, G. A. Riggs, A. T. C. Chang, and J. L. Foster. 2002. Assessment of the relative accuracy of hemispheric-scale snow-cover maps. Ann. Glaciol.,vol.34, pp.24–30.

Knowles, K., E. Njoku, R. Armstrong, and M.J. Brodzik. 2002. Nimbus-7 SMMR Pathfinder daily EASE-Grid brightness temperatures. Boulder, CO: National Snow and Ice Data Center. Digital media and CD-ROM.

Knowles, K. W., M. H. Savoie, R. L. Armstrong, and M. J. Brodzik. 2006. AMSR-E/Aqua daily EASE-Grid brightness temperatures, 2002-2008. Boulder, Colorado USA: National Snow and Ice Data Center. Digital media.

Pulliainen, J. 2006. Mapping of snow water equivalent and snow depth in boreal and sub-arctic zones by assimilating space-borne microwave radiometer data and ground-based observations. Remote Sensing of Environment. 101(2): 257-269.

Takala O.M, Pulliainen J, Metsämäki S, Koskinen J. 2009. Detection of Snowmelt Using Spaceborne Microwave Radiometer Data in Eurasia From 1979 to 2007. IEEE Trans. on Geoscience and Remote Sensing, Vol 47, pp. 2996 – 3007.

Takala, M., K. Luojus, J. Pulliainen, C. Derksen, J. Lemmetyinen, J-P Kärnä, and J. Koskinen. 2011. Estimating northern hemisphere snow water equivalent for climate research through assimilation of space-borne radiometer data and ground-based measurements. Remote Sensing of Environment. 115: 3517–3529, doi:10.1016/j.rse.2011.08.014.

18. NASA STANDARD AMSR-E SWE PRODUCT

By Richard Kelly (Univ. Waterloo, Canada) et.al.

18.1 Algorithm

The NASA standard AMSR-E product is described in Kelly (2009), and archived at the National Snow and Ice Data Center (http://nsidc.org/data/docs/daac/ae_swe_ease-grids.gd.html). The processing chain for the retrievals is shown in Figure 18.1. Shallow snow areas are determined using brightness temperature thresholds at 23 and 89 GHz, and an AMSR-E derived physical temperature estimate described in Kelly et al (2003). If shallow snow is detected, depth is set to 5 cm. Areas of non-shallow snow are identified using thresholds applied to 10 and 37 GHz measurements. The dry snow covered area estimates are constrained by climatological snow information (Dewey and Heim, 1981).

SWE retrievals for non-shallow, dry snow covered areas are based on a brightness temperature difference approach, first proposed by Chang et al., 1990:

$$SD = a(Tb19-Tb37) \quad (18.1)$$

where a is a retrieval coefficient. While this is the conceptual basis for the AMSR-E product, a number of enhancements were implemented to account for vegetation, improve sensitivity to deeper snowpacks, and consider the dynamic influence of snow grain size. Each grid cell is separated into forested and non-forested fractions:

$$SD = ff(SD_f) + (1-ff)*(SD_o) \quad (18.2)$$

with ff representing forest fraction, SD_f the retrieval over forested areas and SD_o the retrieval over open areas. The forest retrieval is based on the 37-19 brightness temperature difference, with a correction factors for forest density (*fd*):

$$SD_f = p1 * (Tb18V-Tb36V)/(1-fd*b) \quad (18.3)$$

The value for b is currently set at 0.6. For the non-forested component, the retrieval combines information from the 36-10 brightness temperature difference which is primarily sensitive to moderate snow depths, and 19-10 brightness temperature difference which adds sensitivity to scattering at the lower frequencies from deeper snow:

$$SD_o = [p1*(Tb10V-Tb36V)] + [p2*(Tb10v-Tb18V)] \quad (18.4)$$

The dynamic coefficients p1 and p2 are:

$$p1 = 1/\log10(36V-36H) \quad (18.5)$$

$$p2 = 1/\log10(18V-18H) \quad (18.6)$$

These replace the static coefficient *a* in equation 18.1 in order to capture the evolving influence of snow grain size through the winter (Kelly, 2009). They are based on the assumption that as snow depth increases, the depth average grain size increases, so these two coefficients decrease ensuring that overestimation of snow depth is avoided. To constrain both coefficients, a minimum polarization difference of 3 is applied to ensure that the denominator is not too small, but the values of p1 and p2 tend to fall between 1 and 2 (Kelly, 2009).

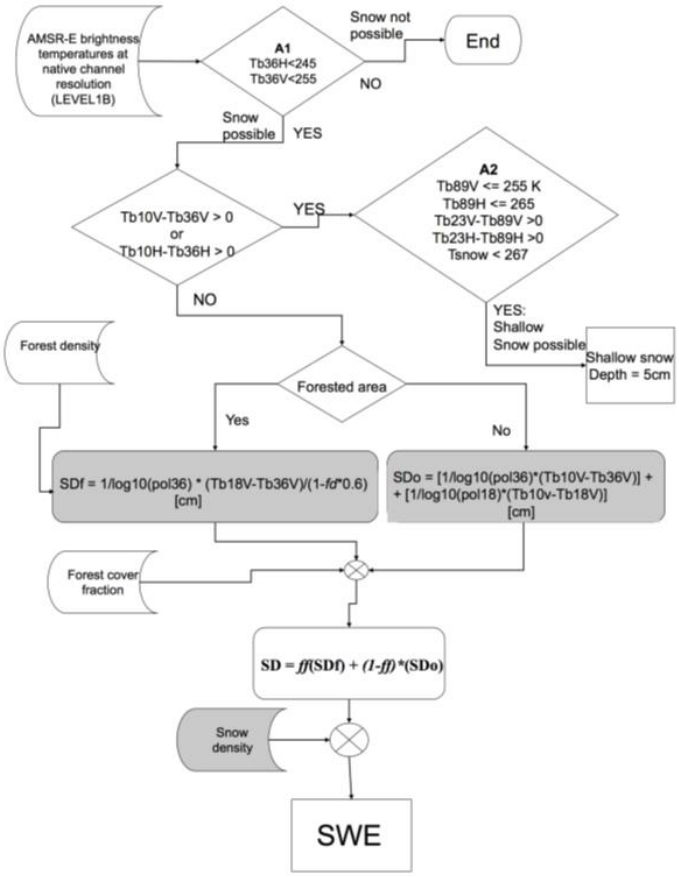

Figure 18.1: Processing chain for the standard NASA AMSR-E SWE algorithm.

All the initial screening for dry snow (shallow versus deep) is performed with V and H pol, with the retrievals subsequently performed using V-pol measurements. The exception is grid cells where only the H pol screening identified snow in which case H-pol brightness temperatures are used for the retrievals.

18.2 Input and Auxiliary Data

SWE and snow depth are estimated at the individual AMSR-E sample or footprint level at raw resolution to ensure that the algorithms can use the native calibrated Tb measurements (and hence exploit the improved resolution of raw AMSR-E measurements compared to previous satellite radiometers) and not a smoothed average that results from re-gridding to level 3 products. SWE and snow depth estimates are subsequently averaged to a 25 x 25 km grid and a 0.25 x 0.25 degree latitude/longitude grid respectively. Snow depth estimates (produced for JAXA) result from a two-step process: the presence of snow is detected, then the depth of snow is estimated as described in Section 16.4.1. For the SWE product (produced for NASA), the snow depth estimates are converted to SWE. Both SWE and depth processing streams utilize calibrated Tb measurements at 10, 18, 23, 36 and 89 GHz. The snow climatology of Dewey and Heim (1981) is applied to constrain the retrievals to a physically plausible domain.

Forest fraction (ff in equation 2) is determined from the MODIS MOD12Q1 data with approximately 1x1 km grid cell resolution. A forest fraction percentage is calculated for each MODIS grid cell using a 7 pixel kernel which approximates the 36 GHz AMSR-E footprint dimension of 14 x 12 km. The forest fraction map has the same grid cell spacing as the original MOD12Q1 product but with each cell representing the approximate forest fraction that contributes to each AMSR-E footprint at the AMSR-E resolution. Information on forest spatial structure (fd in equation 3) is estimated from the University of Maryland Vegetation Continuous Field (VCF) MODIS product, MOD44B. The same kernel based resampling procedure is used as for forest fraction, but the MOD44B segmentation of forest from herbaceous and open areas allows the derivation of a forest density estimate. Land/ocean and permanent ice masks are derived from MODIS MOD12Q1 IGBP land cover data.

For final production of the standard NASA product, snow depth is converted to SWE using the snow climate classification of Sturm et al (1995) and snow density climatologies from Brown and Braaten (1998) and Krenke (2004).

18.3 Product Specs

Until its failure on October 4th, 2011 estimates of daily, pentad and monthly SWE and snow covered area (SCA) at global scale were produced operationally by NASA from the Advanced Microwave Scanning Radiometer for EOS (AMSR-E) brightness temperatures (Tbs) on the NASA's AQUA spacecraft. The AMSR-E was successfully launched on NASA's EOS Aqua spacecraft on May 4th, 2002 therefore providing more than ten years of data that complement those acquired by other spaceborne microwave sensors such as the Special Sensor Microwave Imager (SSM/I). Though many algorithms have been proposed by the scientific community, the AMSR-E SWE product represents the only NASA satellite-based SWE product available to the scientific community.

Data are in the EASE-Grid Northern and Southern Hemisphere EASE-Grid projections (HDF-EOS format). Actual SWE values are scaled down by a factor of 2 for storing in the HDF-EOS file, resulting in a stored data range of 0-240. Users must multiply the SWE values in the file by a factor of 2 to scale the data up to the correct range of 0-480 mm. Flags are included for grid cells outside of the climatologically defined snow cover domain, permanent ice, water, and missing data.

The pentad maps consist of the composite of the daily SWE data. Derived snow parameters from daily product over the same grid cell are screened for consistency based on statistical tests and maximum snow storage is produced. There are 73 pentads in a year; for leap years the pentad including February 28 has an extra day. The monthly maps are generated by composite of the daily data.

Each HDF-EOS file contains core metadata with Quality Assessment (QA) metadata flags that are set by the Science Investigator-led Processing System (SIPS) at the Global Hydrology and Climate Center (GHCC) prior to delivery to NSIDC. A separate metadata file in XML format is also delivered to NSIDC with the HDF-EOS file; it contains the same information as the core metadata. Three levels of QA are conducted with the AMSRE Level-2 and Level-3 products: automatic, operational, and science QA. If a product does not fail QA, it is ready to be used for higher-level processing, browse generation, active science QA, archive, and distribution.

18.4 Validation

The NASA standard AMSR-E product draws on a long heritage of microwave snow research at NASA (Chang et al., 1987; 1990; Foster eta l., 1997; Hall et al., 1991; Kelly et al., 2003). Validation of the current version of the algorithm using snow depth stations reporting to WMO is described in Kelly (2009). RMSE ranges between 16 and 25 cm, and bias between 1 and 5 cm depending on the forest

fraction and year. Correlation values are not reported in Kelly (2009), but only modest correlations values between 0.1 and 0.3 are reported in Tedesco and Narvekar (2010), for the AMSR-E retrievals compared to both climate station snow depth measurements, and SWE estimates from the SNODAS assimilation produced by the U.S. National Weather Service (Figure 18.2).

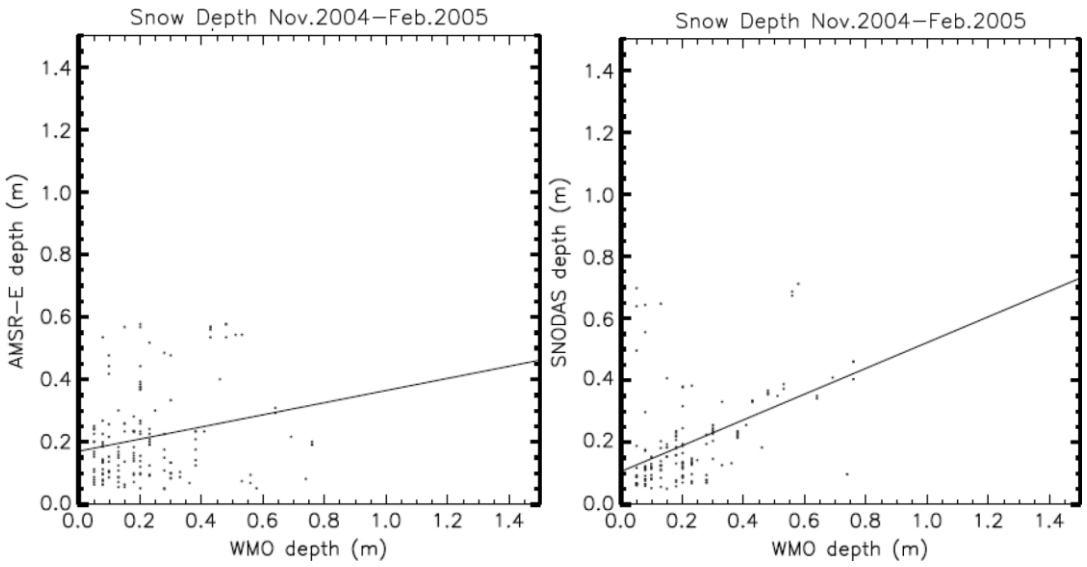

Figure 18.2: AMSR-E retrievals versus WMO stations (left) and SNODAS (right) for November 2004 – February 2005.

18.5 References

Brown, R., and R. Braaten. 1998. Spatial and temporal variability of Canadian monthly snow depths, 1946-1995. Atmosphere-Ocean. 36: 37-54.

Chang, A., J. Foster, and D. Hall. 1987. Nimbus-7 SMMR derived global snow cover parameters. Annals of Glaciology. 9: 39-44.

Chang, A., J. Foster, and D. Hall. 1990. Satellite sensor estimates of northern hemisphere snow volume. International Journal of Remote Sensing. 11(1): 167-171.

Chang, A., J. Foster, D. Hall, B. Goodison, A. Walker, J. Metcalfe, and A. Harby. 1997. Snow parameters derived from microwave measurements during the BOREAS winter field campaign. Journal of Geophysical Research. 102(D24): 29 663-29 671.

Dewey, K., and R. Heim. 1981. Satellite observations of variations in Northern Hemisphere snow cover. U.S. Department of Commerce, NOAA Technical Report NESS 87.

Foster, J. A. Chang, D. Hall. 1997. Comparison of snow mass estimates from a prototype passive microwave snow algorithm, a revised algorithm and a snow depth climatology. Remote Sensing of Environment. 62: 132-142.

Hall, D., M. Sturm, C. Benson, A. Chang, J. Foster, H. Garbeil, and E. Chacho. 1991. Passive microwave remote and in situ measurements of Arctic and Subarctic snow covers in Alaska. Remote Sensing of Environment. 38: 161-172.

Kelly, R., A. Chang, L.Tsang, and J. Foster. 2003. A prototype AMSR-E global snow area and snow depth algorithm. IEEE Transactions on Geoscience and Remote Sensing. 41(2): 230-242.

Kelly, R.E.J. 2009. The AMSR-E Snow Depth Algorithm: Description and Initial Results, Journal of The Remote Sensing Society of Japan. 29(1): 307-317.

Krenke, A. 2004. Former soviet union hydrological snow surveys. NSIDC, Boulder, CO.

Sturm, M., J. Holmgren, and G. Liston. 1995. A seasonal snow cover classification system for local to global applications. Journal of Climate. 8: 1261-1283.

Tedesco, M., and P. Narvekar. 2010. Assessment of the NASA AMSR-E SWE product. IEEE Journal of Selected Topics in Applied Earth Observations and Remote Sensing. 3(1): 141-159.

19. NASA PROTOTYPE AMSR-E PRODUCT

By Marco Tedesco (University College New York, USA) et. al.

19.1 Algorithm

A prototype algorithm for AMSR-E was recently developed to address uncertainties in the baseline NASA product described in Section 18 (Tedesco, personal communication). A combination of numerical techniques (e.g., artificial neural networks), snow emission modelling, and ancillary climatological data are utilized for the estimation of snow depth and SWE, and the detection of dry/wet snow conditions (Figure 19.1).

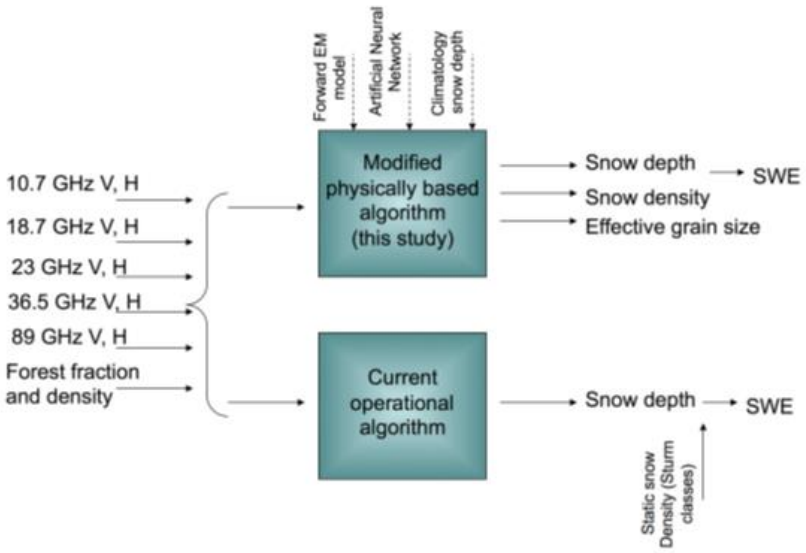

Figure 19.1: Flow chart for the prototype NASA AMSR-E algorithm relative to the baseline described in Section .18.1

The prototype algorithm addresses three issues. First, instead of the p1 and p2 coefficients computed using equations 18.5 and 18.6, the coefficients are computed using estimates of effective grain size obtained from an artificial neural network (ANN) trained with the outputs from the HUT snow emission model (Pulliainen et al., 1999). The grain size estimate via the ANN requires a snow depth first guess, (which is also the unknown in the retrieval scheme) so a snow depth climatology is used to initialize

the grain size estimates from the ANN. Snow density is also required (and unknown) and is obtained based on the method described in Sturm et al. (2010) using the snow depth climatology, the day of the year, and snow climate class as inputs to the density model. Finally, snow temperature is obtained from a combination of measured brightness temperatures (as described below). In summary, the input vector to the ANN to estimate grain size is made of snow depth monthly climatology values, daily snow density climatology computed from Sturm et al. (2010), estimated near-surface temperature and measured brightness temperatures. This configuration means the prototype algorithm retains the characteristics of a 'standalone' satellite algorithm (like the NASA standard algorithm and unlike the GlobSnow approach) but could be modified to use real-time weather station data or to ingest additional information. The grain size estimated from the ANN is then used for the retrieval of snow depth through the definition of new dynamic coefficients based on the standard algorithm approach shown in equations 18.5 and 18.6. These are further differentiated by considering whether the snow is overlying permafrost.

Second, the estimation of snow surface temperature in the standard algorithm is computed using an empirical method described in Kelly (2009). This linear regression is replaced with a non-linear multivariate regression approach based on ANN output. This is similar to what has been described above for the grain size with the difference that the input to the ANN is made of the brightness temperatures measured at 19- and 37 – GHz, both vertical and horizontal polarization, the ~ 22 GHz brightness temperature, vertical polarization, and the ~ 89 GHz brightness temperatures, all collected during the descending orbit (which is the one used for retrieval as it is collected in early morning, hence reducing the probability of the presence of wet snow, which precludes snow depth retrieval.

Third, in the current version of the SWE algorithm, though the spatial variability of the density mask is dictated by the different Sturm et al (1995) snow climate classes, a temporally fixed mask of snow density values are used however it remains static within each snow class. However, density evolves during the snow season and within each snow class and it is therefore important to account for this process to improve SWE estimates (Tedesco and Narvekar, 2010). In the new algorithm, therefore, daily snow density maps are obtained following the formulas reported in Sturm et al. (2010). Here, a statistical model based on a Bayesian analysis of a set of 25,688 depth-density-SWE data collected in the U.S., Canada, and Switzerland uses snow depth (SD), day of the year (DOY), and the climate class of snow (SC) to produce estimates of a local bulk density.

19.2 Input and Auxiliary Data

The prototype AMSR-E algorithm utilizes the same brightness temperature and ancillary datasets as the standard NASA product described in section 18.2. The only additional auxiliary dataset is permafrost information obtained from Brown et al. (1998, updated 2001).

19.3 Product Specs

The same product specifications as for the standard algorithm, see Section 18.3.

19.4 Validation

Tedesco (2012) provides an intercomparison of the standard NASA AMSR-E product, the modified prototype described in section 19.1, and the northern hemisphere operational snow depth analysis produced daily at the Canadian Meteorological Centre (Brasnett, 1998). As shown in Table 19.1, the modified algorithm produces reduced RMSE and bias, and strengthened correlation for all months considered. A similar comparison of the AMSR-E datasets with station measurements at locations reporting to WMO produced similar improvement for all cases (not shown). A comparison of the difference in the AMSR-E products (baseline and modified) with the GlobSnow product identified closer agreement in retrievals for the modified algorithm (Tedesco, 2012).

Table 19.1:
Monthly averaged correlation values, RMSE, slope and bias between the AMSR-E retrievals and the CMC analysis (from Tedesco, 2012).

	Original				*Modified*			
	Correlation	***RMSE***	***Slope***	***Bias***	***Correlation***	***RMSE***	***Slope***	***Bias***
January	0.2197	21.3003	0.2137	21.3983	**0.351**	**17.0357**	**0.224**	**15.9389**
February	0.1923	23.4831	0.1809	26.5166	**0.2874**	**19.778**	**0.2046**	**21.3222**
March	0.0644	25.6249	0.0574	33.5941	**0.1482**	**23.2104**	**0.1137**	**27.3179**
April	-0.0631	27.6975	-0.062	38.3672	**0.2082**	**21.2398**	**0.1525**	**25.9138**
October	0.037	12.3247	0.0335	11.9423	**0.1536**	**10.3858**	**0.1159**	**9.1645**
November	0.1238	14.3137	0.1098	14.5536	**0.1895**	**12.7779**	**0.133**	**11.4269**
December	0.2005	17.9307	0.1882	16.9576	**0.3091**	**14.9568**	**0.1969**	**12.4535**

While not evaluating the prototype algorithm directly, Tedesco et al (2010) used ancillary snow depth information to dynamically update parameters in a similarly structured retrieval algorithm. All the

approaches that utilized weekly updates to the retrieval coefficients performed better than a standard regression based approach using fixed retrieval coefficients.

19.5 References

Brasnett, B. 1999. A global analysis of snow depth for numerical weather prediction. Journal of Applied Meteorology. 38: 726-740.

Brown, J., O. Ferrians, J. A. Heginbottom, and E. Melnikov. 2002. Circum-Arctic Map of Permafrost and Ground-Ice Conditions. Version 2. Boulder, Colorado USA: National Snow and Ice Data Center.

Kelly, R.E.J. (2009) The AMSR-E Snow Depth Algorithm: Description and Initial Results, Journal of The Remote Sensing Society of Japan. 29(1): 307-317.

Pulliainen, J., Grandell, J., & Hallikainen, M., 1999. HUT snow emission model and its applicability to snow water equivalent retrieval. IEEE Trans. Geosci. Remote Sens., 37, 1378−1390.

Sturm, M., B. Taras, G. Liston, C. Derksen, T. Jonas, and J. Lea. 2010. Estimating snow water equivalent using snow depth data and climate classes. Journal of Hydrometeorology. 11: 1380-1394.

Sturm, M., J. Holmgren, and G. Liston. 1995. A seasonal snow cover classification system for local to global applications. Journal of Climate. 8: 1261-1283.

Tedesco, M., and P. Narvekar. 2010. Assessment of the NASA AMSR-E SWE product. IEEE Journal of Selected Topics in Applied Earth Observations and Remote Sensing. 3(1): 141-159.

Tedesco, M., R. Reichle, A. Löw, T. Markus, and J. Foster. 2010. Dynamic approaches for snow depth retrieval from spaceborne microwave brightness temperature. IEEE Transactions on Geoscience and Remote Sensing. 48: 1955-1967.

Tedesco, M. 2012. Algorithm theoretical basis document, NASA AMSR-E SWE Product. Unpublished.